NATIONAL ADVISORY COMMITTEE FOR AERONAUTICS

TECHNICAL NOTE 2465

EXPERIMENTAL AERODYNAMIC DERIVATIVES OF A SINUSOIDALLY OSCILLATING AIRFOIL IN TWO-DIMENSIONAL FLOW

By Robert L. Halfman

Massachusetts Institute of Technology

Washington
November 1951

NATIONAL ADVISORY COMMITTEE FOR AERONAUTICS

TECHNICAL NOTE 2465

EXPERIMENTAL AERODYNAMIC DERIVATIVES OF A SINUSOIDALLY OSCILLATING AIRFOIL IN TWO-DIMENSIONAL FLOW

By Robert L. Halfman

SUMMARY

Experimental measurements of the aerodynamic reactions on a symmetrical airfoil oscillating harmonically in a two-dimensional flow are presented and analyzed. Harmonic motions include pure pitch and pure translation, for several amplitudes and superimposed on an initial angle of attack, as well as combined pitch and translation.

The apparatus and testing program are described briefly and the necessary theoretical background is presented.

In general, the experimental results agree remarkably well with the theory, especially in the case of the pure motions. The net work per cycle for a motion corresponding to flutter is experimentally determined to be zero.

Considerable consistent data for pure pitch were obtained from a search of available reference material, and several definite Reynolds number effects are evident.

INTRODUCTION

The purpose of the work described in this report was to determine experimentally the lift and moment on an oscillating airfoil and compare the results with the predictions of the vortex-sheet theory as described in reference 1. The use of the theory on aero-elastic problems such as flutter could then be verified or modified. The general plan of the program was to break down the flutter motion into its simplest components so as to examine each one individually before superimposing them to check the flutter condition itself.

The entire project was undertaken in a succession of phases by the Aero-Elastic Research Laboratory of the Massachusetts Institute of

Technology over a considerable period of time and should be considered as the combined efforts of the groups which worked on each phase. The phases were:

(1) The design and construction of the oscillating actuator mechanism

(2) The development of the support of the model on the actuator and the subsequent installation of the apparatus in the wind tunnel

(3) The development of the force-recording equipment

(4) Systematic tests with the equipment developed in phases (1) to (3) and design study of equipment for higher frequencies

(5) The thorough analysis of the test results of phase (4)

Since a substantial amount of data for similar tests has been compiled independently by various other research groups and no known résumé or comparison has been made, a portion of this report is given over to the reproduction and comparison of typical data reduced to a common form of presentation. (See appendix.)

This work was conducted at the Massachusetts Institute of Technology under the sponsorship and with the financial assistance of the National Advisory Committee for Aeronautics.

SYMBOLS

n	frequency of forced motion
ω	angular frequency of forced motion ($2\pi n$)
b	semichord
V	air-stream velocity
k	reduced-frequency parameter $\left(\frac{\omega b}{V}\right)$
ρ	density of air
q	dynamic pressure $\left(\frac{1}{2}\rho V^2\right)$
α	pitching angle of wing; positive in direction of stall
α_o	amplitude of pitch

α_i	initial angle of attack
h	vertical translation of wing at 37-percent chord; positive downward
h_o	amplitude of translation
θ	angle by which pitching motion leads translation motion
β	phase angle between front and rear actuator wheels
a	ratio of distance of elastic axis aft of midchord point to semichord
$\overline{x}$	distance of center of gravity aft of midchord
m	mass of wing per unit span
F	Theodorsen's function
G	Theodorsen's function
C	Theodorsen's function (F + iG)
S_α	static moment of wing about elastic axis $((\overline{x} - ab)m)$
I_a	moment of inertia of wing per unit span about elastic axis
ω_h	natural frequency in bending
C_h	effective linear spring constant $\left(m\omega_h^2\right)$
ω_α	natural frequency in torsion
C_α	effective torsional spring constant $\left(I_a\omega_\alpha^2\right)$
W_M	work per cycle due to moment
W_L	work per cycle due to lift
W_N	net work per cycle $\left(- W_L - W_M\right)$
C_{W_L}	coefficient of work due to lift $\left(\frac{W_L}{4qba_o h_o}\right)$
C_{W_M}	coefficient of work due to moment $\left(- \frac{W_M}{4qba_o h_o}\right)$

C_W	coefficient of net work $\left(\frac{W_N}{4qba_o h_o}\right)$
ΔC_D(ave.)	average drag-amplitude coefficient
C_{LS}	steady state or static lift
$C_{MS_{EA}}$	steady-state moment coefficient about elastic axis
R.N.	Reynolds numbers based on airfoil chord
A.R.	aspect ratio
3-DIM	three-dimensional
2-DIM	two-dimensional
Exp.	experimental data
T	theoretical data
BT	theoretical data from references 2 and 3
B_1	experimental data from reference 2
B_2	experimental data from reference 3
S	experimental data from Stanford University
M	experimental data from Massachusetts Institute of Technology
A(i), B(i), C(i), D(i)	data from Stanford University models not corrected to 37-percent chord elastic-axis location
A(c), B(c), C(c), D(c)	data from Stanford University models corrected to 37-percent chord elastic-axis location

(i) experimental data from references 2 and 3 not corrected to 37-percent chord elastic-axis location

(c) experimental data from references 2 and 3 corrected to 37-percent chord elastic-axis location

The following symbols are usually combined with subscripts:

L lift per unit span; positive downward

M moment per unit span; positive in direction of stall

R real part of complex quantity

R' dimensionless real part of complex quantity

I imaginary part of complex quantity

I' dimensionless imaginary part of complex quantity

$\sqrt{R^2 + I^2}$ magnitude

A,B,D,E components of lift or moment

ϕ phase angle $\left(\tan^{-1} \frac{I}{R}\right)$

Subscripts:

P due to pitching motion

T due to translational motion

R due to combination of translational and pitching motion

L lift

M moment

DESCRIPTION OF APPARATUS

The mechanical apparatus is designed to oscillate an airfoil in pure pitch, pure translation, and combinations of the two at various frequencies and amplitudes. The installation in the test section of the tunnel is shown in figure 1 and the entire oscillator mechanism is

illustrated schematically in figure 2. The range of motions obtainable is shown in figure 3.

The airfoil which was constructed for these tests is rectangular in plan form with a 1-foot chord, 2-foot span, and NACA 0012 profile. An extremely rigid and light magnesium two-spar stressed-skin construction was necessary to minimize inertia loads and prevent appreciable deflection during oscillation. The tests were performed in the M.I.T. 5- by $7\frac{1}{2}$- foot flutter tunnel which was modified by the installation of two vertical fairings as shown in figure 1. The presence of these fairings insured essentially two-dimensional flow over the airfoil while any deviations from the usual flow could be detected by the pitot-tube rake installation also shown in figure 1.

The oscillator mechanism consists primarily of an actuator unit located just below the test section and two identical linkages extending up through the vertical fairings on each side of the airfoil. As may be seen in figure 2, the actuator (3) has two pairs of circular crank wheels on each side. The rotational motion of each pair is transformed into sinusoidal vertical motion by means of a connecting rod sliding on a member constrained to move vertically. This vertical motion is transmitted up into the test section by thin steel bands (1) which terminate at the "dumbbell" cams (6). Additional bands continue from the cams to the adjustable overhead springs (9) which maintain tension in the bands at all times. The resultant motion of the cams is transmitted to the wing through the linkage (12). Each pair of crank wheels can be set to produce either 1-, 2-, or 3-inch-amplitude vertical motion and the front pairs can be set and phased independently of the rear pairs. Thus with the rear pairs exactly 180° out of phase with respect to the front, the cam (6) is rocked about its center in pure pitch.

Two sockets in each end rib of the airfoil receive the ball ends of short cantilever beams supported by the linkage (12) with the forward sockets located on the center-of-gravity axis of the wing at 37-percent chord. Resistance wire strain gages mounted on these cantilevers measure the forces required to oscillate the airfoil in a given motion. Since these forces include inertia reactions as well as aerodynamic forces it was necessary to design the "multiple accelerometers" (13) to produce signals equal to the inertia reactions of the airfoil which could be electrically subtracted from the total force signals. This difference, then, represents aerodynamic forces only. The inertia cancellation process is necessary only for the lift and moment signals since there is no inertia force in the drag direction. The signals are amplified and recorded with Consolidated Engineering Corporation 1000-cycle-per-second carrier equipment. The correct attenuator settings for the accelerometer signals are determined experimentally by substituting a

"dummy wing" for the airfoil. This wing is of open construction to minimize aerodynamic reactions but has mass and moment-of-inertia properties identical with those of the airfoil. Because of the relatively large range of forces to be covered during the tests it was necessary to design and use two complete sets of force-measuring elements, a "soft" set for low frequencies and amplitudes and a "stiff" set to handle the higher forces at higher frequencies and amplitudes.

A reference-position signal was at first obtained from an undamped accelerometer mounted on the rear crossbar (2) and later from a Kollsman rotatable transformer (14) attached to the rear crank wheel.

SYSTEMATIC TESTS

The four general types of tests included in the testing program are:

(1) Pure pitching motion

(2) Pure translation

(3) Pure motions superimposed on an initial angle of attack

(4) Combined pitching and translation with special emphasis in the neighborhood of a motion corresponding to flutter

In order to obtain the best results throughout the testing program, the least difficult tests were performed first and the experience thus gained was applied to the remaining tests as they were encountered. Thus the pure motions were examined first at the two amplitudes corresponding to the 1- and 2-inch crank-wheel settings on the actuator using the soft force-measuring elements. Next the turnbuckles, (16) in figure 2, were adjusted to produce an initial angle of attack of 6.1° and the lower-amplitude pure motions were superimposed on this initial angle.

Since there are so many possible combined motions it was necessary to restrict the testing to a survey of the field. Thus tests were made at a constant "reduced frequency" k of 0.3 for phasings between the pure motions of 0°, 90°, 180°, and 270°. Ideally the ratio of translation amplitude to pitch amplitude should also have been kept constant to permit simple and accurate comparisons of the four conditions; but this was not possible, unfortunately, because of the limitations of the oscillator. Another series of tests at constant reduced frequency was made in the neighborhood of a case corresponding to flutter. The derivation of the correct motions for the flutter condition is described in the next section.

Because of strength limitations, tests using the soft elements could not be run in the high-frequency range for the larger-amplitude motions. Thus, in order to extend the frequency ranges already covered in the pure motion tests, the stiff set of elements was installed and high-frequency tests at the larger amplitudes were made. It was also decided to run another series of tests near the flutter condition partly as a check on the previous runs corresponding to a condition near flutter. This second flutter series was made with a constant phasing between the pure motions, with a constant amplitude ratio, and at a constant airspeed. The only variable was the frequency of the motion which produced a corresponding variation in reduced frequency k.

For all but the combined-motion tests, either two or three airspeeds were used, averaging about 95 miles per hour, and the frequency range was covered for each airspeed in half-cycle per second steps. The combined-motion tests were run at only one airspeed and for each test the frequency was varied slowly and smoothly over a range from slightly above to slightly below the frequency corresponding to the desired value $k = 0.3$.

The over-all instrument system was calibrated by applying known forces directly to the wing and noting the corresponding galvanometer deflections in the recording oscillograph. Typical records are shown in figures 4 and 5, and include traces of lift, moment, reference position, and in some cases drag, as well as zero traces. Despite the relatively high-frequency "hash" on most of the records, consistent values of amplitudes and phase angles were measured and are plotted in figures 6 to 17 and recorded in tables I through X.

THEORETICAL BACKGROUND

To obtain the theoretical values of the aerodynamic derivatives for comparison with the experimental results of this report, the analytical methods used were based on Theodorsen's work (reference 1). In this analysis separate solutions are given for pure harmonic pitching and pure translation, and a combination of the two requires only a vector addition of the derivatives due to the pure motions.

The two-dimensional lift and moment equations, as rearranged by Hunter[1] are as follows:

$$\left.\begin{aligned}
\frac{L_R}{4qb} &= -\pi\left(-\frac{k^2}{2}+ikC\right)\frac{h}{b}-\pi\left\{\frac{1}{2}\left[ik+ak^2\right]+\left[1+ik\left(\frac{1}{2}-a\right)\right]C\right\}\alpha \\
\frac{M_R}{4qb^2} &= -\pi\left[\frac{ak^2}{2}-\left(\frac{1}{2}+a\right)ikC\right]\frac{h}{b}-\pi\left\{\frac{1}{2}\left[ik\left(\frac{1}{2}-a\right)-k^2\left(\frac{1}{8}+a^2\right)\right]\right. \\
&\qquad \left.\left(\frac{1}{2}+a\right)\left[1+ik\left(\frac{1}{2}-a\right)\right]C\right\}\alpha
\end{aligned}\right\} \quad (1)$$

These results are conveniently expressed in complex notation. For example, the lift force resulting from a sinusoidally varying translational motion may be written as

$$L_T = 4qb\left(R_{LT}+iI_{LT}\right)e^{i\omega t}$$

Here ω represents the angular frequency of the forced motion. The subscript T is used to designate the translational mode, and the restriction that the real term R and the imaginary term I be those that apply only to the lift force is specified by the subscript L. This expression of the lift force due to the translational motion can be written in another form as a nondimensional derivative:

$$\frac{L_T}{4qb} = \sqrt{R_{LT}^2+I_{LT}^2}\,e^{i\left(\omega t+\phi_{LT}\right)} \quad (2)$$

where $\phi_{LT} = \tan^{-1}\frac{I_{LT}}{R_{LT}}$.

The expression for the theoretical aerodynamic moment derivative in the translational mode may be written:

$$\frac{M_T}{4qb^2} = \sqrt{R_{MT}^2+I_{MT}^2}\,e^{i\left(\omega t+\phi_{MT}\right)} \quad (3)$$

where $\phi_{MT} = \tan^{-1}\frac{I_{MT}}{R_{MT}}$.

---

[1]Unpublished M.I.T. Master's thesis by Maxwell W. Hunter, "Calculation of the Aerodynamic Span Effect in Flutter Analysis," June 1944.

For the pitching motion, the form of the equations is identical to that for the translation; the lift L_P due to pitch is expressed in in terms of R_{LP}, I_{LP}, and ϕ_{LP} and the moment M_P due to pitch is expressed in terms of R_{MP}, I_{MP}, and ϕ_{MP}. The combined motion case is differentiated from the above by the use of the subscript R (meaning resultant) instead of the subscripts P and T.

The real and imaginary factors given by the theory for a two-dimensional wing are as follows:

$$R_{LT} = \frac{\pi h_o}{b}\left(\frac{k^2}{2} + kG\right)$$

$$I_{LT} = -\frac{\pi h_o}{b} kF$$

$$R_{MT} = -\frac{\pi h_o}{b}\left[\frac{ak^2}{2} + \left(\frac{1}{2} + a\right)kG\right]$$

$$I_{MT} = \frac{\pi h_o}{b}\left(\frac{1}{2} + a\right)kF$$

$$R_{LP} = -\pi\alpha_o\left[\frac{ak^2}{2} + F - \left(\frac{1}{2} - a\right)kG\right]$$

$$I_{LP} = -\pi\alpha_o\left[\frac{k}{2} + G + \left(\frac{1}{2} - a\right)kF\right]$$

$$R_{MP} = \pi\alpha_o\left\{\frac{k^2}{2}\left(\frac{1}{8} + a^2\right) + \left(\frac{1}{2} + a\right)\left[F - \left(\frac{1}{2} - a\right)kG\right]\right\}$$

$$I_{MP} = -\pi\alpha_o\left\{\frac{k}{2}\left(\frac{1}{2} - a\right) - \left(\frac{1}{2} + a\right)\left[G + \left(\frac{1}{2} - a\right)kF\right]\right\}$$

$$R_{LR} = R_{LT} + R_{LP}\cos\theta - I_{LP}\sin\theta$$

$$I_{LR} = I_{LT} + R_{LP}\sin\theta + I_{LP}\cos\theta$$

$$R_{MR} = R_{MT} + R_{MP}\cos\theta - I_{MP}\sin\theta$$

$$I_{MR} = I_{MT} + R_{MP}\sin\theta + I_{MP}\cos\theta$$

and the corresponding phase angles are:

$$\phi_{LT} = \tan^{-1} \frac{I_{LT}}{R_{LT}}$$

$$\phi_{LP} = \tan^{-1} \frac{I_{LP}}{R_{LP}}$$

$$\phi_{LR} = \tan^{-1} \frac{I_{LR}}{R_{LR}}$$

$$\phi_{MT} = \tan^{-1} \frac{I_{MT}}{R_{MT}}$$

$$\phi_{MP} = \tan^{-1} \frac{I_{MP}}{R_{MP}}$$

$$\phi_{MR} = \tan^{-1} \frac{I_{MR}}{R_{MR}}$$

with the additional condition derived from the following table:

R	+	-	-	+
I	+	+	-	-
Quadrant	1	2	3	4

The angle θ is the amount by which the pitching displacement vector α leads the reference displacement vector h; the ratio $\frac{\omega b}{V}$ is the reduced frequency parameter k; F and G are respectively the real and the imaginary parts of the Theodorsen function C(k); the symbol a denotes the ratio of the distance of the elastic axis aft of the midchord point to the half chord b; h_o represents the amplitude in inches of the translational oscillations and α_o represents the amplitude in radians of the pitching oscillations; h and L are positive downward and α and M are positive for a rotation toward the stall.

One of the outstanding advantages of the apparatus that was designed for this research is that not only can pure pitching and pure translating motions be imparted to the airfoil at a choice of amplitudes in either

pure motion, but a wide range of combinations of pitching and translating motions can also be used with an equally wide choice of phase intervals between the motions. Thus if a combined motion corresponding to a typical flutter is imparted to the airfoil a study can be made of the aerodynamic reactions for this critical condition.

Since the airfoil is inherently extremely rigid, it follows the forcing motion of the linkage without perceptible deviation. This motion can be adjusted to simulate that of a spanwise segment of a wing under a wide range of dynamic conditions. Although the chord and profile are fixed, values of elastic-axis location, center-of-gravity location, mass and inertia per unit span, and effective spring constants may be chosen to represent a typical wing with a flutter mode which corresponds to a possible setting of the oscillator. The actual determination of a flutter condition, as outlined in the following paragraphs, follows the method of finding all the possible flutter motions which can easily be duplicated by the oscillator and then choosing one which corresponds to a reasonable wing.

The conditions for the flutter of a two-dimensional wing in bending-torsion flutter are expressed by the following set of differential equations if the effects of structural damping are neglected:

$$m\ddot{h} + S_\alpha \ddot{\alpha} + C_h h - L_R = 0$$

$$I_a \ddot{\alpha} + S_\alpha \ddot{h} + C_\alpha \alpha - M_R = 0$$

If the assumption that the motions are simple harmonic is introduced, one may write the equations in the complex forms:

$$-m\omega^2 h_o - S_\alpha \omega^2 \alpha_o e^{i\theta} + m\omega_h^2 h_o - 4qb\left(R_{LR} + iI_{LR}\right) =$$

$$-I_a \omega^2 \alpha_o - S_\alpha \omega^2 h_o e^{-i\theta} + I_a \omega^2 \alpha_o - 4qb^2 e^{-i\theta}\left(R_{MR} + iI_{MR}\right) = 0$$

or

$$-m\omega^2 h_o - S_\alpha \omega^2 \alpha_o e^{i\theta} + m\omega_h{}^2 h_o + 4q\pi h_o \left(-\frac{k^2}{2} + ikC\right) +$$

$$4q\alpha_o e^{i\theta} \pi b \left\{\frac{1}{2}\left(ik + ak^2\right) + \left[1 + ik\left(\frac{1}{2} - a\right)\right] C\right\} = 0$$

$$-I_a \omega^2 \alpha_o - S_\alpha \omega^2 h_o e^{-i\theta} + I_a \omega_\alpha{}^2 \alpha_o + 4qbh_o e^{-i\theta} \pi \left[\frac{ak^2}{2} - \left(\frac{1}{2} + a\right) ikC\right] +$$

$$4qb^2 \alpha_o \pi \left\{\frac{1}{2}\left[ik\left(\frac{1}{2} - a\right) - k\left(\frac{1}{8} + a^2\right)\right] -$$

$$\left(\frac{1}{2} + a\right)\left[1 + ik\left(\frac{1}{2} - a\right)\right] C\right\} = 0$$

where $h = h_o e^{i\omega t}$ and $\alpha = \alpha_o e^{i(\omega t + \theta)}$.

In order to satisfy the equations of motion, the sums of the real and the imaginary components of each of these equations must be independently equal to zero. By this fact and the identity $e^{\pm i\theta} = \cos\theta \pm i \sin\theta$,

$$\left.\begin{aligned} -m\omega^2 h_o - S_\alpha \omega^2 \alpha_o \cos\theta + m\omega_h{}^2 h_o - 4qbR_{LR} &= 0 \\ -S_\alpha \omega^2 \alpha_o \sin\theta - 4qbI_{LR} &= 0 \\ -I_a \omega^2 \alpha_o - S_\alpha \omega^2 h_o \cos\theta + I_a \omega_\alpha{}^2 \alpha_o - 4ab^2\left(R_{MR} \cos\theta + I_{MR} \sin\theta\right) &= 0 \\ -S_\alpha \omega^2 h_o \sin\theta + 4qb^2\left(I_{MR} \cos\theta - R_{MR} \sin\theta\right) &= 0 \end{aligned}\right\} \quad (4)$$

These four equations must be satisfied to determine the flutter condition for a wing.

The second and the fourth equations may be written in the forms:

$$\left.\begin{aligned} 4qbI_{LR}h_o &= -S_\alpha\omega^2\alpha_o h_o \sin\theta \\ -4qb^2\alpha_o\left(R_{MR}\sin\theta - I_{MR}\cos\theta\right) &= S_\alpha\omega^2 h_o\alpha_o \sin\theta \end{aligned}\right\} \quad (5)$$

These two expressions have left-hand sides which are proportional to the work done by the lift and the moment as will be shown below. In the absence of structural damping in bending-torsion flutter, the total work done on the wing during a cycle must be zero. Any work done in one degree of freedom must therefore be offset by equal and opposite work done in the other degree of freedom. The means of an energy transfer from one degree of freedom to another lies in the inertia coupling between the pure motions.

That energy transfer exists only if an inertia coupling term S_α is present may be easily seen if one studies the work equations closely. The air forces may be written as:

$$\frac{L_R}{4qb} = \sqrt{R_{LT}^2 + I_{LT}^2}\, e^{i\left(\omega t+\phi_{LT}\right)} + \sqrt{R_{LP}^2 + I_{LP}^2}\, e^{i\left(\omega t+\phi_{LP}+\theta\right)}$$

$$\frac{M_R}{4qb^2} = \sqrt{R_{MT}^2 + I_{MT}^2}\, e^{i\left(\omega t+\phi_{MT}\right)} + \sqrt{R_{MP}^2 + I_{MP}^2}\, e^{i\left(\omega t+\phi_{MP}+\theta\right)}$$

Then the work per cycle done by the lift force is:

$$\oint L_R\, dh = -4qb\omega h_o\left\{\int_0^{\frac{2\pi}{\omega}}\left[\sqrt{R_{LT}^2 + I_{LT}^2}\cos\left(\omega t + \phi_{LT}\right) + \sqrt{R_{LP}^2 + I_{LP}^2}\cos\left(\omega t + \phi_{LP}^2 + \theta\right)\right]\sin\omega t\, dt\right\}$$

But

$$\int_0^{\frac{2\pi}{\omega}} \cos(\omega t + \phi)\sin \omega t \, dt = -\frac{\sin \phi}{\omega}\int_0^{2\pi} \sin^2\omega t \, d(\omega t) = -\pi\frac{\sin \phi}{\omega}$$

Therefore,

$$W_L = \oint L_R \, dh = 4qb\pi h_o\left[\sqrt{R_{LT}^2 + I_{LT}^2}\sin \phi_{LT} + \sqrt{R_{LP}^2 + I_{LP}^2}\sin\left(\phi_{LP} + \theta\right)\right]$$

Similarly the work done by the moment per cycle is:

$$W_M = \oint M_R \, d\alpha = 4qb^2\pi\alpha_o\left[\sqrt{R_{MT}^2 + I_{MT}^2}\sin\left(\phi_{MT} - \theta\right) + \sqrt{R_{MP}^2 + I_{MP}^2}\sin \phi_{MP}\right]$$

The same results may be expressed in the simpler forms:

$$\left.\begin{aligned} W_L &= 4qb\pi h_o\left(I_{LT} + R_{LP}\sin\theta + I_{LP}\cos\theta\right) = 4qb\pi h_o I_{LR} \\ W_M &= 4qb^2\pi\alpha_o\left(I_{MP} - R_{MT}\sin\theta + I_{MT}\cos\theta\right) = -4qb^2\alpha_o\pi\left(R_{MR}\sin\theta - I_{MR}\cos\theta\right) \end{aligned}\right\} \quad (6)$$

These values of work per cycle are proportional to the left-hand sides of equation (5), the constant of proportionality being π. Thus it is seen that the coupling term S_α makes possible the exchange of energy between the motions in such a way that the net work done by the airfoil at flutter is zero:

$$W_{net} = W_N = -\left(W_L + W_M\right) = 0$$

To proceed now to the actual solution of equations (5), it is convenient to introduce the dimensionless auxiliary quantities:

$$I_{LT}' = \frac{b}{h_o} I_{LT}$$

$$I_{MT}' = \frac{b}{h_o} I_{MT}$$

$$R_{MT}' = \frac{b}{h_o} R_{MT}$$

$$I_{LP}' = \frac{1}{\alpha_o} I_{LP}$$

$$R_{LP}' = \frac{1}{\alpha_o} R_{LP}$$

$$I_{MP}' = \frac{1}{\alpha_o} I_{MP}$$

Then,

$$\left.\begin{aligned} W_L &= 4qbh_o^2\left[\frac{I}{b} I_{LT}' + \left(\frac{\alpha_o}{h_o}\right)\left(R_{LP}' \sin\theta + I_{LP}' \cos\theta\right)\right] = -S_\alpha \omega^2 \alpha_o h_o \sin\theta \\ W_M &= 4qb^2\alpha_o^2\left[I_{MP}' + \left(\frac{h_o}{\alpha_o}\right)\left(\frac{1}{b}\right)\left(I_{MT}' \cos\theta - R_{MT}' \sin\theta\right)\right] = S_\alpha \omega^2 \alpha_o h_o \sin\theta \end{aligned}\right\} \quad (7)$$

These sets of transcendental equations can be solved "graphically" with the use of the nondimensional coefficients:

$$C_{W_L} = \frac{W_L}{4qb\alpha_o h_o} = \left[\frac{h_o}{\alpha_o}\left(\frac{I_{LT}'}{b}\right) + R_{LP}' \sin\theta + I_{LP}' \cos\theta\right]$$

$$C_{W_M} = -\frac{W_M}{4qb\alpha_o h_o} = -\left[\frac{1}{\left(\frac{h_o}{\alpha_o}\right)}\left(bI_{MP}'\right) + I_{MT}' \cos\theta - R_{MT}' \sin\theta\right]$$

If these coefficients are plotted against the ratio h_o/α_o for several values of θ at a given value of k, wherever C_{W_M} is equal to C_{W_L} at the same value of θ, there exists a point of zero work. Plotting θ against h_o/α_o for these points of zero work produces the curves shown in figure 18. Superimposed on the same plot are curves showing possible oscillator settings and the particular condition chosen for testing is marked with a large dot on the curve for $k = 0.3$ at $h_o/\alpha_o = 15$ and $\theta = 225^\circ$. The properties of the corresponding wing, as determined from the solution of all four equations of motion, are:

$$\frac{m}{\pi\rho b^3} \approx 14, \quad a \approx -0.26, \quad S_\alpha \approx 0.013, \quad \text{and} \quad \bar{x} - ab \approx 1.2 \text{ inches},$$

where $b = 5.75$ inches.

ANALYSIS OF RESULTS

General Discussion

A prime consideration throughout the entire program has been the desire to obtain really quantitative results, and a great deal of energy has been expended to this end. An arbitrary error limit of ±5 percent which was set early in the development program required that each component of the entire system have a predictable behavior within a few percent.

An examination of figures 6 to 17 reveals some clues as to how accurate the results actually are. Looking first at the pure motions in figures 6 to 10, it may be seen that especially for the smaller amplitudes the experimental points lie in narrow even bands. The width of these bands is an indication of the uncertainty of the measurements and can be attributed to items such as unevenness of air flow, small variations in airspeed, and difficulty in finding amplitudes and phase angles from the galvanometer traces. For the larger-amplitude pure motions the series of solid points do not necessarily fall in the same bands as the other points, undoubtedly because of the fact that they are derived from tests using the stiff set of force-measuring elements rather than the soft. Since these tests with the stiff elements were made some months after the other tests, a comparison of the results gives an indication of the consistency of the over-all apparatus. The moment phase-angle data in large-amplitude pitch, for example, show that while the inaccuracy or spread is consistent the averages of the two series differ by as much as 8°. Similar trends are evident in 2-inch-translation lift magnitude and moment phase angle. These differences probably arise from such sources as variations in accelerometer-signal amplitudes, carrier-voltage variations, and even improvements in technique and equipment.

A variation more difficult to account for is the apparent shift in the lift magnitude and phase angle in 1-inch translation at a reduced frequency of 0.2. This shift does not indicate some failure or sudden change in the mechanism or instruments because it is in the same place for each airspeed and the entire frequency range was covered for first one airspeed and then another. The static calibrations gave no clue and some preliminary tests for the 2-inch amplitude showed the same shift. A minor breakdown in the oscillator linkage at this point prevented further investigation and the trend was completely absent from subsequent tests.

A fact pertinent to this discussion is that, although phase angles are inherently difficult to measure on the records, they are not changed by variations in carrier voltage, element sensitivities, or calibrations and are thus in a sense surer to be right than magnitude measurements. The absolute magnitudes of the phase angles, however, are dependent on the accuracy of the reference-position indicator. For the earlier tests the output of the position accelerometer was badly obscured by natural-frequency hash as shown in figure 4, since it was necessarily an undamped accelerometer. The use of a Kollsman rotatable transformer eliminated the hash but introduced the problem of setting the transformer in phase with the oscillator. An unceasing effort was made to reduce the general hash level on the records, but little improvement could actually be achieved.

Pure Motions

Viewing the data with the reservations dictated by the previous discussion, several general trends are noticeable. The agreement between theory and experiment is remarkably good for phase angles with the possible exception of lift in 2-inch translation. The magnitudes of lift and moment are in close agreement for translation but show definite deviations from the theory in the case of pitch. For the smaller pitch amplitude the moment checks better than the lift while for the larger amplitude the reverse is true. In general, however, the deviations become more pronounced at the small values of reduced frequency. This trend is discussed further in the section Component Analysis.

Although the drag forces are very small compared with the lift, and the drag trace is sometimes almost totally obscured by hash, it was possible to obtain "average" values of the magnitude of the oscillating portion of the drag in the case of pure pitch. Since drag is positive for both positive and negative angles of attack and since there is a very slight tilt to the air stream in the test section, the drag trace appears as a displaced nonsinusoidal double-frequency curve with alternate peaks of slightly different amplitude. It is the average amplitude

of these peaks that leads to the coefficients plotted in figure 8. The most noticeable characteristic of these curves is the definite positive slope, especially for the larger-amplitude motion. A probable cause is an increased turbulence or breaking away of the flow at the higher reduced frequencies, which is not unreasonable when it is remembered that the airfoil is oscillating through a total amplitude of 27° at frequencies as high as 17 cycles per second.

When the pure motions are superimposed on an initial angle of attack, the magnitudes of the oscillatory components of lift and moment drop off noticeably although the phase angles still show good agreement with the theory. In the case of superimposed pitch, for instance, the moment magnitude is somewhat less than for the larger-amplitude pure-pitch case. It is interesting to note that although the records for these tests were not so clean and consistent as for previous tests, the uncertainty or spread of points is not noticeably worse.

Figure 14 contains the data for the components of lift and moment due to the initial angle. These values were obtained by measuring the displacement of the center line of the sinusoidal trace from the galvanometer zero position and for the range covered there appears to be no definite trend either up or down. Although the uncertainty of the points is usually small, there is definitely a greater possibility of error than in measurements on the oscillating portion of the traces because of the greater complexity of the record-analysis procedure for the component data. In all cases the points at zero reduced frequency are values obtained from the static coefficient tests.

Combined Motions

The combined-motion tests were run in two sections at two different times. The tests illustrated in figures 15 and 16 were run at a constant reduced frequency of 0.3 with the phasing between the pure motions as the variable, using the soft elements. The tests illustrated in figure 17 were run with the stiff elements at a later date, holding the phasing constant at 225° and varying the reduced frequency. In this way the flutter condition, at $k = 0.3$ and $\theta = 225°$ as found in the previous section, was approached from two directions with the hope that the experimental values at the common point would check. As can be seen by comparing figures 16 and 17 this is not the case, especially for moment. A thorough investigation of the possible sources of the error indicates that incorrect signals must have been coming from the multiple accelerometer at least for part of the range of phase variation in the case of lift in figure 16. The fact that the ratio of translation amplitude to pitch amplitude could not be kept constant as the phasings between the motions was varied hindered and complicated the search. The reason for

the considerable difference in the moment data could be adequately determined only by a repetition of the tests.

The above-mentioned discrepancies are damaging, however, only in a quantitative sense as the data are still valuable in showing that the trends predicted by the theory are, in general, correct. When the total work per cycle is calculated and plotted against k and θ in figure 19 (data in tables VIII through X) the points follow the theoretical curves in a remarkably consistent manner. Closer investigation yields the fact that at this flutter condition the work per cycle due to lift has a far more important contribution to the total than the work per cycle due to moment. Thus, since the work per cycle due to lift is the product of the imaginary component of the lift and translational velocity, it becomes apparent that the good agreement on the work done is readily possible in spite of the comparatively poor data in figures 16 and 17.

The three-dimensional plot in figure 20 (data in table XI) is an attempt to show graphically the variation in work per cycle at the amplitude ratio of the flutter condition. For any value of reduced frequency the variation is sinusoidal although the amplitude, phase, and mean value all change for different values of reduced frequency. Thus the theoretical curve of work per cycle against reduced frequency in figure 19 corresponds to the element of the surface at 225° in figure 20. The intersection of the surface with the zero work plane shows all possible flutter conditions at this amplitude ratio although they are not, of course, all for a wing of the same characteristics as assumed in this report.

Component Analysis

With the hope of gaining a better understanding of the factors which determine the aerodynamic reactions on a simple airfoil in two-dimensional flow, a study has been made of the magnitude and effect of each term in the theoretical equations.

Looking first at the equations given by Theodorsen in reference 1,

$$L = -\rho b^2(V\pi\dot{\alpha} + \pi\ddot{h} - \pi ba\ddot{\alpha}) - 2\pi\rho VbC\left[V\alpha + \dot{h} + b\left(\frac{1}{2} - a\right)\dot{\alpha}\right]$$

$$M = -\rho b^2\left[\pi\left(\frac{1}{2} - a\right)Vb\dot{\alpha} + \pi b^2\left(\frac{1}{8} + a^2\right)\ddot{\alpha} - a\pi b\ddot{h}\right] +$$

$$2\rho Vb^2\pi\left(a + \frac{1}{2}\right)C\left[V\alpha + \dot{h} + b\left(\frac{1}{2} - a\right)\dot{\alpha}\right]$$

it is simple to reduce these equations to the cases of pure translation and pure pitch.

$$L_T = -\pi\rho b^2\ddot{h} - 2\pi\rho bVC\left(\dot{h}\right)$$

$$L_P = \pi\rho b^3 a\ddot{\alpha} - \pi\rho b^2 V\dot{\alpha} - 2\pi\rho bVC\left[V\alpha + b\left(\frac{1}{2} - a\right)\dot{\alpha}\right]$$

$$M_T = \pi\rho b^3 a\ddot{h} + 2\pi\rho b^2 V\left(a + \frac{1}{2}\right)C\left(\dot{h}\right)$$

$$M_P = -\pi\rho b^4\left(\frac{1}{8} + a^2\right)\ddot{\alpha} - \pi\rho b^3 V\left(\frac{1}{2} - a\right)\dot{\alpha} +$$

$$2\pi\rho b^2 V\left(a + \frac{1}{2}\right)C\left[V\alpha + b\left(\frac{1}{2} - a\right)\dot{\alpha}\right]$$

The lift force L_T, for example, is made up of only two terms, of which the first is a pure inertia reaction term, and the second is a lift due to induced angle of attack modified by the wake according to Theodorsen's function $C = F + iG$. Similarly, L_P consists of an inertia reaction term proportional to angular acceleration, another type of acceleration term involving the product $V\dot{\alpha}$, and terms due to angle of attack and rate of change of angle of attack modified by the function C. The moment terms are quite similar to the lift terms except for the addition of various functions of a, a measure of elastic-axis position.

If the substitutions

$$h = h_o e^{i\omega t}$$

$$\alpha = \alpha_o e^{i\omega t}$$

are made and the reduced frequency $k = \omega b/V$ is introduced, the

equations become:

$$\frac{L_T}{4\pi q h_o} = \frac{k^2}{2} - ikC = B_{LT} + E_{LT}$$

$$\frac{L_P}{4\pi q b \alpha_o} = -\frac{ik}{2} - \frac{ak^2}{2} - C - ik\left(\frac{1}{2} - a\right)C = A_{LP} + B_{LP} + D_{LP} + E_{LP}$$

$$\frac{M_T}{4\pi q b h_o} = -\frac{ak^2}{2} + ik\left(\frac{1}{2} + a\right)C = B_{MT} + E_{MT}$$

$$\frac{M_P}{4\pi q b^2 \alpha_o} = -\frac{ik}{2}\left(\frac{1}{2} - a\right) + \frac{k^2}{2}\left(\frac{1}{8} + a^2\right) + \left(\frac{1}{2} + a\right)C + ik\left(\frac{1}{2} - a\right)\left(\frac{1}{2} + a\right)C$$

$$= A_{MP} + B_{MP} + D_{MP} + E_{MP}$$

Each of these individual terms has been plotted in figures 21 to 24 (data in tables XII through XIV) for an airfoil with elastic axis at 37-percent chord ($a = -0.26$). The total of each group of terms is marked 2-DIM (meaning two-dimensional).

Since tables of spanwise load distribution and modified C-function for an aspect ratio of six were readily available in reference 4 by Reissner and Stevens, an approximate correction has been calculated and applied to each two-dimensional theoretical curve and is marked 3-DIM. These three-dimensional corrections have been included in this analysis because absolutely perfect two-dimensional flow conditions did not exist during the tests. At all times there was a clearance between the edges of the wing and the vertical end plates of the order of 1/32 or 1/16 inch through which air could move from one surface to the other during the oscillations. The three-dimensional curves, then, indicate the direction and magnitude of a correction for an aspect ratio of six.

The dotted curves indicate the average of the experimental data for the smaller-amplitude pure motions. It is interesting to note that in the case of pitch the experimental curves fall between the two-dimensional and the three-dimensional curves and appear to correspond to an aspect ratio considerably higher than six. The inconsistent behavior of the experimental data for lift in translation may be attributed entirely to the shift in the curves shown on the upper part of figure 9. Far more consistent results would be obtained if the data for the 2-inch translation were plotted instead. For moment in pure translation the data plotted are consistently higher than even the two-dimensional

theoretical curve although the curve for the higher amplitude would be in far better agreement. The poorer data are plotted primarily for the purpose of gathering additional clues to the reasons for their trends.

Harmonic Analysis

An assumption which is rather easily checked from the experimental data is that the aerodynamic reactions on a wing are perfectly sinusoidal for sinusoidal motions.

During the course of the data analysis, periodic checks were made to be sure that the galvanometer traces were very nearly sinusoidal so that the measuring of amplitudes and phase angles was a valid procedure. Since a more careful check was desired, two typical larger-amplitude pure-motion records were carefully enlarged photographically and examined thoroughly. Pure-motion records were used because they are relatively free of hash and the traces are fairly large. Also the larger-amplitude records were more likely to deviate from perfect sinusoids than those for the smaller amplitude.

The results of the investigation were negative for both pitch and translation in that no deviations were found of an order greater than might have been caused by small variations in the oscillator motion or by slight nonlinearity of the instrumentation system.

CONCLUSIONS

The most general conclusion to be drawn from this analysis is that the experimental data corroborate the predictions of the theory over an important range of reduced frequency.

The component analysis indicates that two-dimensional conditions were not quite realized for the M.I.T. tests, although the effective aspect ratio was well above six. A reduction of the clearances between airfoil and vertical end plates would undoubtedly raise the effective aspect ratio to a very high value.

For pure motions the effects of amplitude and initial angle of attack appear to be small for reasonable amplitudes. If the stall range is approached, however, or if very small angles of attack are under consideration, very definite deviations from the theory must be expected.

The combined-motion tests indicate that, for the typical flutter condition chosen, the experimental and theoretical work-per-cycle conditions check very well. Unfortunately generalizations in a quantitative sense for the remaining combined-motion data are not justified because of the inconsistencies of some portions of the data. Qualitatively, the trends predicted by theory are followed quite accurately although the combined-motion field is so broad that the present test program only touched some of the high spots.

In the case of pure pitch there is an encouraging agreement between various independent groups of data. Tests made on wings of different dimensions and profiles in various types of wind tunnels and with entirely different measurement systems all seem to check quite well. Although several minor Reynolds number effects are noticeable the basic trend indicates that the agreement between theory and experiment becomes better as the Reynolds number is increased. Tests below a Reynolds number of 150,000 may actually give incorrect trends as well as poor quantitative data.

Massachusetts Institute of Technology
Cambridge, Mass., April 1, 1948

APPENDIX

SURVEY OF REFERENCE MATERIAL

An intensive search of available material yielded a considerable amount of experimental data compiled both in the United States and Europe dealing with the aerodynamic reactions resulting from pure pitch. Apparently no previous work of this type has been done on pure translation or true combined motions and none of the experimenters in pitch measured both lift and moment. Curiously, previous work in this country has been concerned only with lift in pure pitch while the British have made extensive measurements on moment in pure pitch. The material dealing with lift will be examined first, followed by the material concerning moment. A summary of airfoils used in the experiments described on the following pages appears in figure 25.

The first attempt in this country to corroborate the then new theory as put forth by Theodorsen was made in 1939 by Silverstein and Joyner (reference 5) who presented some experimental data on the lift phase angle in pure pitch. Their relatively long and narrow airfoil was driven at one end and supported by a cantilever beam at the other. Minute vertical deflections of the beam were amplified optically and recorded on film. The results demonstrate qualitative agreement with the theory but, when plotted against reduced frequency rather than its reciprocal, they show a very considerable spread above $k = 0.3$. The points which could be read from the published graph with a reasonable degree of accuracy are reproduced in figure 26.

The next known work was done by Vincenti under the supervision of Reid at Stanford University (reference 6). Measurements of both the magnitude and phase of the lift in pure pitch were made on a considerably larger wing (fig. 25) with an apparatus basically quite similar to that used by Silverstein and Joyner. Fairly good qualitative agreement for both magnitude and phase angle was obtained. Only the phase-angle results are reproduced in figure 26. Insufficient information was available in the published report to permit conversion of the magnitudes to the notation used in this report. As will be seen later, the poor quantitative results can be attributed largely to the low Reynolds numbers $R.N._{max} = 200{,}000$ at which the tests were performed.

After Vincenti's rather promising results were obtained a comprehensive program was undertaken by Reid (reference 7) using the same basic apparatus. As illustrated in figure 25, four different models were used which permitted various combinations of chord and elastic-axis position. Representative results are reproduced in figures 27 and 28, marked (i),

(data in tables XV and XVI) for an oscillation amplitude of 2.5° and for frequencies of 6.67 and 10 cycles per second for models A and B and models C and D, respectively. Since the range of reduced frequency was covered by varying the airspeed rather than the frequency, the Reynolds number decreases in inverse proportion to the reduced frequency.

In order to put these Stanford results on a basis directly comparable with the M.I.T. results for the purpose of a Reynolds number survey, the data have been slightly modified to correct for the differences in elastic-axis position. Thus for models A and C the correction is:

$$\frac{L}{4qb\alpha_o} = -\pi\left[\frac{1}{2}(-0.26 + 0.20)k^2 + ikC(0.26 - 0.20)\right]$$

$$= 0.0492k^2 - 0.1885ikC$$

and for B and D,

$$\frac{L}{4qb\alpha_o} = -0.2199k + 0.4398ikC$$

These corrected results are marked (c) and should be compared with the theoretical curves which are for $a = -0.26$.

In first presenting his results, Reid plotted the ratio of the magnitude of the oscillating lift to the magnitude of the lift under steady-state conditions at a corresponding amplitude. After noticing several apparent inconsistencies in the trends of his data, he discarded his previous assumption that identical stream-boundary effects occur under both steady and oscillating conditions. All of the oscillating lift magnitudes were then divided by the values corresponding to the infinite-aspect-ratio lift-curve slope for the NACA 0015 profile of 0.100 per degree. These revised calculations are the basis of the plots reproduced in this report. The conversion in nomenclature is simply:

$$R_{LP} - iI_{LP} = \alpha_o(-\pi A - i\pi B)$$

where A and B are the real and imaginary components of the lift magnitude as given by Reid. Actually, to provide a comparison with the theory of the same form as used with the other data in this report, the

Stanford lift magnitudes should be reduced by the ratio of 5.73 to 2π or almost 10 percent because of Reid's introduction of the lift-curve slope of 0.100. With this reduction the magnitudes would fall on or slightly below the theoretical curve and thus be quite consistent with the average M.I.T. results.

In general, the results obtained by Reid are in good agreement with the theory, both as to magnitude and phase angle, as long as the Reynolds number remains above at least 125,000. The effect of either amplitude or mean angle of oscillation appears to be negligible so long as the former is not too small and the angles of attack do not exceed the linear range of the steady-state lift curve. Serious deviations for an amplitude of $\pm 1^{\circ}$ indicate that the ratio of linear displacements of points on the airfoil to the transverse dimensions of the boundary layer may be important for very small amplitudes.

To provide a comparison between the Stanford data and those obtained at M.I.T., values of lift magnitude and phase angle for various reduced frequencies have been plotted against Reynolds number in figure 29 (data in tables XV through XVII). Trends for each value of reduced frequency are indicated by short curves for Stanford (S) and M.I.T. (M). The corresponding theoretical values are marked T. The agreement between trends is remarkably consistent. Quantitatively the check is also quite good for both magnitude and phase angle if the Stanford lift magnitudes are given the previously discussed 10-percent reduction.

The available data on British measurements of moment in pure pitch are contained principally in references 2 and 3. The apparatus used to obtain these data rotates the airfoil in the tunnel with one steel band and an identical airfoil outside of the tunnel with another steel band. The difference in the tensions of the two bands is a measure of the aerodynamic moment and operates a mechanical balance with a magnetostriction stress unit. The resultant electrical signal is photographed as it appears on the face of a cathode-ray oscilloscope.

The British are apparently primarily interested in the effect of initial angles of attack on the damping or imaginary part of the moment signal so that data at zero initial angle are not very plentiful. Quite a few tests on wings of finite aspect ratio were also made as well as with wings of different profiles.

Inasmuch as a complete airfoil was used as a moment-of-inertia balance, not only the structural moment of inertia was canceled out by the balancing procedure, but the effective moment of inertia of the air surrounding the airfoil as well. This term, $\frac{k^2}{2}\left(\frac{1}{8} + a^2\right)$ according to the theory, becomes quite appreciable at higher values of reduced

frequency and makes the comparison of the British and M.I.T. results rather difficult, especially in view of the almost certain inaccuracy of the theory at zero airspeed. A correction for one-half- and one-third-chord elastic-axis positions must also be made to permit comparison of the two sets of data. Thus the plots in figures 30 to 33 show the British data first simply converted to the method of presentation of this report (i) and second corrected for ideal air inertia and elastic-axis position (c). Theoretical curves are given for both conditions. In figure 30 and tables XV and XVIII the data from reference 2 show good phase-angle agreement with the theoretical, especially for the higher Reynolds numbers, but the magnitudes are somewhat too high. Figures 31 and 32 and tables XV and XIX from reference 3 are also for a half-chord axis and the curves show the same general trends. Because the flexibility of the airfoil was resulting in appreciable deflections of the center section under load, the data of figure 32 were taken with an additional center support for the airfoil as a check against the original data of figure 31. The surprisingly high moment magnitudes at zero reduced frequency in figure 31 "were obtained from static pitching-moment curves by integration over a complete cycle of incidence variation" (reference 3). The results for a third-chord axis in figure 33 and tables XV and XIX show similar trends although the agreement for both magnitude and phase is poorer than with the tests about the half-chord axis. It is interesting that the higher Reynolds number gives a somewhat better agreement with the theoretical predictions.

When the corrected British data are plotted with corresponding M.I.T. data against Reynolds number in figure 34, several definite trends may be noticed. The rate of change of moment magnitude with Reynolds number apparently increases markedly at the higher reduced frequencies for all three sets of data. For moment phase angle, however, the data from reference 2 (B_1) appear to be somewhat out of step with the remarkably consistent data from reference 3 (B_2) and M.I.T. (M).

REFERENCES

1. Theodorsen, Theodore: General Theory of Aerodynamic Instability and the Mechanism of Flutter. NACA Rep. 496, 1935.

2. Bratt, J. B., and Scruton, C.: Measurements of Pitching Moment Derivatives for an Aerofoil Oscillating about the Half-Chord Axis. R. & M. No. 1921, British A.R.C., Nov. 1938.

3. Bratt, J. B., and Wight, K. C.: The Effect of Mean Incidence, Amplitude of Oscillation, Profile and Aspect Ratio on Pitching Moment Derivatives. R. & M. No. 2064, British A.R.C., June 4, 1945.

4. Reissner, Eric, and Stevens, John E.: Effect of Finite Span on the Airload Distributions for Oscillating Wings. II - Methods of Calculation and Examples of Application. NACA TN 1195, 1947.

5. Silverstein, Abe, and Joyner, Upshur T.: Experimental Verification of the Theory of Oscillating Airfoils. NACA Rep. 673, 1939.

6. Reid, Elliott G., and Vincenti, Walter: An Experimental Determination of the Lift of an Oscillating Airfoil. Jour. Aero. Sci., vol. 8, no. 1, Nov. 1940, pp. 1-6.

7. Reid, Elliott G.: Experiments on the Lift of Airfoils in Non-Uniform Motion. Stanford Univ. Rep., July 23, 1942.

TABLE I

THEORETICAL VALUES OF MAGNITUDES AND PHASE ANGLES AGAINST REDUCED FREQUENCY FOR PURE MOTIONS

[Elastic axis, 37-percent chord; semichord b, 5.80 in.]

Pure translation, h = 1.00 in.				k	Pure pitch; α_o = 6.74°			
Lift		Moment			Lift		Moment	
$\sqrt{R_{LT}^2 + I_{LT}^2}$	ϕ_{LT}	$\sqrt{R_{MT}^2 + I_{MT}^2}$	ϕ_{MT}		$\sqrt{R_{LP}^2 + I_{LP}^2}$	ϕ_{LP}	$\sqrt{R_{MP}^2 + I_{MP}^2}$	ϕ_{MP}
0	270.00	0	90.00	0	0.3697	180.00	0.0887	360.00
.0054	267.48	.0013	86.87	.010	.3636	177.90	.0874	356.70
.0129	265.52	.0031	83.97	.025	.3542	176.60	.0854	353.52
.0202	264.10	.0049	81.54	.040	.3448	175.83	.0837	350.78
.0248	263.38	.0059	80.16	.050	.3389	175.56	.0827	349.17
.0293	262.80	.0071	78.90	.060	.3332	175.42	.0818	347.66
.0377	262.04	.0092	76.41	.080	.3224	175.50	.0802	344.94
.0455	261.64	.0112	74.78	.100	.3128	176.00	.0790	342.52
.0530	261.52	.0132	73.08	.120	.3266	176.76	.0781	340.30
.0667	261.96	.0168	70.22	.160	.2893	178.81	.0771	336.37
.0794	263.05	.0204	67.80	.200	.2779	181.68	.0770	332.93
.0912	264.56	.0239	65.65	.240	.2691	184.83	.0776	329.87
.1082	267.48	.0291	62.80	.300	.2606	190.00	.0795	325.88
.1191	269.66	.0327	61.03	.340	.2574	193.57	.0814	323.56
.1357	273.21	.0380	58.58	.400	.2559	198.97	.0850	320.55
.1469	275.68	.0418	57.03	.440	.2566	202.52	.0877	318.82
.1642	279.44	.0475	54.82	.500	.2600	207.67	.0923	316.57
.1825	283.19	.0536	52.70	.560	.2657	212.54	.0974	314.70
.1954	285.64	.0577	51.35	.600	.2705	215.62	.1010	313.65
.2159	289.27	.0644	49.42	.660	.2793	219.96	.1068	312.32
.2306	291.55	.0689	48.18	.700	.2860	222.64	.1109	311.60
.2697	297.10	.0811	45.22	.800	.3045	228.87	.1214	310.12
.3638	306.53	.1089	40.03	1.000	.3227	239.05	.1446	308.60
.4793	314.03	.1415	35.70	1.200	.3957	247.00	.1701	308.30
.6939	322.40	.2002	30.45	1.500	.4841	256.18	.2122	309.10
1.1626	331.43	.3249	24.20	2.000	.6379	267.32	.2921	311.40

TABLE II

EXPERIMENTAL VALUES OF MAGNITUDES AND PHASE ANGLES FOR

PURE PITCH; PITCH AMPLITUDE, 6.74°

[Elastic axis 37-percent chord; semichord b, 5.80 in.; initial angle α_i, 0°]

Record number	Velocity (mph)	k	Lift		Moment	
			$\sqrt{R_{LP}^2 + I_{LP}^2}$	ϕ_{LP}	$\sqrt{R_{MP}^2 + I_{MP}^2}$	ϕ_{MP}
1817	105.4	0.053	0.273	180	0.0755	351
1818	105.4	.060	.268	178	.0742	343
1819	105.4	.075	.268	180	.0742	349
1820	105.4	.079	.266	180	.0740	346
1822	105.4	.086	.268	184	.0704	352
1823	105.4	.094	.264	177	.0705	344
1824	105.4	.102	.260	174	.0696	338
1825	105.4	.115	.257	178	.0696	337
1827	105.4	.123	.251	180	.0738	341
1828	105.4	.134	.251	178	.0740	336
1829	105.4	.140	.249	178	.0742	334
1830	105.4	.149	.249	178	.0742	332
1832	105.4	.160	.249	182	.0725	337
1833	105.4	.168	.244	183	.0715	332
1834	105.4	.181	.242	180	.0763	333
1835	105.4	.148	.249	180	.0755	338
1837	93.2	.059	.268	178	.0773	351
1838	93.2	.070	.266	179	.0750	351
1839	93.2	.078	.263	182	.0704	351
1840	93.2	.087	.266	179	.0712	346
1842	93.2	.099	.256	180	.0707	348
1843	93.2	.109	.252	178	.0712	342
1844	93.2	.119	.256	176	.0718	339
1845	93.2	.127	.254	175	.0712	339
1847	93.2	.139	.254	180	.0751	343
1848	93.2	.151	.249	183	.0736	339
1849	93.2	.160	.249	180	.0752	337
1850	93.2	.170	.240	180	.0748	332
1852	93.2	.181	.245	183	.0774	332
1853	93.2	.195	.240	186	.0766	337
1854	93.2	.206	.240	186	.0802	336
1861	81.0	.113	.251	182	.0710	342
1862	81.0	.121	.248	184	.0718	342
1863	81.0	.134	.251	180	.0710	339
1864	81.0	.144	.248	181	.0700	335
1866	81.0	.157	.251	181	.0700	334
1867	81.0	.170	.247	184	.0718	338
1868	81.0	.180	.247	182	.0710	333
1869	81.0	.195	.244	183	.0700	333
1871	81.0	.208	.244	182	.0718	326
1872	81.0	.221	.244	187	.0718	330
1873	81.0	.234	.236	189	.0749	330

TABLE II

EXPERIMENTAL VALUES OF MAGNITUDES AND PHASE ANGLES FOR PURE PITCH; PITCH AMPLITUDE, 6.74° - Concluded

[Elastic axis, 37-percent chord; semichord b, 5.80 in.; initial angle α_i, 0°]

Record number	Velocity (mph)	k	Lift		Moment	
			$\sqrt{R_{LP}^2 + I_{LP}^2}$	ϕ_{LP}	$\sqrt{R_{MP}^2 + I_{MP}^2}$	ϕ_{MP}
1875	81.0	0.068-	0.274	Bad hash in position curve	0.0690	Bad hash in position curve
1876	81.0	.078	.270		.0690	
1877	81.0	.090	.270		.0690	
1878	81.0	.106	.284		.0690	
1879	105.4	.190	.240	182	.0704	332
1880	105.4	.196	.246	184	.0715	328
1881	105.4	.203	.244	182	.0715	336
1882	105.4	.213	.242	185	.0730	334
1884	105.4	.227	.234	185	.0725	332
1885	105.4	.238	.236	188	.0730	330
1886	105.4	.244	.232	188	.0765	330
1887	105.4	.244	.236	185	.0730	324
1889	105.4	.256	.238	185	.0730	324
1890	105.4	.262	.240	187	.0776	328
1891	105.4	.281	.240	186	------	326
1892	105.4	.283	.236	186	------	324
1896	105.4	.309	.249	187	------	321
1908	93.2	.216	.250	186	------	338
1909	93.2	.227	.238	187	.0739	328
1910	93.2	.236	.244	187	.0739	326
1911	93.2	.246	.241	187	.0749	324
1913	93.2	.257	.244	187	.0749	324
1914	93.2	.271	.238	188	.0763	324
1915	93.2	.278	.241	187	.0763	325
1916	93.2	.289	.241	187	.0784	324
1918	93.2	.300	.238	187	.0840	325
1919	93.2	.308	.238	187	.0840	320
1920	93.2	.304	.238	188	.0826	320
1921	93.2	.315	.233	189	.0784	323
1923	93.2	.344	.236	193	.0815	320
1924	93.2	.352	.238	194	.0810	323
1925	93.2	.374	.248	194	.0890	320
1928	81.0	.248	.244	188	.0753	329
1929	81.0	.257	.234	188	.0738	331
1930	81.0	.276	.239	188	.0753	329
1931	81.0	.283	.234	188	.0768	324
1933	81.0	.294	.239	190	.0768	329
1934	81.0	.308	.234	190	.0798	322
1935	81.0	.316	.243	190	.0814	318
1936	81.0	.330	.239	194	.0783	319
1938	81.0	.344	.243	194	.0753	318
1939	81.0	.358	.237	195	.0814	318
1940	81.0	.366	.239	195	.0814	317
1941	81.0	.374	.234	196	.0814	318
1943	81.0	.394	.243	197	.0844	319
1944	81.0	.410	.244	197	.0859	338
1945	81.0	.416	.243	197	------	344
1947	105.4	.330	.243	191	------	324
1948	105.4	.336	.240	191	------	319
1949	105.4	.341	.238	191	------	318
1950	105.4	.368	.243	192	------	321
1952	93.2	.373	.248	194	------	317
1953	93.2	.389	.238	199	------	320
1954	93.2	.389	.243	199	------	320
1955	93.2	.404	.248	200	.0895	325
1957	81.0	.426	.247	194	.0894	323
1958	81.0	.445	.247	195	.0911	318
1959	81.0	.445	.247	195	.0976	318
1960	81.0	.460	.264	199	.1020	320

TABLE III

EXPERIMENTAL VALUES OF MAGNITUDES AND PHASE ANGLES FOR

PURE PITCH; PITCH AMPLITUDE, 13.48°

[Elastic axis, 37-percent chord; semichord b, 5.80 in.; initial angle α_1, 0°]

Record number	Velocity (mph)	k	Lift		Moment	
			$\sqrt{R_{LP}^2 + I_{LP}^2}$	ϕ_{LP}	$\sqrt{R_{MP}^2 + I_{MP}^2}$	ϕ_{MP}
3060	80.2	0.147	0.502	178	0.134	334
3061	80.2	.137	.502	177	.135	336
3062	80.2	.128	.506	176	.136	337
3063	80.2	.115	.502	177	.134	339
3065	80.2	.204	.488	180	.139	327
3066	80.2	.186	.488	179	.140	329
3067	80.2	.172	.498	179	.139	334
3068	80.2	.168	.495	176	.140	333
3070	80.2	.250	.497	181	.132	324
3071	80.2	.238	.497	182	.132	324
3072	80.2	.222	.504	181	.130	326
3073	80.2	.208	.504	180	.132	330
3075	80.3	.286	.509	186	.130	323
3076	80.3	.271	.504	182	.132	325
3077	80.3	.255	.493	184	.130	324
3105	91.5	.130	.494	178	.135	337
3106	91.5	.121	.510	178	.138	337
3107	91.6	.106	.510	177	.134	340
3109	91.7	.174	.497	181	.135	335
3110	91.7	.161	.494	181	.135	335
3111	91.7	.150	.494	180	.135	336
3112	91.7	.140	.502	179	.138	338
3120	91.7	.212	.481	182	.134	329
3121	91.7	.207	.481	183	.130	330
3122	91.7	.191	.488	179	.134	331
3123	91.7	.183	.500	176	.134	330
3125	91.8	.245	.488	179	.135	320
3126	91.8	.237	.488	179	.135	321
3127	91.8	.230	.481	183	.138	324
3129	103.6	.116	.509	173	.130	335
3130	103.6	.104	.509	172	.132	338
3131	103.6	.097	.499	171	.132	337
3133	103.7	.154	.504	174	.130	331
3134	103.7	.144	.509	175	.133	333
3135	103.7	.132	.504	172	.130	332
3136	103.7	.124	.499	175	.133	336
3138	103.8	.186	.505	175	.130	325
3139	103.8	.180	.499	174	.129	326
3140	103.8	.173	.495	173	.130	327
3141	103.8	.160	.499	173	.133	328
3143	103.9	.220	.495	174	.140	324
3144	103.9	.210	.490	174	.140	324
3145	103.9	.200	.490	175	.138	328
3682	91.5	.302	.512	182	.127	321
3683	91.5	.300	.500	187	.127	327
3684	91.5	.287	.500	184	.131	331
3685	91.5	.275	.512	184	.132	326
3687	91.7	.266	.496	186	.127	329
3688	91.7	.248	.515	184	.129	333
3689	91.7	.240	.492	185	.129	335
3690	91.7	.226	.505	189	.131	335
3699	91.8	.212	.505	187	.129	339
3700	91.8	.205	.500	182	.127	331
3701	91.8	.194	.505	186	.126	336
3702	91.8	.181	.520	188	.132	341
3703	92.0	.175	.515	182	.129	338
3704	92.0	.158	.520	185	.137	340
3705	92.0	.153	.524	184	.136	341
3706	92.0	.141	.527	183	.132	343
3708	92.0	.218	.515	182	.134	335
3709	92.0	.205	.512	183	.129	331
3710	92.0	.203	.512	185	.131	332
3711	92.0	.181	.520	183	.129	335
3713	91.7	.322	.496	184	.129	316
3714	91.7	.322	.496	184	.131	317
3715	91.7	.317	.512	181	.136	322
3717	91.7	.383	.500	191	.134	317
3718	91.7	.369	.500	192	.138	318
3719	91.7	.353	.492	186	.138	318
3720	91.7	.338	.500	186	.131	318

TABLE IV

EXPERIMENTAL VALUES OF MAGNITUDES AND PHASE ANGLES FOR PURE TRANSLATION; TRANSLATION AMPLITUDE, 1.00 INCH

[Elastic axis, 37-percent chord; semichord b, 5.80 in.; initial angle α_i, 0°]

Record number	Velocity (mph)	k	Lift		Moment	
			$\sqrt{R_{LT}^2 + I_{LT}^2}$	ϕ_{LT}	$\sqrt{R_{MT}^2 + I_{MT}^2}$	ϕ_{MT}
2004	105.4	0.307	0.1224	256	0.0370	56
2005	105.4	.305	.1224	252	.0283	58
2006	105.4	.300	.1260	258	.0324	60
2007	105.4	.280	.1154	253	.0310	61
2009	105.4	.274	.1214	256	.0354	64
2010	105.4	.261	.1127	257	.0338	60
2011	105.4	.253	.1025	255	.0318	61
2014	105.4	.235	.0880	254	.0203	60
2015	105.4	.228	.0798	254	.0242	64
2016	105.4	.218	.0783	258	.0256	68
2017	105.4	.208	.0708	258	.0228	68
2019	105.4	.201	.0671	260	.0208	64
2020	105.4	.189	.0701	262	.0212	65
2021	105.4	.182	.0656	262	.0201	64
2022	105.4	.171	.0587	259	.0196	65
2024	105.4	.160	.0553	261	.0181	68
2025	105.4	.153	.0514	266	.0181	73
2026	105.4	.143	.0493	267	.0161	74
2027	105.4	.133	.0471	265	.0150	74
2028	105.4	.121	.0424	263	.0142	68
2029	105.4	.114	.0397	261	.0126	70
2030	105.4	.104	.0397	261	.0132	68
2031	105.4	.094	.0354	261	.0118	73
2035	105.4	.088	.0357	264	.0113	72
2036	105.4	.082	.0323	264	.0105	73
2037	105.4	.071	.0289	267	.0091	73
2042	93.2	.363	.1340	262	.0396	64
2043	93.2	.350	.1253	260	.0364	62
2044	93.2	.340	.1295	261	.0342	64
2046	93.2	.324	.1253	260	.0342	56
2048	93.2	.313	.1077	255	.0345	57
2049	93.2	.298	.1160	257	.0328	63
2050	93.2	.294	.1133	258	.0295	62
2051	93.2	.279	.1078	255	.0290	62
2053	93.2	.267	.1040	254	.0299	64
2054	93.2	.258	.1040	254	.0285	63
2055	93.2	.246	.1031	257	.0258	65
2056	93.2	.239	.0952	255	.0262	61
2058	93.2	.224	.0979	255	.0267	64
2059	93.2	.216	.0946	256	.0252	66
2060	93.2	.203	.0899	255	.0238	64
2061	93.2	.197	.0850	261	.0239	67
2063	93.2	.186	.0629	265	.0224	70
2064	93.2	.173	.0610	262	.0197	66
2065	93.2	.160	.0581		.0185	
2066	93.2	.149	.0562		.0167	
2068	93.2	.139	.0500	bad	.0158	bad
2069	93.2	.128	.0455	posi-	.0151	posi-
2070	93.2	.118	.0408	tion	.0143	tion
2071	93.2	.110	.0374	curve	.0126	curve
2074	93.2	.097	.0362		.0125	
2075	93.2	.089	.0362		.0121	
2076	93.2	.081	.0307	264	.0105	68
2077	93.2	.072	.0286	272	.0098	76
2102	81.0	.274	.1018	254	.0254	59
2104	81.0	.266	.1050	251	.0261	59
2105	81.0	.255	.1069	256	.0258	63
2106	81.0	.250	.1029	260	.0254	66
2107	81.0	.228	.0942	261	.0245	64
2110	81.0	.213	.0760	257	.0242	66
2111	81.0	.199	.0735	bad posi-	.0234	bad posi-
2112	81.0	.187	.0635	tion curve	.0198	tion curve
2113	81.0	.174	.0561	258	.0191	66
2115	81.0	.159	.0578	259	.0198	65
2116	81.0	.152	.0534	262	.0179	62
2117	81.0	.133	.0455	262	.0172	66
2118	81.0	.126	.0437	259	.0146	70
2120	81.0	.111	.0430	264	.0131	76
2121	81.0	.104	.0401	264	.0123	70
2122	81.0	.092	.0367	264	.0112	69
2123	81.0	.079	.0322	265	.0103	73
2124	81.0	.069	.0299	261	.0088	69
2038	105.4	.062	.0241	271	.0081	75
2039	105.4	.055	.0202	272	.0074	74
2094	81.0	.370	.140	263	.0414	54
2095	81.0	.343	.140	254	.0388	58
2096	81.0	.332	.132	254	.0402	58
2097	81.0	.324	.121	255	.0371	58
2099	81.0	.314	.132	255	.0417	60
2100	81.0	.300	.123	255	.0385	58
2101	81.0	.284	.112	253	.0321	59

TABLE V

EXPERIMENTAL VALUES OF MAGNITUDES AND PHASE ANGLES FOR PURE TRANSLATION; TRANSLATION AMPLITUDE, 2.00 INCH

[Elastic axis, 37-percent chord; semichord b, 5.80 in.; initial angle α_i, 0°]

Record number	Velocity (mph)	k	Lift		Moment	
			$\sqrt{R_{LT}^2 + I_{LT}^2}$	ϕ_{LT}	$\sqrt{R_{MT}^2 + I_{MT}^2}$	ϕ_{MT}
3457	103.0	0.166	0.119	268	0.0316	66
3458	103.0	.155	.114	269	.0310	70
3459	103.0	.143	.105	270	.0295	68
3460	103.1	.134	.102	271	.0299	70
3462	103.2	.124	.0914	272	.0253	68
3463	103.2	.114	.0849	271	.0243	69
3464	103.2	.105	.0829	271	.0232	69
3465	103.2	.099	.0746	272	.0214	73
3466	103.2	.086	.0643	272	.0190	73
3477	91.7	.179	.124	272	.0358	65
3478	91.7	.172	.124	271	.0351	70
3479	91.7	.155	.117	270	.0320	67
3480	91.7	.153	.111	269	.0317	67
3482	91.7	.137	.0966	272	.0281	69
3483	91.7	.128	.0919	274	.0258	71
3484	91.7	.120	.0848	274	.0253	73
3485	91.7	.109	.0813	275	.0238	70
3486	91.7	.097	.0742	275	.0211	71
3488	80.2	.208	.149	277	.0402	64
3489	80.2	.200	.142	276	.0388	66
3490	80.2	.183	.135	272	.0366	65
3491	80.2	.169	.121	272	.0339	69
3493	103.2	.210	.151	273	.0402	64
3495	103.2	.199	.143	273	.0392	64
3497	91.7	.242	.170	275	.0453	62
3498	91.7	.226	.163	278	.0418	64
3500	80.2	.273	.191	282	.0505	60
3501	80.2	.264	.177	281	.0486	59
Stiff Elements						
3659	91.4	0.166	0.136	272	0.0348	79
3660	91.4	.162	.134	270	.0336	77
3661	91.4	.153	.124	267	.0325	75
3662	91.4	.144	.124	272	.0310	77
3665	91.5	.216	.167	267	.0434	69
3666	91.5	.208	.165	267	.0408	72
3667	91.5	.199	.157	271	.0408	81
3668	91.5	.191	.148	273	.0382	83
3672	91.6	.259	.202	266	.0507	71
3673	91.6	.248	.192	273	.0483	75
3674	91.6	.242	.186	271	.0488	69
3675	91.6	.229	.178	269	.0467	72
3678	91.7	.299	.230	273	.0566	74
3679	91.7	.280	.215	263	.0546	70
3680	91.7	.270	.207	266	.0521	66
3722	92.0	.309	.228	262	.0625	51
3723	92.0	.298	.216	262	.0566	61

TABLE VI

EXPERIMENTAL VALUES OF MAGNITUDES AND PHASE ANGLES FOR PURE PITCH ABOUT AN INITIAL ANGLE; PITCH AMPLITUDE, 6.74°

[Elastic axis, 37-percent chord; semichord b, 5.80 in.; initial angle α_i, 6.10°]

Record number	Velocity (mph)	k	Lift			Moment		
			$\sqrt{R_{LP}^2 + I_{LP}^2}$	ϕ_{LP}	$C_L(\alpha_i)$	$\sqrt{R_{MP}^2 + I_{MP}^2}$	ϕ_{MP}	$C_M(\alpha_i)$
3196	91.8	0.282	0.233	193	0.485	0.064	332	0.072
3197	91.8	.266	.233	189	.466	.066	327	.073
3198	91.8	.254	.230	185	.441	.065	326	.071
3199	91.8	.243	.230	189	.451	.067	329	.076
3202	91.9	.230	.243	186	.465	.065	329	.072
3203	91.9	.217	.238	187	.462	.065	329	.069
3204	91.9	.205	.242	185	.469	.066	336	.065
3205	92.0	.198	.240	185	.480	.064	336	.067
3208	92.0	.188	.240	189	.458	.062	333	.065
3209	92.0	.177	.240	190	.465	.063	337	.070
3210	92.0	.168	.238	187	.454	.064	338	.065
3211	92.1	.156	.240	185	.458	.063	343	.070
3215	92.1	.139	.238	183	.462	.062	341	.066
3216	92.1	.134	.236	187	.458	.063	345	.064
3217	92.1	.122	.236	183	.458	.060	345	.064
3218	92.1	.110	.236	179	.450	.061	343	.061
3219	92.2	.102	.246	182	.458	.064	345	.062
3234	80.0	.296	.248	193	.465	.069	326	.066
3235	80.0	.289	.246	191	.469	.063	320	.060
3236	80.0	.277	.244	191	.471	.062	326	.064
3239	80.1	.268	.241	188	.448	.061	332	.067
3240	80.1	.248	.236	187	.462	.060	327	.063
3241	80.1	.250	.237	195	.459	.059	335	.067
3245	80.2	.215	.234	189	.459	.060	336	.068
3246	80.2	.202	.233	186	.456	.062	328	.065
3248	80.2	.175	.233	188	.456	.060	340	.068
3255	80.2	.167	.234	186	.466	.064	335	.070
3256	80.2	.153	.233	182	.456	.064	339	.073
3257	80.2	.141	.234	182	.453	.062	339	.070
3258	80.2	.134	.234	184	.440	.062	346	.068
3259	80.2	.115	.234	184	.434	.062	349	.068

TABLE VII

EXPERIMENTAL VALUES OF MAGNITUDES AND PHASE ANGLES FOR PURE TRANSLATION ABOUT AN INITIAL ANGLE; TRANSLATION AMPLITUDE, 1.00 INCH

[Elastic axis, 37-percent chord; semichord b, 5.80 in.; initial angle α_i, 6.10°]

Record number	Velocity (mph)	k	Lift			Moment		
			$\sqrt{R_{LT}^2 + I_{LT}^2}$	ϕ_{LT}	$C_L(\alpha_i)$	$\sqrt{R_{MT}^2 + I_{MT}^2}$	ϕ_{MT}	$C_M(\alpha_i)$
3273	91.3	0.270	0.0905	270	0.46	0.0170	64	0.073
3274	91.3	.267	.0905	264	.46	.0178	58	.074
3275	91.3	.258	.0850	262	.46	.0157	58	.074
3276	91.3	.233	.0815	267	.46	.0149	57	.074
3279	91.3	.229	.0795	262	.47	.0137	68	.074
3280	91.3	.216	.0757	267	.47	.0137	68	.074
3281	91.3	.204	.0721	264	.49	.0135	68	.074
3282	91.3	.197	.0695	259	.48	.0125	64	.075
3285	91.4	.181	.0587	259	.47	.0117	64	.073
3286	91.4	.176	.0614	261	.48	.0113	64	.073
3287	91.4	.164	.0568	259	.48	.0105	63	.073
3288	91.4	.151	.0517	261	.48	.0101	70	.075
3291	91.4	.144	.0486	263		.0095	64	
3292	91.4	.131	.0430	265		.0081	71	
3293	91.4	.125	.0418	261		.0081	72	
3294	91.4	.113	.0357	262		.0068	72	
3295	91.4	.098	.0320	259		.0061	67	
3302	79.9	.312	.1050	272	.43	.0203	66	.072
3303	79.9	.302	.1050	272	.43	.0171	57	.072
3304	79.9	.291	.0973	269	.42	.0186	64	.071
3305	79.9	.276	.0924	271	.44	.0186	62	.071
3308	79.9	.265	.0895	268	.47	.0172	65	.074
3309	79.9	.248	.0848	265	.47	.0156	63	.073
3310	79.9	.238	.0848	265	.46	.0158	60	.073
3311	79.9	.232	.0796	266	.47	.0140	60	.073
3314	79.9	.211	.0730	262	.48	.0128	64	.074
3315	79.9	.204	.0715	267	.48	.0134	62	.074
3316	79.9	.188	.0644	261	.51	.0118	61	.073
3317	79.9	.178	.0600	266	.47	.0116	64	.073
3324	82.8	.159	.0540	263	.45	.0119	Hash bad	.075
3325	82.9	.143	.0530	263	.47	.0094	---do---	.075
3326	82.9	.131	.0452	260	.46	.0103	---do---	.074
3327	82.9	.122	.0443	258	.46	.0093	---do---	.074
3328	83.0	.110	.0428	261	.46	.0085	---do---	.075

TABLE VIII

THEORETICAL VALUES OF MAGNITUDES, PHASE ANGLES, AND NET WORK PER CYCLE FOR COMBINED MOTIONS

[Elastic axis 37-percent chord; semichord b, 5.80 in.; initial angle α_i, 0°]

k	Motion phase angle, θ (deg)	Translation amplitude, h_o (in.)	Pitch amplitude, α_o (deg)	Lift		Moment		Net work cycle (in.-lb)
				$\sqrt{R_{LR}^2 + I_{LR}^2}$	ϕ_{LR}	$\sqrt{R_{MR}^2 + I_{MR}^2}$	ϕ_{MR}	
Variable reduced frequency								
0	225.10	1.37	5.19	0.2854	45.10	0.0685	225.10	-53.045
.050	225.10	1.37	5.19	.2376	35.08	.0584	208.45	-34.157
.100	225.10	1.37	5.19	.1979	29.15	.0518	194.88	-22.644
.200	225.10	1.37	5.19	.1418	19.50	.0465	170.35	-8.600
.240	225.10	1.37	5.19	.1263	15.38	.0466	161.57	-4.605
.300	225.10	1.37	5.19	.1097	8.22	.0484	150.07	.601
.340	225.10	1.37	5.19	.1026	2.97	.0502	143.23	3.595
.400	225.10	1.37	5.19	.0975	354.45	.0539	134.28	7.878
.440	225.10	1.37	5.19	.0966	349.6	.0565	129.8	
.500	225.10	1.37	5.19	.1009	342.2	.0612	123.2	
.560	225.10	1.37	5.19	.1098	336.5	.0661	117.4	
.600	225.10	1.37	5.19	.1181	333.7	.0695	114.0	
Variable translation amplitude, pitch amplitude, and motion phase angle								
0.300	0	1.5000	3.37	0.2310	233.64	0.0566	16.72	52.392
.300	90	1.4142	9.53	.5203	276.13	.1540	57.35	155.298
.300	180	.5000	10.11	.3829	2.02	.1216	139.07	13.868
.300	270	1.4142	9.53	.2212	108.97	.0712	233.08	-67.457
.300	0	.5000	10.11	.4070	197.50	.1121	333.07	22.244
.300	180	1.5000	3.37	.1850	310.40	.0620	100.81	44.400
.300	219.2	1.4295	4.56	.1094	348.23	.0460	276.98	10.127
.300	233.2	1.1100	7.53	.1875	48.08	.0564	307.43	-23.095
.300	232.6	1.0271	8.10	.2165	50.25	.0762	183.11	-23.639
.300	232.1	.9956	8.28	.2267	50.47	.0788	183.45	-23.826
.300	231.7	.9636	8.45	.2364	50.75	.0816	183.92	-23.870
.300	230.9	.9313	8.61	.2463	50.45	.0841	183.81	-23.553
.300	230.1	.8987	8.77	.2558	50.12	.0868	183.68	-23.088
.300	229.1	.8660	8.92	.2653	49.51	.0894	183.35	-22.366
.300	219.1	.6756	9.64	.3182	40.92	.1039	139.10	14.287

NACA

TABLE IX

EXPERIMENTAL VALUES OF MAGNITUDES, PHASE ANGLES, AND NET WORK PER CYCLE FOR COMBINED MOTIONS; VARIABLE TRANSLATION AMPLITUDE, PITCH AMPLITUDE, AND MOTION PHASE ANGLE

[Elastic axis, 37-percent chord; semichord b, 5.80 in.; initial angle α_i, 0°; reduced frequency k, 0.30]

Record number	Velocity (mph)	Translation amplitude, h_o (in.)	Pitch amplitude, α_o (deg)	Motion phase angle, θ (deg)	Lift		Moment		Net work cycle (in.-lb)
					$\sqrt{R_{LR}^2 + I_{LR}^2}$	ϕ_{LR}	$\sqrt{R_{MR}^2 + I_{MR}^2}$	ϕ_{MR}	
3633	80.0	1.50	3.37	0	0.227	231	0.0785	24	
3647	80.0	1.41	9.53	90	.512	270	.142	49	
3645	79.8	1.41	9.53	270	.186	102	.0420	254	
3635	80.0	.50	10.11	0	----	198	.100	338	
3360	79.2	1.50	3.37	180.0	.246	331	.0687	125	37.90
3378	79.2	1.43	4.56	219.2	.192	354	.0699	163	10.62
3380	80.0	1.11	7.53	233.2	.203	30	.0976	196	-12.97
3382	80.0	1.03	8.10	232.6	.230	45	.102	201	-23.50
3384	79.7	1.00	8.28	232.1	.236	46	.109	197	-22.27
3386	79.8	.96	8.45	231.7	.241	41	.117	192	-16.22
3401	79.9	.93	8.61	230.9	.240	45	.112	199	-20.11
3403	79.9	.90	8.77	230.1	.251	39	.114	197	-16.63
3406	79.9	.87	8.92	229.1	.257	48	.117	198	-16.26
3408	80.0	.68	9.64	219.1	.315	41	.134	187	-13.14
3410	80.0	.50	10.11	180.0	.367	3	.148	155	10.43

TABLE X

EXPERIMENTAL VALUES OF MAGNITUDES, PHASE ANGLES, AND NET WORK PER CYCLE FOR COMBINED MOTIONS; VARIABLE REDUCED FREQUENCY

[Elastic axis, 37-percent chord; semichord b, 5.80 in.; translation amplitude h_o, 1.37 in.; pitch amplitude α_o, ±5.19°; initial angle α_i, 0°; motion phase angle θ, 225.10°]

Record number	Velocity (mph)	k	Lift		Moment		Net work cycle (in.-lb)
			$\sqrt{R_{LR}^2 + I_{LR}^2}$	ϕ_{LR}	$\sqrt{R_{RM}^2 + I_{RM}^2}$	ϕ_{RM}	
3569	80.0	0.379	0.095	0	0.0378	120	3.635
3570	80.0	.365	.095	355	.0369	98	4.907
3571	80.0	.350	.095	356	.0326	125	4.638
3572	80.0	.342	.102	356	.0370	125	5.929
3574	80.0	.330	.104	2	.0292	125	1.895
3575	80.0	.316	.104	12	.0280	112	-3.149
3576	80.0	.302	.104	8	.0292	110	-1.201
3595	80.0	.326	.104	6	.0280	109	-.390
3596	80.0	.312	.099	3	.0356	111	1.872
3597	80.0	.300	.104	17	.0356	123	-4.544
3598	80.0	.288	.109	5	.0292	132	.392
3600	80.0	.280	.107	14	.0304	95	-4.560
3601	80.0	.265	.111	15	.0304	137	-4.556
3602	80.0	.251	.118	12	.0321	152	-3.425
3603	80.0	.236	.114	15	.0330	160	-4.849
3605	80.0	.224	.127	21	.0347	156	-8.792
3606	80.0	.213	.132	18	.0330	172	-8.160
3607	80.0	.203	.140	19	.0408	168	-8.596
3608	80.0	.189	.142	22	.0391	179	-11.274
3609	80.0	.174	.142	20	.0391	176	-9.917
3610	80.0	.162	.152	26	.0451	184	-14.684
3612	80.0	.291	.110	11	.0356	138	-1.791
3613	80.0	.288	.112	16	.0330	139	-4.848
3614	80.0	.267	.112	16	.0330	140	-4.854
3615	80.0	.253	.117	15	.0321	156	-5.003
3617	80.0	.338	.097	8	.0344	118	.222
3618	80.0	.328	.097	13	.0343	138	-2.315
3619	80.0	.314	.097	9	.0343	132	-.574
3620	80.0	.297	.101	6	.0331	121	.419
3622	80.0	.349	.099	11			
3623	80.0	.370	.104	359			
3624	80.0	.370	.099	3			

TABLE XI

WORK-PER-CYCLE COEFFICIENT - THEORETICAL VALUES

[Elastic axis, 37-percent chord; semichord b, 5.80 in.; translation amplitude h_o, 1.37 in.; pitch amplitude α_o, $\pm 5.19^\circ$; amplitude ratio $\frac{h_o}{\alpha_o}$, 15; $C_W = C_{W_M} - C_{W_L} = \frac{W_N}{4qb\alpha_o h_o}$]

θ (deg)	k = 0	k = 0.10	k = 0.20	k = 0.30	k = 0.40	k = 0.50
0	0	0.5114	1.2661	2.0140	2.7432	3.4566
30	1.5708	1.8787	2.4738	3.1118	3.7592	4.4071
60	2.7206	2.9460	3.3688	3.8527	4.3640	4.8883
90	3.1416	3.4277	3.7113	4.0384	4.3957	4.7716
120	2.7206	3.1944	3.4094	3.6189	3.8456	4.0879
150	1.5708	2.3089	2.5442	2.7068	2.8614	3.0209
180	0	1.0082	1.3473	1.5464	1.7064	1.8560
210	-1.5708	-.3591	.1396	.4486	.6904	.9055
240	-2.7206	-1.4264	-.7554	-.2923	.0856	.4243
270	-3.1416	-1.9081	-1.0979	-.4780	.0539	.5410
300	-2.7206	-1.6748	-.7960	-.0585	.6040	1.2247
330	-1.5708	-.7893	.0692	.8536	1.5882	2.2917
360	0	.5114	1.2661	2.0140	2.7432	3.4566

TABLE XII

COMPONENT ANALYSIS - THEORETICAL VALUES FOR LIFT AND MOMENT IN PURE TRANSLATION

Lift in pure translation

k	B_{LT}	E_{LT}	$L_T/4\pi qh_o = B_{LT} + E_{LT}$
0	0	0 + 0i	0 + 0i
.05	.00125	-0.00653 - 0.04545i	-0.00528 - 0.04545i
.10	.0050	-.01723 - 0.0832i	-.01223 - 0.0832i
.20	.0200	-.03732 - 0.14552i	-.01732 - 0.14552i
.30	.0450	-.05379 - 0.1995i	-.00879 - 0.1995i
.40	.0800	-.066 - 0.2500i	.01400 - 0.2500i
.50	.1250	-.07535 - 0.29895i	.04965 - 0.29895i
.60	.1800	-.08268 - 0.34728i	.09732 - 0.34728i
.80	.3200	-.0932 - 0.44328i	.2268 - 0.44328i
1.00	.5000	-.1003 - 0.5394i	.3997 - 0.5394i

k	Av. 3-DIM $L_T/4\pi qh_o$ (1)
0	0 + 0i
.167	-0.004105 - 0.1023i
.333	.01114 - 0.18414i
.667	.13136 - 0.33582i

k	3-DIM	
	Magnitude	Phase (deg)
0	0	270
.167	.1023	267.7
.333	.1845	273.5
.667	.3606	291.5

Moment in pure translation

k	B_{MT}	E_{MT}	$M_T/4\pi qbh_o = B_{MT} + E_{MT}$
0	0	0 + 0i	0 + 0i
.05	.000325	0.001567 + 0.01091i	0.001892 + 0.01091i
.10	.00130	.00414 + 0.01997i	.005435 + 0.019968i
.20	.0052	.00896 + 0.3492i	.014157 + 0.03492i
.30	.0117	.01291 + 0.04788i	.02461 + 0.4788i
.40	.0208	.01584 + 0.06000i	..03664 + 0.0600i
.50	.0325	.01808 + 0.07175i	.05058 + 0.07175i
.60	.0468	.01984 + 0.08335i	.06664 + 0.08335i
.80	.0832	.02237 + 0.10639i	.10557 + 0.10639i
1.00	.1300	.02407 + 0.12946i	.15407 + 0.12946i

k	Av. 3-DIM $M_T/4\pi qbh_o$ (1)
0	0 + 0i
.167	0.00788 + 0.0245i
.333	.0251 + 0.0442i
.667	.07964 + 0.08064i

k	3-DIM	
	Magnitude	Phase (deg)
0	0	90
.167	.0257	72.1
.333	.05082	60.4
.667	.11335	45.2

[1]Average along span, A.R. = 6.

TABLE XIII

COMPONENT ANALYSIS - THEORETICAL VALUES FOR LIFT AND MOMENT IN PURE PITCH

Lift in pure pitch

k	A_{LP}	B_{LP}	D_{LP}	E_{LP}	$\frac{L_P}{4qb\alpha_o\pi}$
0	0	0	-1.0000 + 0.0000i	-0 - 0.0000i	-1.0000 + 0i
.05	-.025i	.000325	-.9090 + 0.1305i	-.0050 - 0.0345i	-.9137 + 0.0710i
.10	-.050i	.0013	-.8320 + 0.1723i	-.0131 - 0.0632i	-.8438 + 0.0591i
.20	-.100i	.0052	-.7276 + 0.1886i	-.0287 - 0.1106i	-.7511 + 0.0220i
.30	-.150i	.0117	-.6650 + 0.1793i	-.0409 - 0.1516i	-.6942 - 0.1223i
.40	-.200i	.0208	-.6250 + 0.1650i	-.0502 - 0.1900i	-.6544 - 0.2250i
.50	-.250i	.0325	-.5979 + 0.1507i	-.0573 - 0.2272i	-.6277 - 0.3265i
.60	-.300i	.0468	-.5788 + 0.1378i	-.0628 - 0.2639i	-.5948 - 0.4261i
.80	-.400i	.0832	-.5541 + 0.1165i	-.0708 - 0.3369i	-.5417 - 0.6204i
1.00	-.500i	.1300	-.5394 + 0.1003i	-.0762 - 0.4099i	-.4856 - 0.8096i

k	Av. 3-DIM $\frac{L_P}{4qb\alpha_o\pi}$ (1)
0	-0.6797 + 0i
.167	-.6234 - 0.0533i
.333	-.5298 - 0.1828i
.667	-.5148 - 0.4521i

k	3-DIM	
	Magnitude	Phase (deg)
0	0.6797	180
.167	.6256	184.9
.333	.5605	199.0
.667	.6851	221.3

Moment in pure pitch

k	A_{MP}	B_{MP}	D_{MP}	E_{MP}	$\frac{M_P}{4qb^2\alpha_o\pi}$
0	0.0000i	0.	0.2400 - 0.0i	0 + 0.0000i	0.2400 + 0i
.05	-.0190i	.0002	.2182 - 0.0313i	.0012 + 0.0083i	.2196 - 0.0420i
.10	-.0380i	.0010	.1997 - 0.0414i	.0031 + 0.0152i	.2038 - 0.0642i
.20	-.0760i	.0039	.1746 - 0.0453i	.0069 + 0.0265i	.1854 - 0.0948i
.30	-.1140i	.0087	.1596 - 0.0430i	.0098 + 0.0364i	.1781 - 0.1206i
.40	-.1520i	.0154	.1500 - 0.0396i	.0120 + 0.0456i	.1774 - 0.1460i
.50	-.1900i	.0241	.1435 - 0.0362i	.0138 + 0.0545i	.1814 - 0.1717i
.60	-.2280i	.0347	.1389 - 0.0331i	.0151 + 0.0633i	.1887 - 0.1978i
.80	-.3040i	.0616	.1330 - 0.0280i	.0170 + 0.0809i	.2116 - 0.2511i
1.00	-.3800i	.0963	.1295 - 0.0241i	.0183 + 0.0984i	.2441 - 0.3057i

k	Av. 3-DIM $\frac{M_P}{4qb^2\alpha_o\pi}$ (1)
0	0.1631 + 0i
.167	.1532 - 0.0706i
.333	.1505 - 0.1228i
.667	.1801 - 0.2244i

k	3-DIM	
	Magnitude	Phase (deg)
0	0.1631	0
.167	.1688	335.3
.333	.1944	320.1
.667	.2878	308.8

[1]Average along span, A.R. = 6.

NACA

TABLE XIV

COMPONENT ANALYSIS - EXPERIMENTAL VALUES; AVERAGE M.I.T. RESULTS

Pure pitch; $\alpha_o = 6.74^o$			Pure translation; $h_o = 1.0$ in.	
k	$\frac{L_p}{4\pi q b \alpha_o}$	$\frac{M_p}{4\pi q b^2 \alpha_o}$	$\frac{L_p}{4\pi q h_o}$	$\frac{M_p}{4\pi q b h_o}$
0.10	-0.704 + 0.0246i	0.1805 - 0.057i	-0.0079 - 0.0690i	0.0071 + 0.0217i
.15	-.677 + 0i	.1790 - 0.0744i	-.0149 - 0.106i	.0129 + 0.0304i
.20	-.659 - 0.0346i	.1770 - 0.0899i	-.0265 - 0.143i	.0180 + 0.0385i
.25	-.646 - 0.0680i	.1750 - 0.103i	-.0412 - 0.178i	.0228 + 0.0458i
.30	-.635 - 0.1120i	.177 - 0.1195i	-.0570 - 0.212i	.0329 + 0.0547i
.40	-.630 - 0.1985i	.1775 - 0.1465i		

TABLE XV

CORRELATION ANALYSIS - THEORETICAL VALUES

(a) For corrected results (a = -0.26)

k	$\frac{L}{4qb\alpha_o}$	ϕ_{LP}	$\frac{M}{4qb^2\alpha_o}$	ϕ_{MP}
0	3.1416	180.0	0.7540	360.0
.1	2.6591	176.0	.6719	342.52
.2	2.3624	181.68	.6549	332.93
.3	2.2153	190.0	.6762	325.88
.4	2.1754	198.97	.7229	320.55
.5	2.2102	207.67	.7846	316.57
.6	2.2995	215.62	.8586	313.65
.8	2.5885	228.87	1.0320	310.12
1.0	2.9659	239.05	1.2292	308.60

(b) For British results (no inertia term)

k	(a = -0.33)		(a = 0)	
	$\frac{M}{4qb^2\alpha_o}$	ϕ_{MP}	$\frac{M}{4qb^2\alpha_o}$	ϕ_{MP}
0	0.5233	0	1.5708	360.0
.1	.4794	337.4	1.3505	347.9
.2	.4956	323.2	1.2205	343.9
.3	.5453	312.9	1.1450	341.6
.4	.6141	305.4	1.1002	340.0
.5	.6943	299.9	1.0736	338.4
.6	.7831	295.7	1.0588	336.9
.8	.9722	289.9	1.0511	333.9
1.0	1.1718	286.2	1.0618	330.7

TABLE XVI

CORRELATION ANALYSIS - STANFORD RESULTS[1]

k	R.N.	Interpolated $L_p/4qba_o$	Interpolated phase, ϕ_{LP}	Correction term	Corrected $L_p/4qba_o$	Correct phase, ϕ_{LP}
Model A (b = 7.5 in., a = -0.20); n = 6.66 cps (table I-A-6R)						
0.2	1.028×10^6	2.405	180	-0.0033 - 0.0274i	2.4080	180.7
.3	.685	2.2708	188	-.0016 - 0.0376i	2.2783	189.0
.4	.514	2.2330	195.7	.0027 - 0.0471i	2.2433	196.9
.6	.343	2.3081	209.3	.0183 - 0.0655i	2.3254	211.0
.8	.257	2.5198	219.4	.0427 - 0.0836i	2.5416	221.5
1.0	.206	2.7674	226.6	.0753 - 0.1017i	2.7923	229.2
Model C (b = 5.0 in., a = -0.20); n = 10 cps (table I-C-10R)						
0.2	1.028	2.482	180	-0.0033 - 0.0274i	2.4855	180.6
.3	.685	2.3552	186.5	-.0016 - 0.0376i	2.3613	187.4
.4	.514	2.3082	194.2	.0027 - 0.0471i	2.31767	195.3
.6	.343	2.3604	206.9	.0183 - 0.0655i	2.3747	208.5
.8	.257	2.5347	217.4	.0427 - 0.0836i	2.5532	219.5
1.0	.206	2.7670	225.8	.0753 - 0.1017i	2.7274	228.3
Model B (b = 7.5 in., a = -0.40); n = 6.66 cps (table I-B-6R)						
0.2	0.686	2.3254	184.4	0.0078 + 0.0641i	2.3136	182.9
.3	.457	2.2307	191.0	.0038 + 0.0877i	2.21195	188.8
.4	.343	2.2010	197.9	-.0062 + 0.1099i	2.1759	195.1
.6	.229	2.3006	211.7	-.0428 + 0.1528i	2.2618	207.9
.8	.172	2.6058	224.4	-.0997 + 0.1949i	2.5494	219.7
1.0	.137	3.0945	234.3	-.1758 + 0.2372i	3.01774	229.0
Model D (b = 5.0 in., a = -0.40); n = 10 cps (table I-D-10R)						
0.2	0.686	2.4150	185.2	0.0078 + 0.0641i	2.4022	183.7
.3	.457	2.3348	190.9	.0038 + 0.0877i	2.3161	188.8
.4	.343	2.3280	197.5	-.0062 + 0.1099i	2.3033	194.9
.6	.229	2.4651	210.2	-.0428 + 0.1528i	2.4301	206.6
.8	.172	2.7957	222.1	-.0997 + 0.1949i	2.7475	217.7
1.0	.137	3.1037	228.9	-.1758 + 0.2372i	3.0540	223.5

[1]These results have been corrected for a theoretical "shift" of elastic axis from 30- and 40- to 37-percent chord.

TABLE XVII

CORRELATION ANALYSIS - M.I.T. RESULTS

[$\alpha_i = 0^\circ$; $\alpha_o = 6.74^\circ$ or $h_o = 1.0$ in.; $a = -0.26$]

k	$\frac{L}{4qba_o}$	ϕ_{LP}	$\frac{M}{4qb^2a_o}$	ϕ_{MP}
R.N. = 0.715×10^6				
0.05	----	---	-----	---
.10	2.38	---	0.587	---
.15	2.12	181	.595	344
.20	2.08	182	.603	333
.25	2.06	188	.639	329
.30	2.01	190	.665	326
.35	2.04	195	-----	---
.40	2.07	197	.722	326
R.N. = 0.823×10^6				
0.05	----	---	-----	---
.10	2.12	180	0.602	348
.15	2.12	183	.626	339
.20	2.04	186	.652	337
.25	2.06	187	.636	324
.30	2.02	187	.716	325
.35	2.02	194	.690	323
.40	2.11	200	.761	325
R.N. = 0.930×10^6				
0.05	2.32	180	0.643	351
.10	2.22	174	.593	338
.15	2.12	178	.632	332
.20	2.08	183	.608	332
.25	2.02	184	.621	324
.30	2.12	187	-----	321
.35	2.04	191	-----	319
.40	----	---	-----	---

TABLE XVIII

CORRELATION ANALYSIS - RESULTS[1] OF REFERENCE 2 ($\alpha_i = 0^\circ$)

k	Interpolated $M/4qb^2\alpha_o$	Corrected $M/4qb^2\alpha_o$	$M_{corr.}/4qb^2\alpha_o$	$\frac{R_{MP}^2 + I_{MP}^2}{\alpha_o}$	ϕ_{MP}
		R.N. = 0.09×10^6			
0	1.6000 - 0i	-0.8168 + 0i	0.7832 + 0i	0.7832	360
.2	1.2950 - 0.355i	-.5902 + 0.0414i	.7048 - 0.3136i	.7714	336
.4	1.0400 - 0.445i	-.4761 - 0.0817i	.5639 - 0.5267i	.7717	317
.6	.8665 - 0.460i	-.3815 - 0.2062i	.4850 - 0.6662i	.8243	306
		R.N. = 0.14×10^6			
0	1.5325 - 0i	-0.8168 + 0i	0.7157 + 0i	0.7157	360.0
.1	1.3810 - 0.290i	-.6803 + 0.0822i	.7007 - 0.2078i	.7308	343.5
.2	1.2400 - 0.378i	-.5902 + 0.0414i	.6498 - 0.3366i	.7318	332.6
.3	1.1090 - 0.422i	-.5274 - 0.0184i	.5816 - 0.4404i	.7295	322.9
.4	1.0230 - 0.431i	-.4761 - 0.0817i	.5469 - 0.5127i	.7497	316.9
.6	.9240 - 0.403i	-.3815 - 0.2062i	.5425 - 0.6092i	.8157	311.7
		R.N. = 0.21×10^6			
0	1.5150 - 0i	-0.8168 + 0i	0.6982 + 0i	0.6982	360.0
.1	1.3450 - 0.277i	-.6803 + 0.0822i	.6647 - 0.1948i	.6927	343.7
.2	1.2520 - 0.345i	-.5902 + 0.0414i	.6618 - 0.3036i	.7281	335.4
.3	1.1420 - 0.374i	-.5274 - 0.0184i	.6146 - 0.3924i	.7292	327.4
.4	1.0800 - 0.395i	-.4761 - 0.0817i	.6039 - 0.4767i	.7694	321.7
		R.N. = 0.28×10^6			
0	1.5140 - 0i	-0.8168 + 0i	0.6972 + 0i	0.6972	360.0
.1	1.414 - 0.280i	-.6803 + 0.0822i	.7337 - 0.1978i	.7599	344.9
.2	1.242 - 0.381i	-.5902 + 0.0414i	.6518 - 0.3396i	.7350	332.5
.3	1.167 - 0.401i	-.5274 - 0.0184i	.6396 - 0.4194i	.7649	326.7
.4	1.151 - 0.418i	-.4761 - 0.0817i	.6749 - 0.4997i	.8398	323.5

[1]Results are for a wing which has its elastic axis at one-half chord. The following corrections have been made: (a) Aerodynamic inertia term added and (b) theoretical "shift" of elastic axis to 37-percent chord.

TABLE XIX

CORRELATION ANALYSIS - RESULTS[1] OF REFERENCE 3 ($\alpha_1 = 0°$; b = 4.5 in.)

k	Interpolated $M/4qb^2\alpha_o$	Corrected $M/4qb^2\alpha_o$	$M_{corr.}/4qb^2\alpha_o$	$\frac{R_{MP}^2 + I_{MP}^2}{\alpha_o}$	ϕ_{MP}
(a) Without center bearing (a = 0)					
R.N. = 0.142 x 10^6					
0	1.886 + 0i	-0.8168 + 0i	1.0692 + 0i	1.0692	360.0
.1	1.395 - 0.3061	-.6803 + 0.08221	.7147 - 0.22381	.7492	342.6
.2	1.210 - 0.3391	-.5902 + 0.04141	.6198 - 0.29761	.6875	334.4
.3	1.106 - 0.3551	-.5274 - 0.01841	.5786 - 0.37341	.6888	327.2
.4	1.306 - 0.3631	-.4761 - 0.08171	.5599 - 0.44471	.7151	321.5
.6	0.956 - 0.3691	-.3815 - 0.20621	.5745 - 0.57521	.8130	315.0
.8	0.925 - 0.360i	-.2788 - 0.32571	.6462 - 0.68571	.9422	313.0
R.N. = 0.283 x 10^6					
0	1.805 + 0i	-0.8168 + 0i	0.9882 + 0i	0.9882	360.0
.1	1.375 - 0.2701	-.6803 + 0.08221	.6947 - 0.18781	.7197	344.8
.2	1.223 - 0.3451	-.5902 + 0.04141	.6328 - 0.30361	.7019	334.4
.3	1.136 - 0.3711	-.5274 - 0.01841	.6086 - 0.38941	.7224	327.4
.4	1.110 - 0.3851	-.4761 - 0.08171	.6339 - 0.46671	.7873	323.6
.6		-.3815 - 0.20621			
.8		-.2788 - 0.32571			
(b) With center bearing (a = 0)					
R.N. = 0.142 x 10^6					
0.2	1.222 - 0.3351	0.5902 + 0.04141	0.6318 - 0.29361	0.6966	335.1
.3	1.122 - 0.3601	-.5274 - 0.01841	.5946 - 0.37841	.7047	327.6
.4	1.057 - 0.3701	-.4761 - 0.08171	.5809 - 0.45171	.7358	322.1
.6	.993 - 0.3591	-.3815 - 0.20621	.6115 - 0.56521	.8328	317.2
R.N. = 0.283 x 10^6					
0.1	1.330 - 0.2611	-0.6803 + 0.08221	0.6497 - 0.17881	0.6739	344.6
.2	1.195 - 0.3351	-.5902 + 0.04141	.6048 - 0.29361	.6722	334.1
.3	1.105 - 0.3551	-.5274 - 0.01841	.5776 - 0.37341	.6878	327.1
.4	1.077 - 0.3581	-.4761 - 0.08171	.6009 - 0.43971	.7446	323.8
(c) Without center bearing (a = -0.333)					
R.N. = 0.142 x 10^6					
0	0.533 + 0i	0.2293 + 0i	0.7623 + 0i	0.7623	360.0
.1	.490 - 0.1551	.1961 - 0.01671	.6861 - 0.17171	.7073	345.7
.2	.450 - 0.2581	.1840 - 0.00051	.6340 - 0.25851	.6847	337.8
.3	.415 - 0.3371	.1870 + 0.02041	.6020 - 0.31661	.6802	332.3
.4	.380 - 0.4041	.2007 + 0.04211	.5807 - 0.36191	.6844	328.0
.5	.343 - 0.4661	.2230 + 0.06341	.5660 - 0.40261	.6945	324.6
.6	.305 - 0.5291	.2528 + 0.08441	.5578 - 0.44461	.7133	321.4
.8	.218 - 0.6501	.3333 + 0.12541	.5513 - 0.52461	.7611	316.4
1.0		.4397 + 0.16511			
R.N. = 0.283 x 10^6					
0	0.550 + 0i	0.2293 + 0i	0.7793 + 0i	0.7793	360.0
.1	.498 - 0.1551	.1961 - 0.01671	.6941 - 0.17171	.7151	346.1
.2	.455 - 0.2581	.1840 - 0.00051	.6390 - 0.25851	.6892	338.0
.3	.425 - 0.3381	.1870 + 0.02041	.6120 - 0.31761	.6895	332.6
.4	.395 - 0.4301	.2007 + 0.04211	.5979 - 0.38791	.7109	326.9
.5		.2230 + 0.06341			
.6		.2528 + 0.08441			
.8		.3333 + 0.12541			
1.0		.4397 + 0.16511			

[1]Results are for wings with elastic axis at one-half chord and one-third chord. The following corrections have been made: (a) Aerodynamic inertia term added and (b) theoretical "shift" of elastic axis to 37-percent chord.

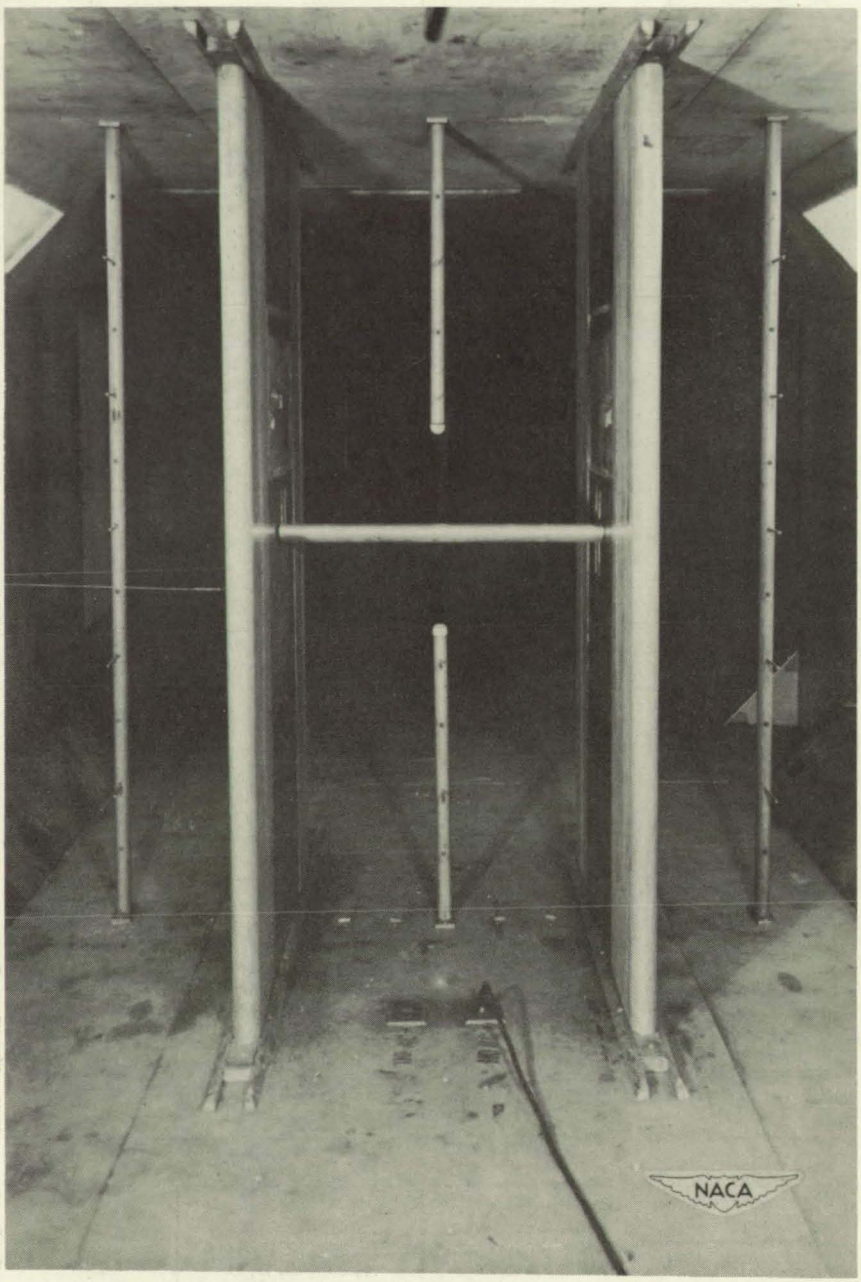

Figure 1.- Test-section arrangement viewed from upstream.

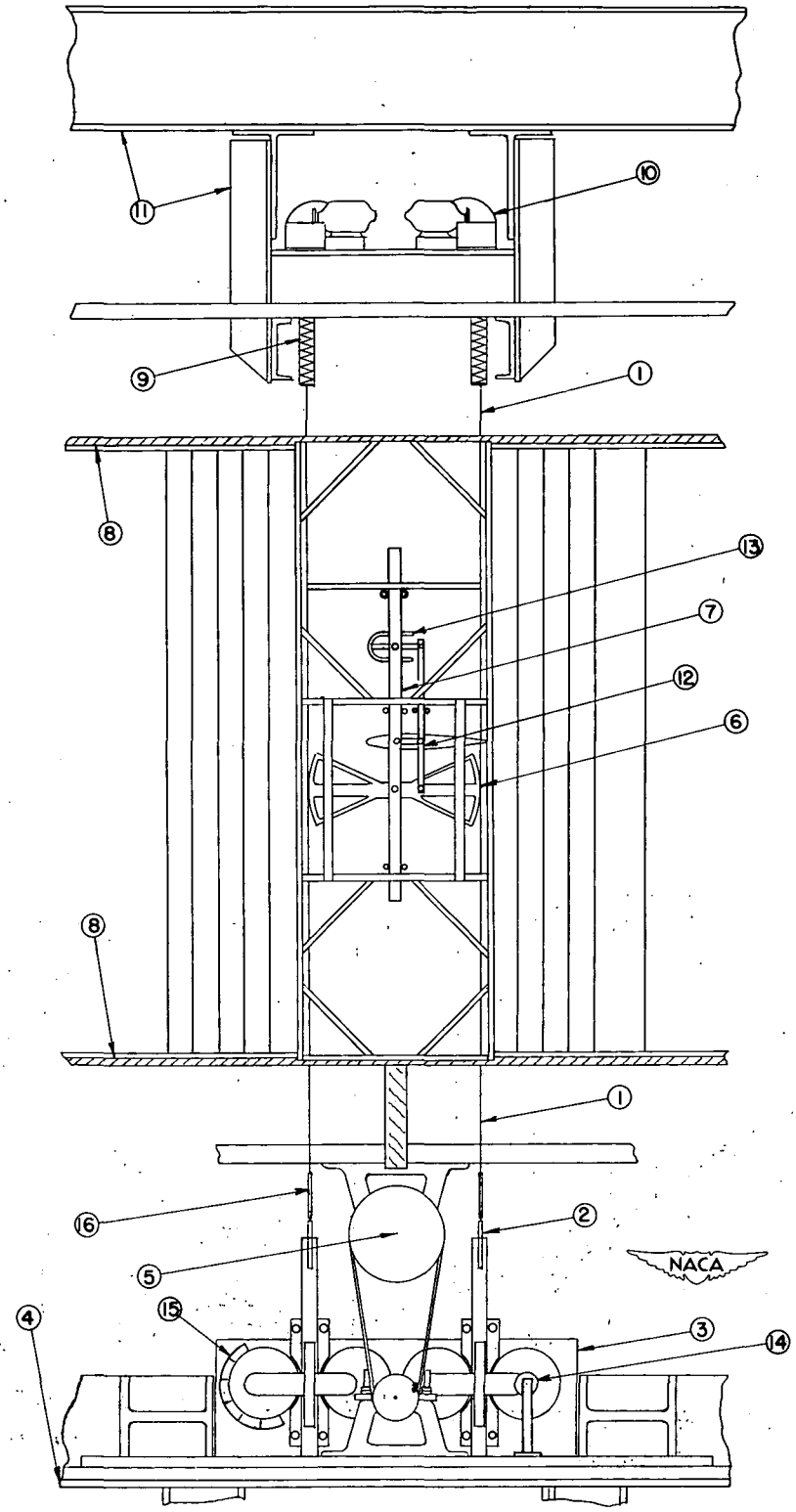

Figure 2.- Diagrammatic layout of oscillator.

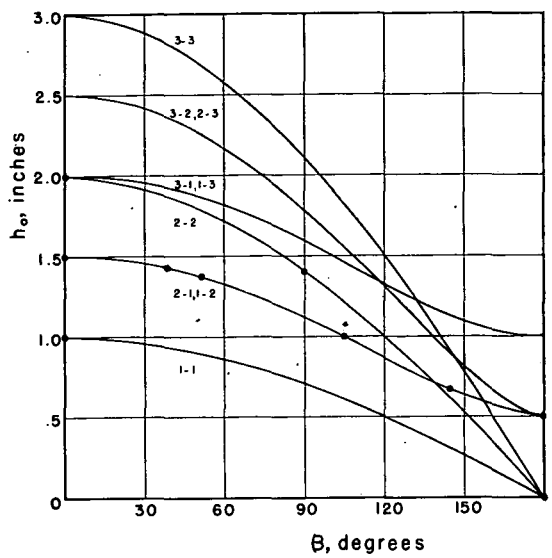

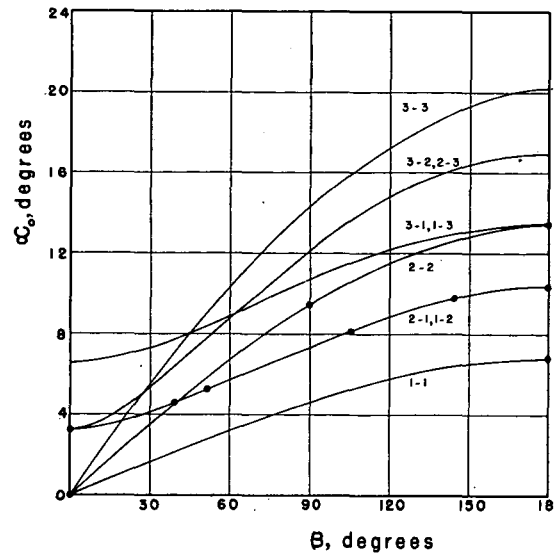

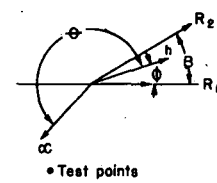

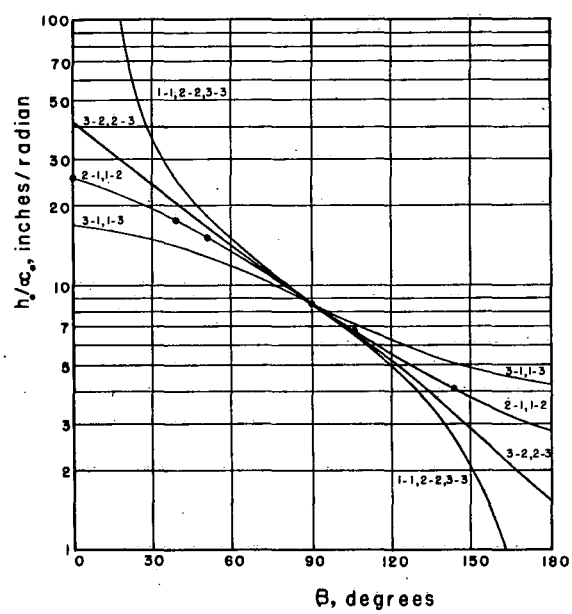

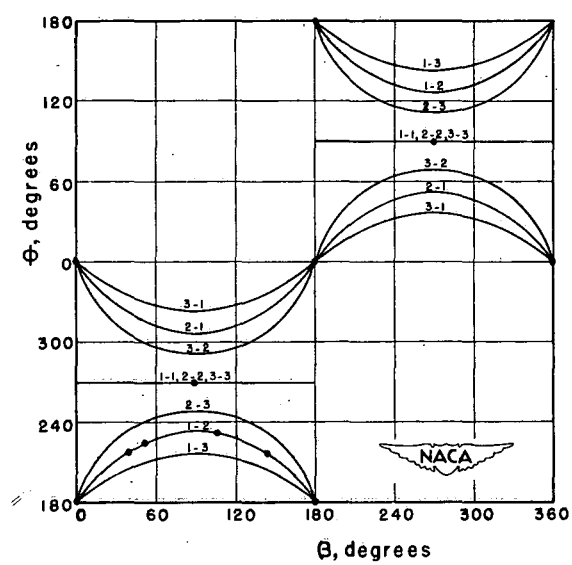

Figure 3.- Oscillator properties for various crank-wheel-amplitude and phase-angle settings.

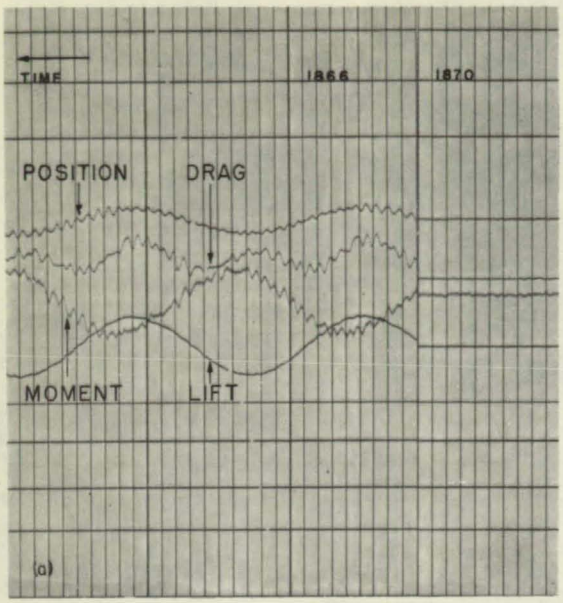

$\alpha_0 = \pm 6.7°$

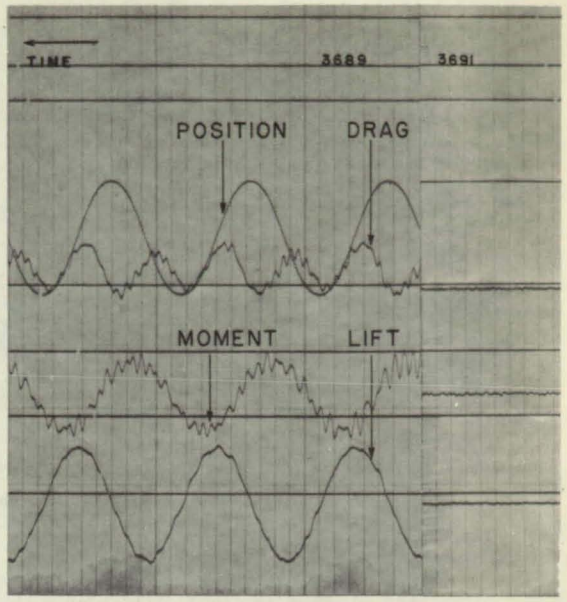

$\alpha_0 = \pm 13.5°$

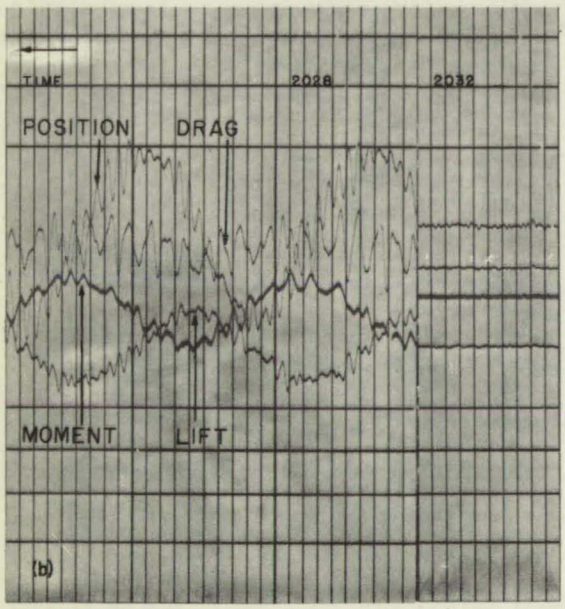

$h_o = 1$ IN.

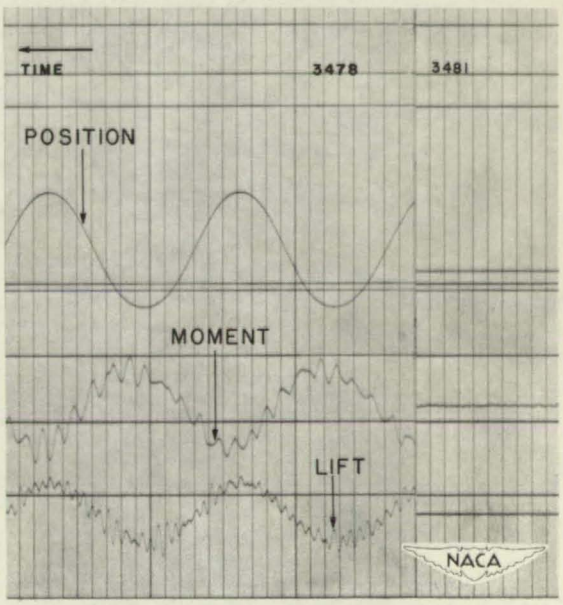

$h_o = 2$ IN.

(a) Pure pitch.

(b) Pure translation.

Figure 4.- Typical records of pure pitch and pure translation.

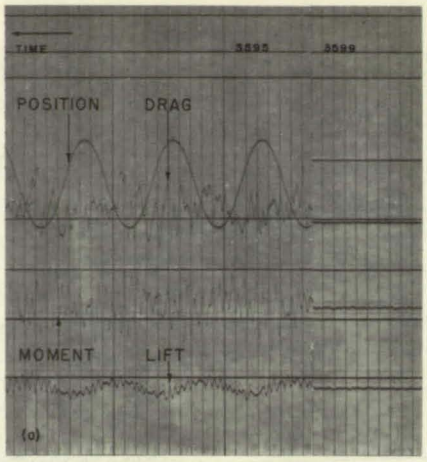

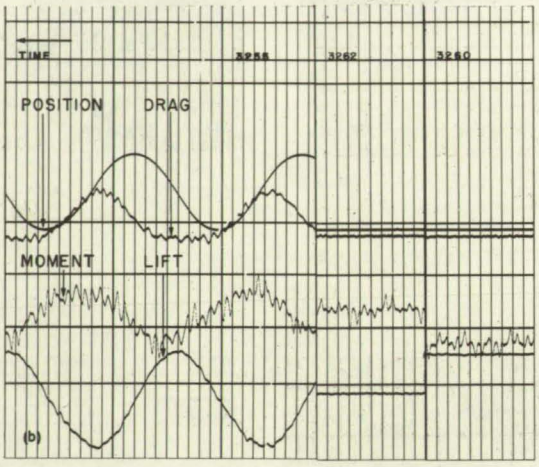

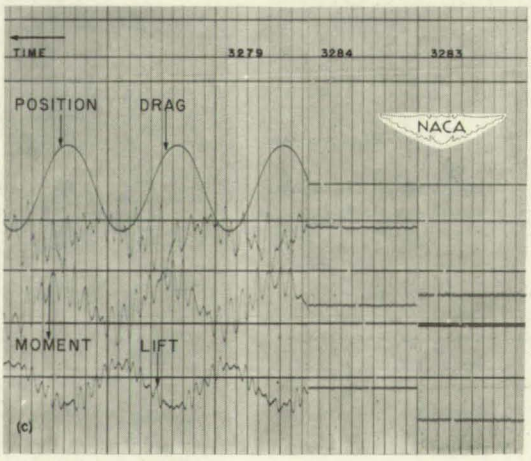

(a) Combined motions.

(b) Pure pitch with initial angle.

(c) Pure translation with initial angle.

Figure 5.- Typical records of combined motions, pure pitch with initial angle, and pure translation with initial angle.

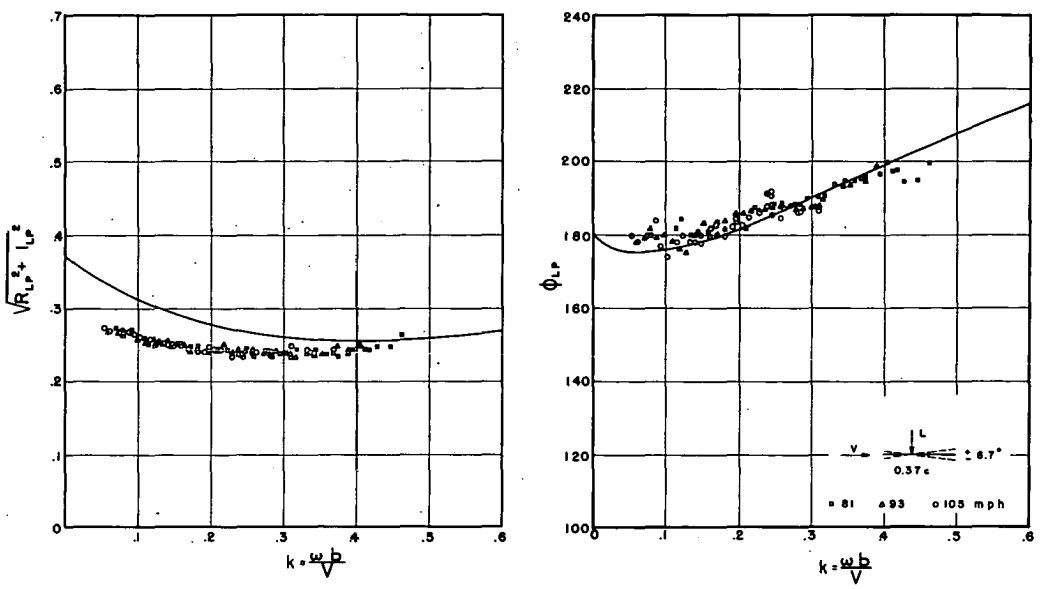

(a) $\alpha_o = \pm 6.7^\circ$.

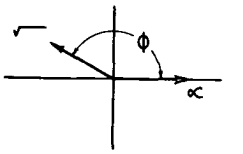

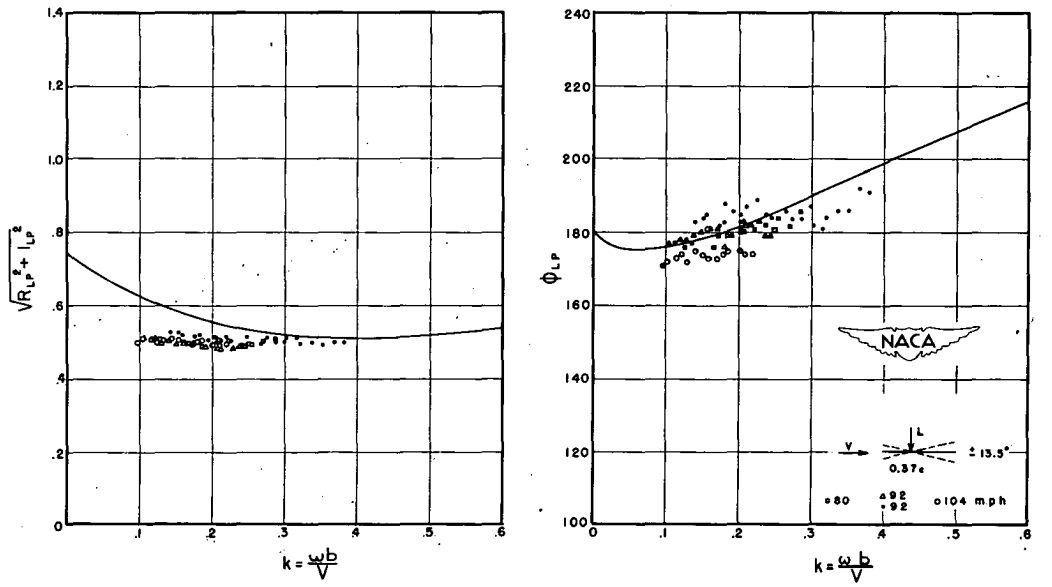

(b) $\alpha_o = \pm 13.5^\circ$.

Figure 6.- Lift in pure pitch.

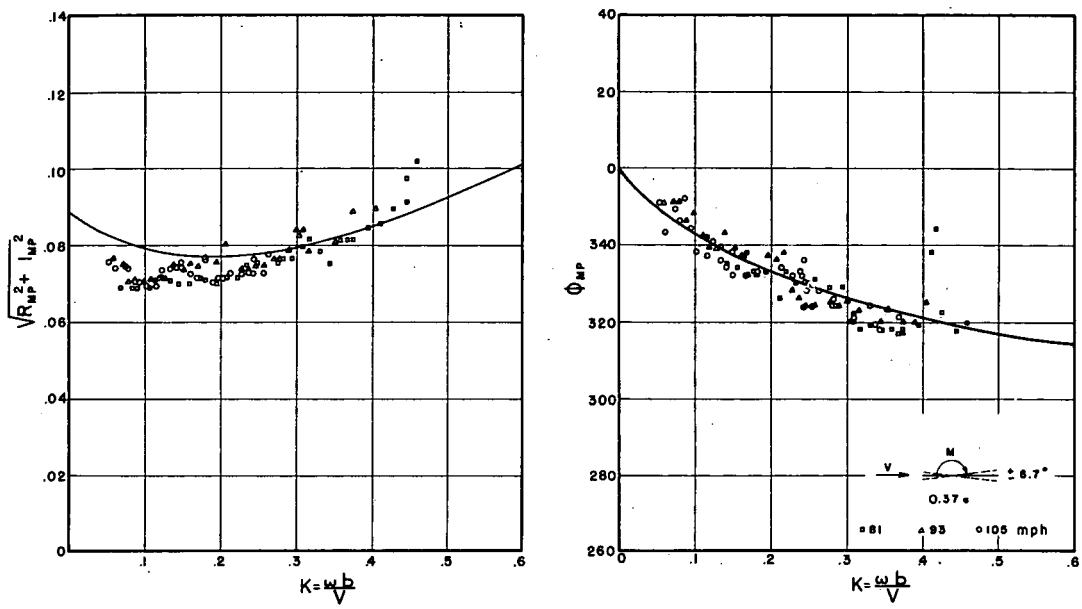

(a) $\alpha_o = \pm 6.7^o$.

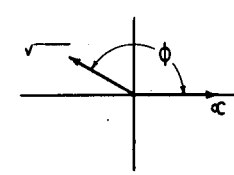

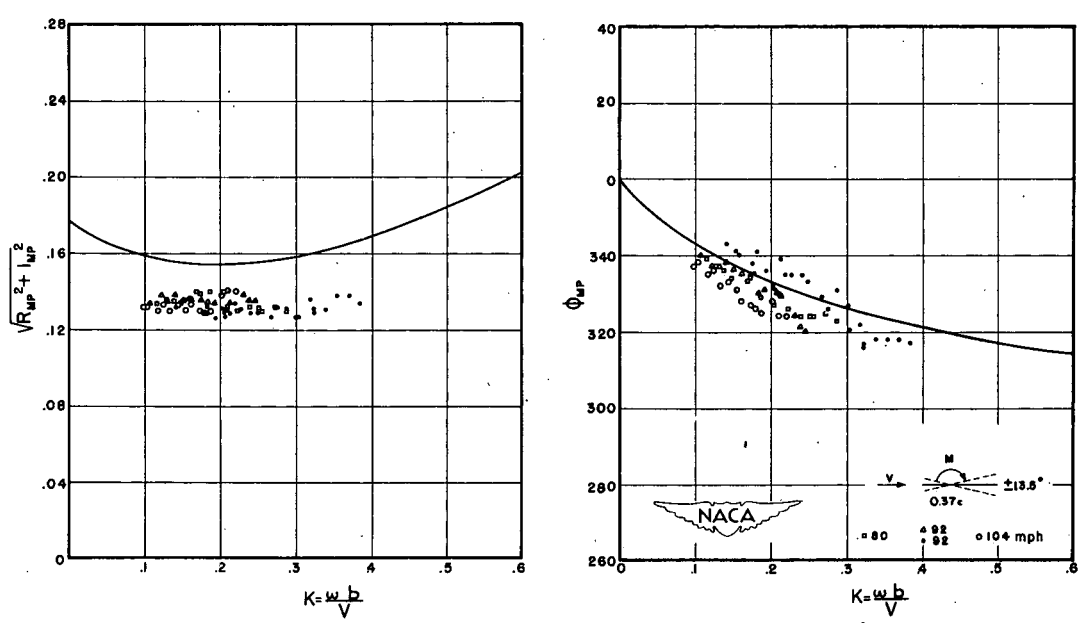

(b) $\alpha_o = \pm 13.5^o$.

Figure 7.- Moment in pure pitch.

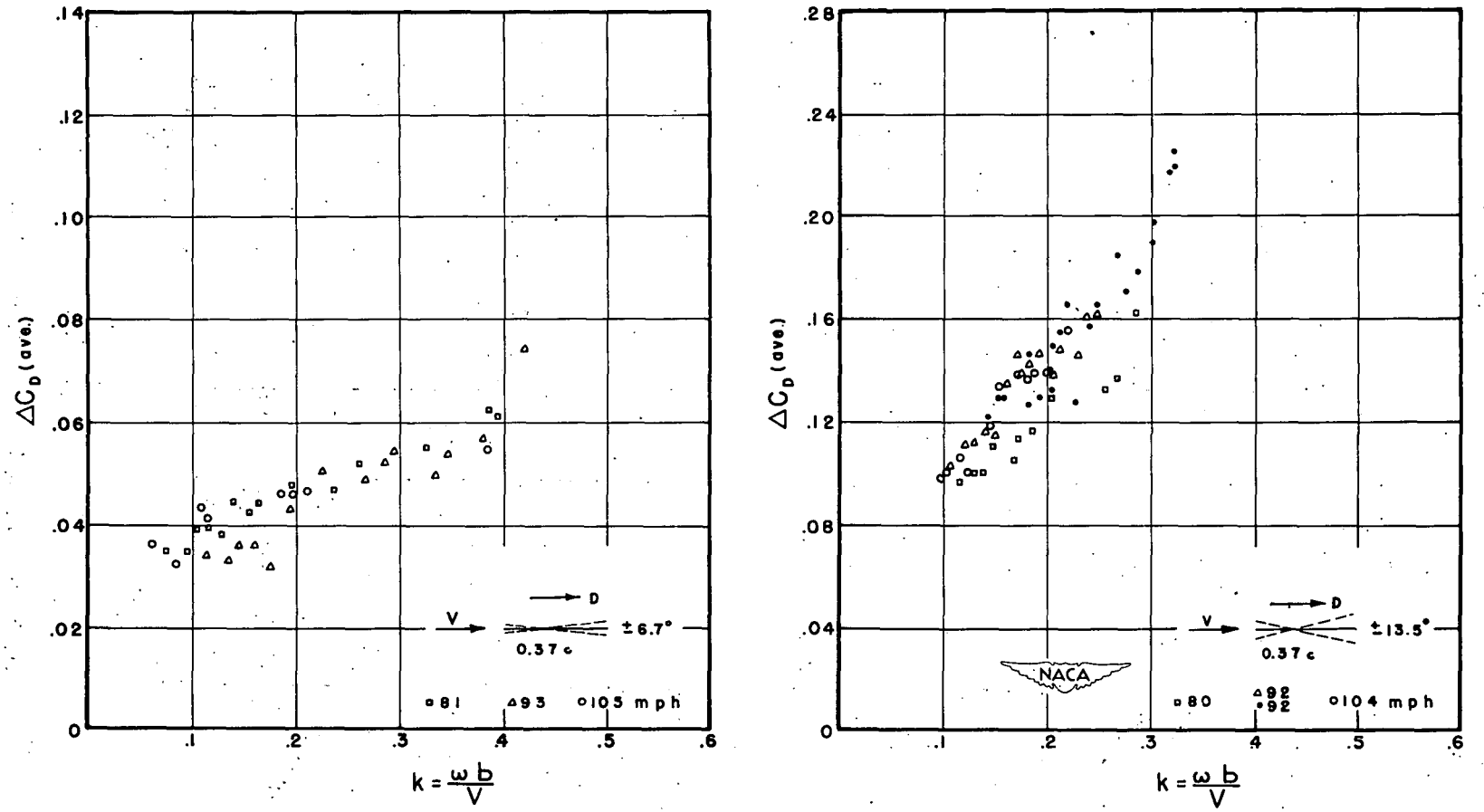

(a) $\alpha_o = \pm 6.7^\circ$.

(b) $\alpha_o = \pm 13.5^\circ$.

Figure 8.- Average drag amplitude coefficients in pure pitch.

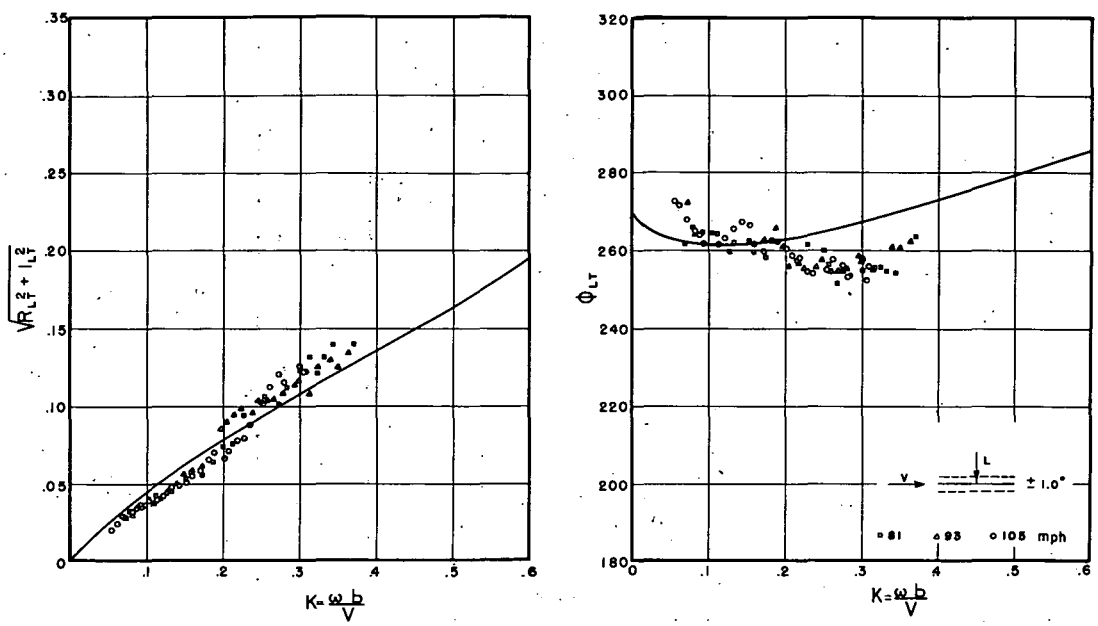

(a) h_o = 1.0 inch.

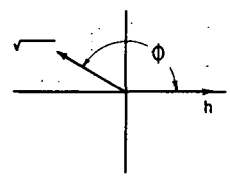

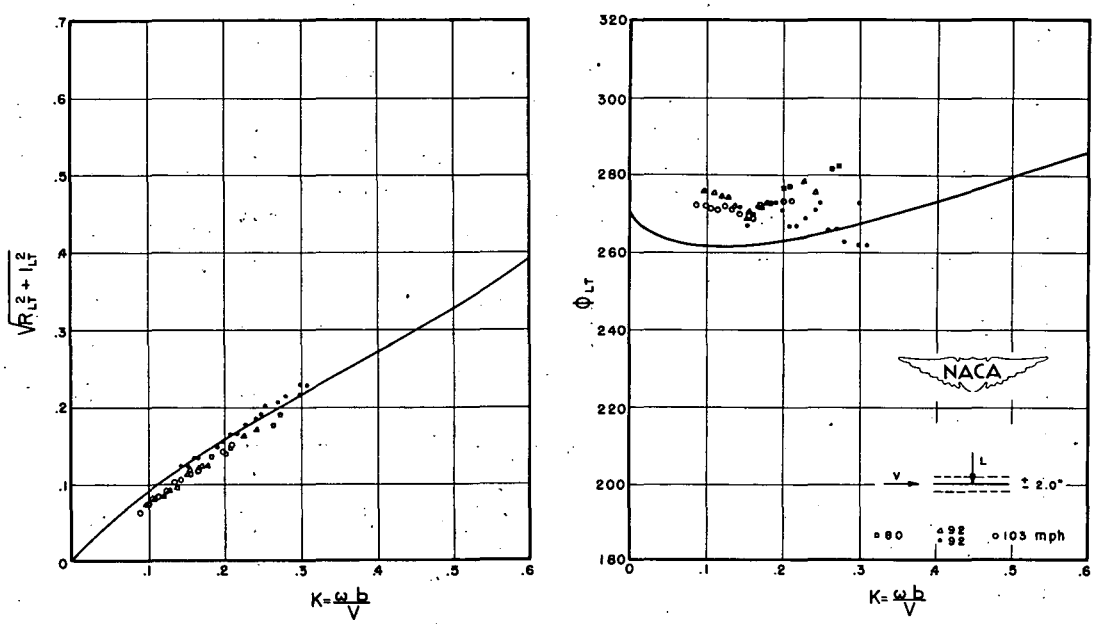

(b) h_o = 2.0 inches.

Figure 9.- Lift in pure translation.

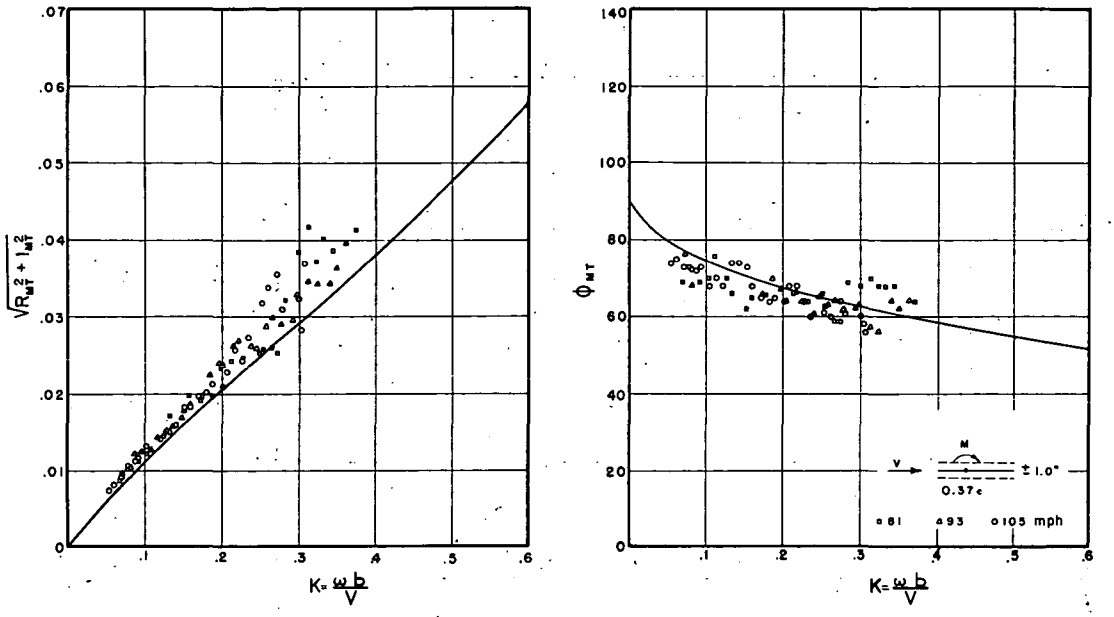

(a) h_o = 1.0 inch.

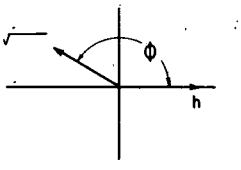

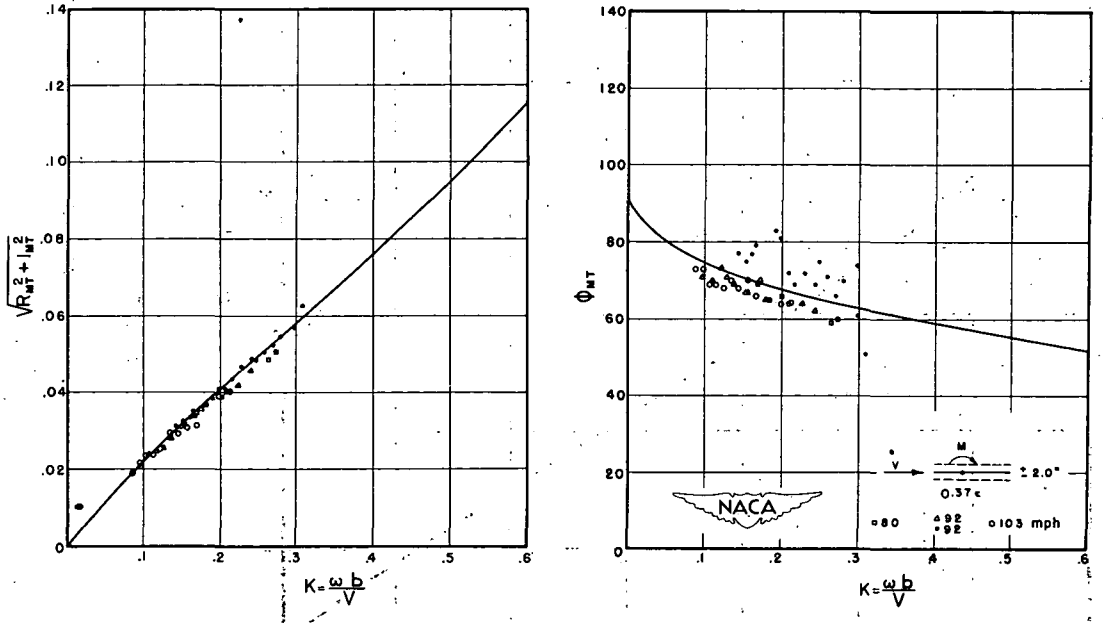

(b) h_o = 2.0 inches.

Figure 10.- Moment in pure translation.

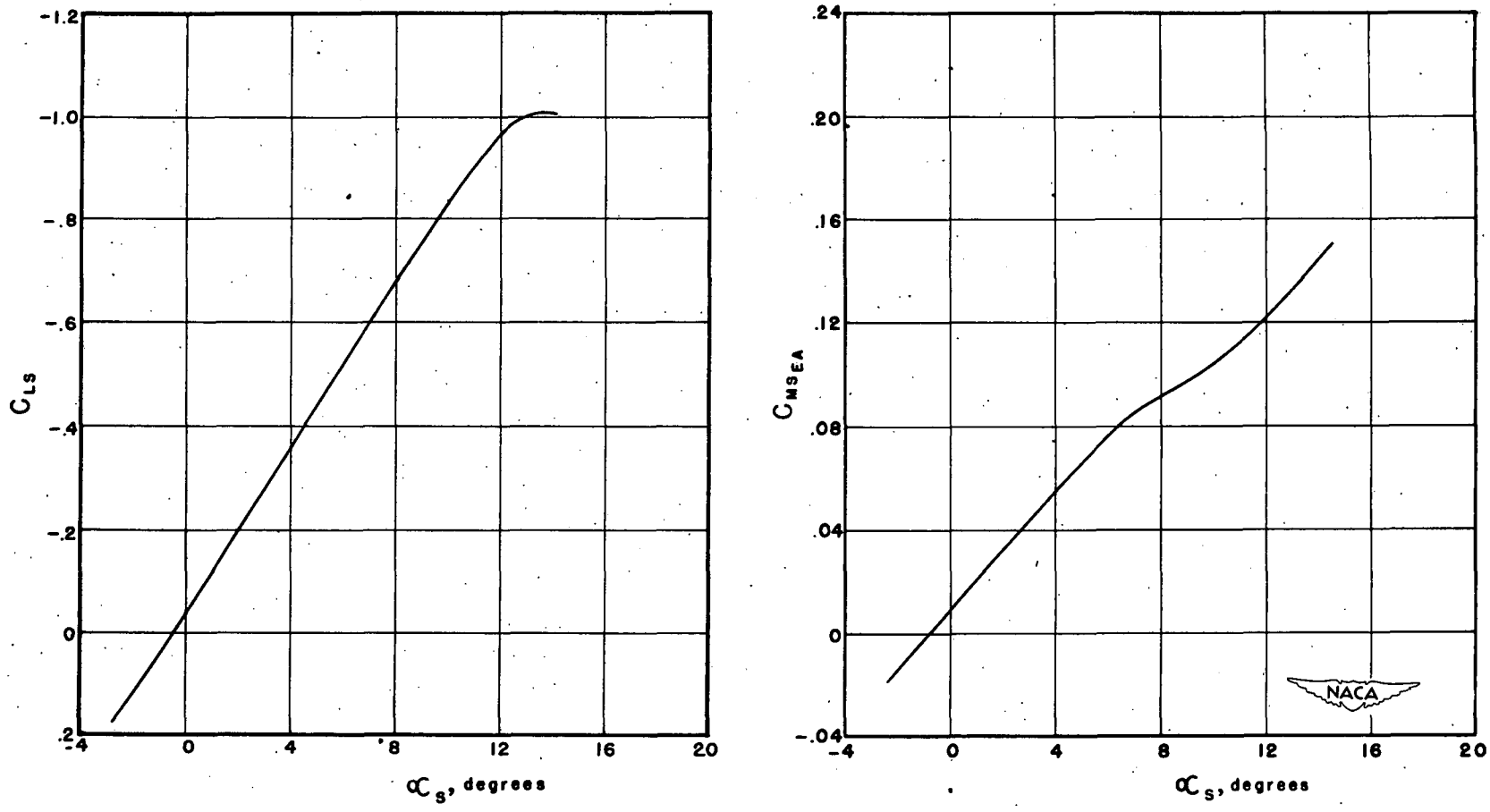

(a) Lift.

(b) Moment.

Figure 11.- Static lift and moment coefficients.

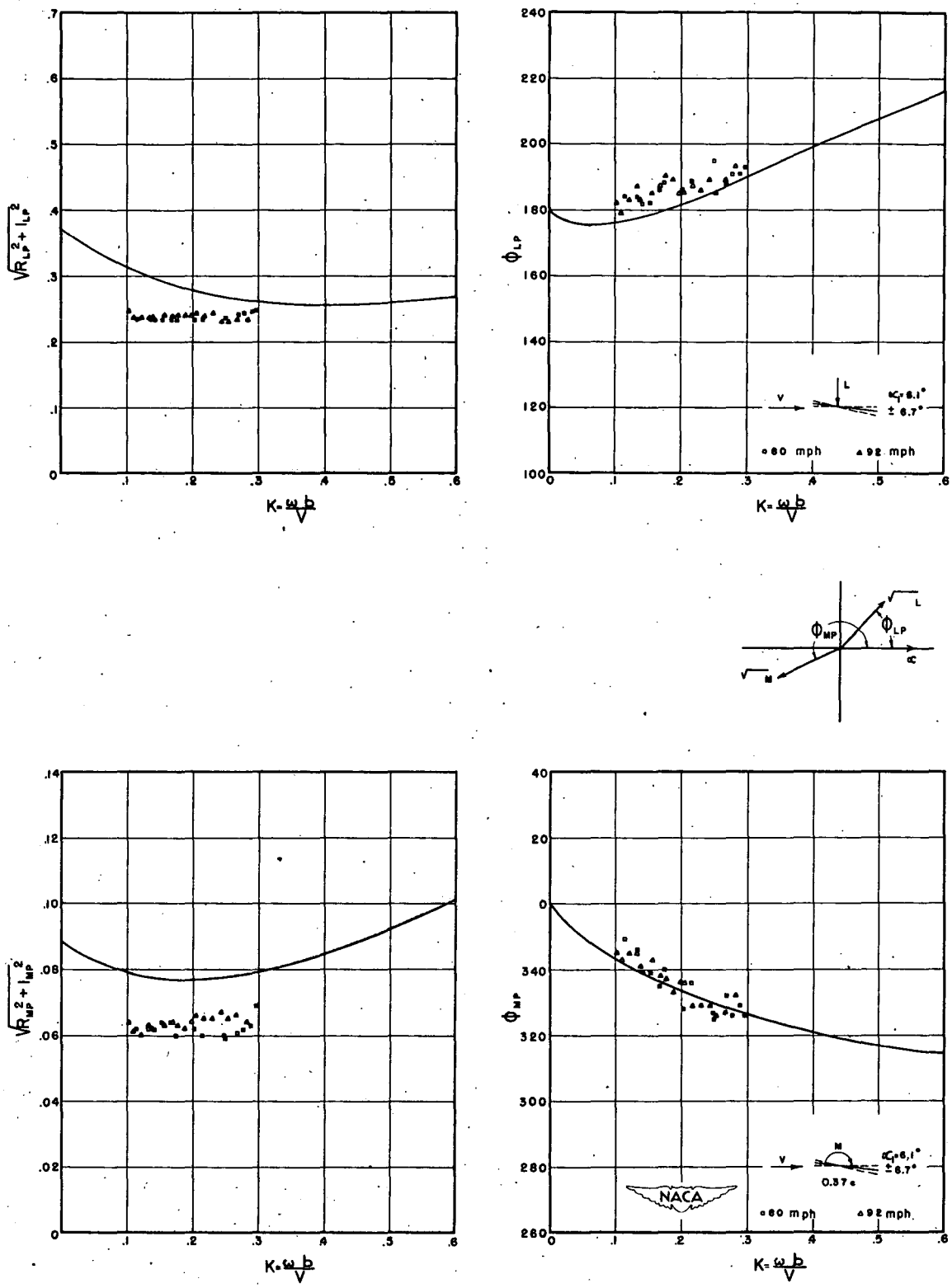

Figure 12.- Lift and moment in pure pitch about an initial angle. $\alpha_o = \pm 6.7^o$; $\alpha_i = 6.1^o$. Oscillatory component.

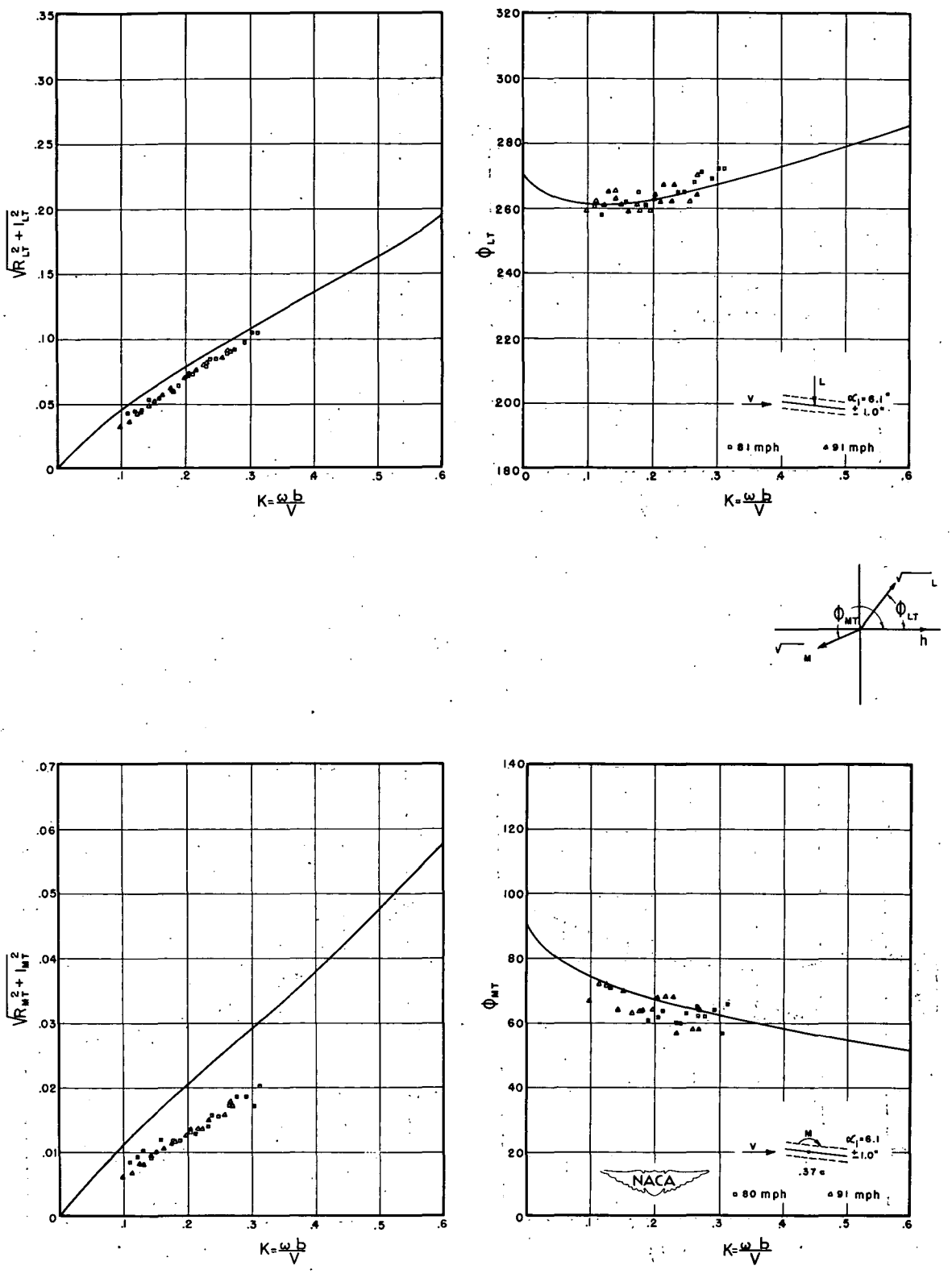

Figure 13.- Lift and moment in pure translation about an initial angle. $h_o = \pm 1.0$ inch; $\alpha_i = 6.1^o$. Oscillatory component.

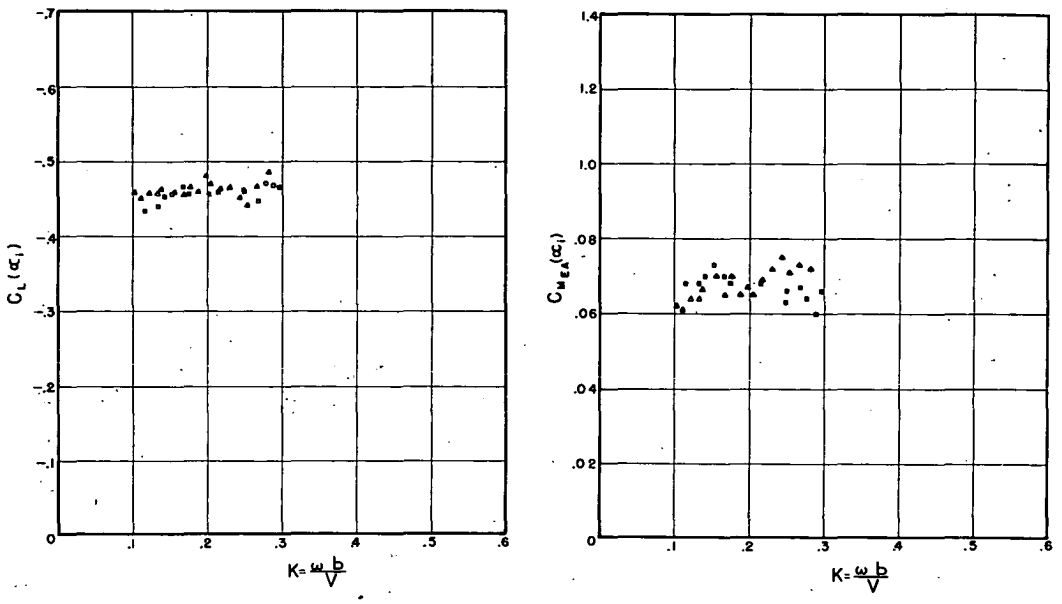

(a) Pure pitch.

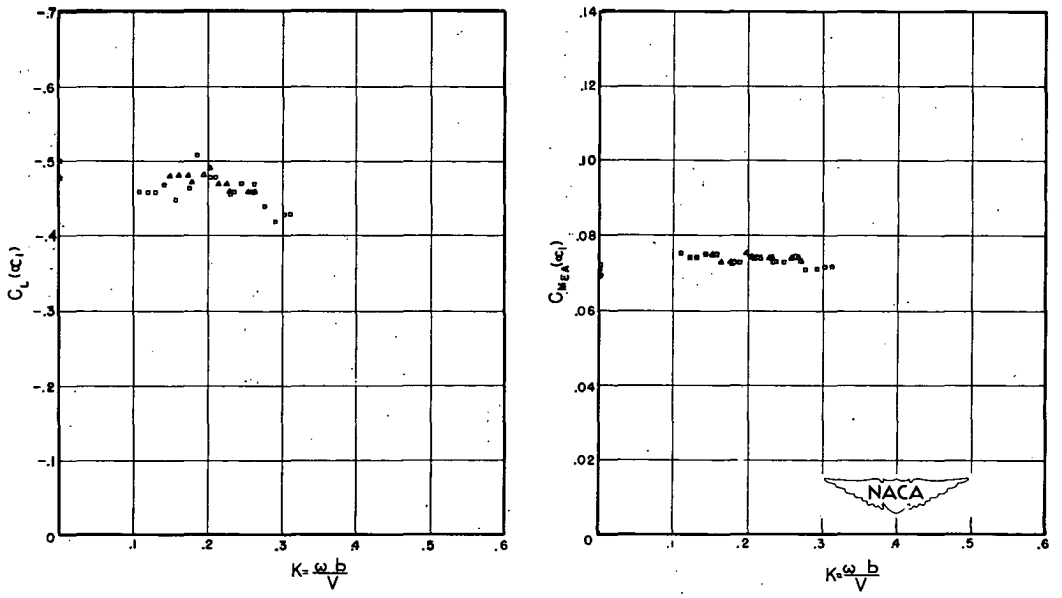

(b) Pure translation.

Figure 14.- Lift and moment in pure pitch and translation about an initial angle. $\alpha_o = \pm 6.7^o$; $h_o = \pm 1.0$ inch; $\alpha_i = 6.1^o$. Mean component.

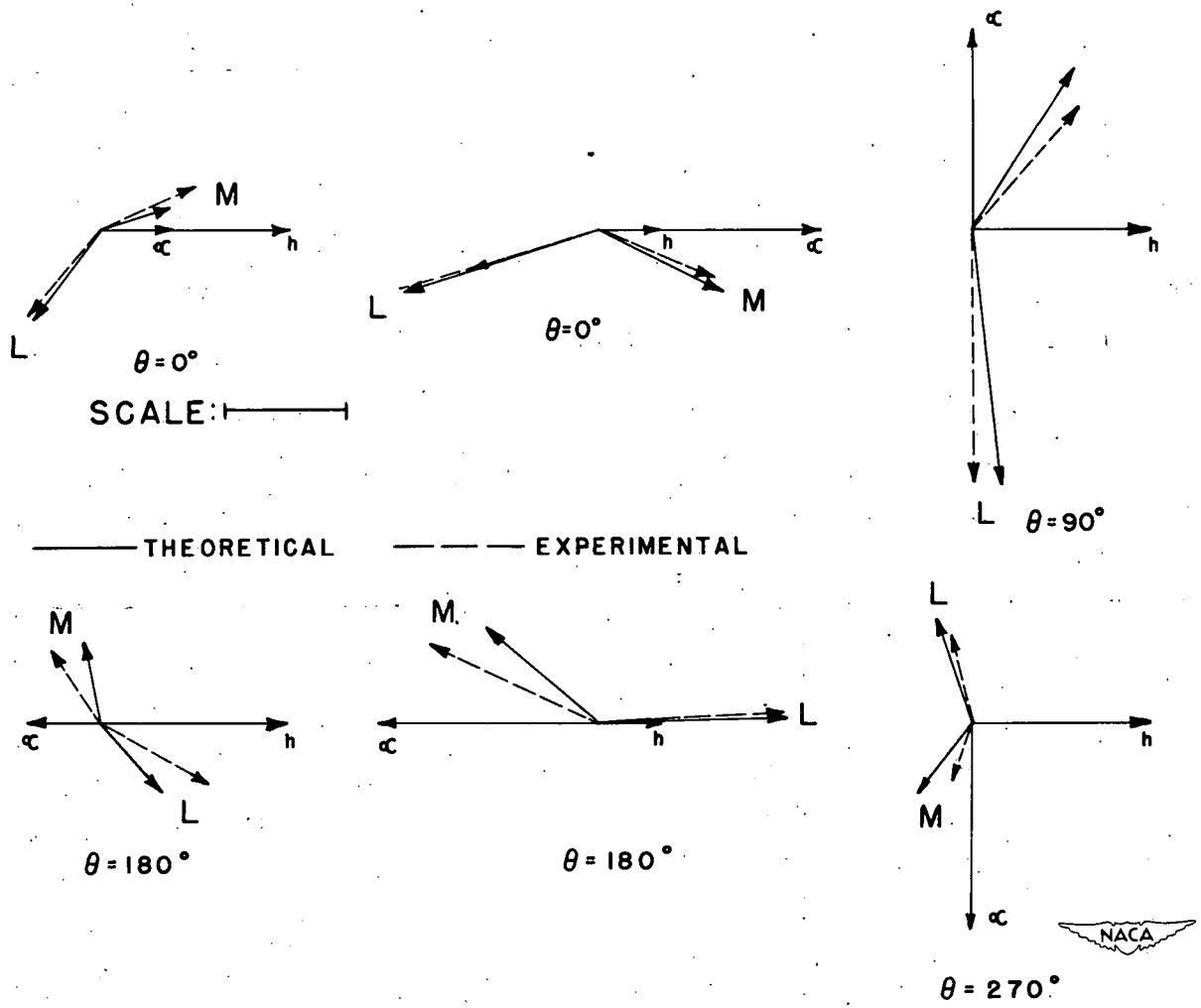

Figure 15.- Vector plots for combined motions. h = 1.0 inch; $\alpha = 5.7^{\circ}$; $\sqrt{R_{LR}^2 + I_{LR}^2} = 0.25$; $\sqrt{R_{MR}^2 + I_{MR}^2} = 0.10$.

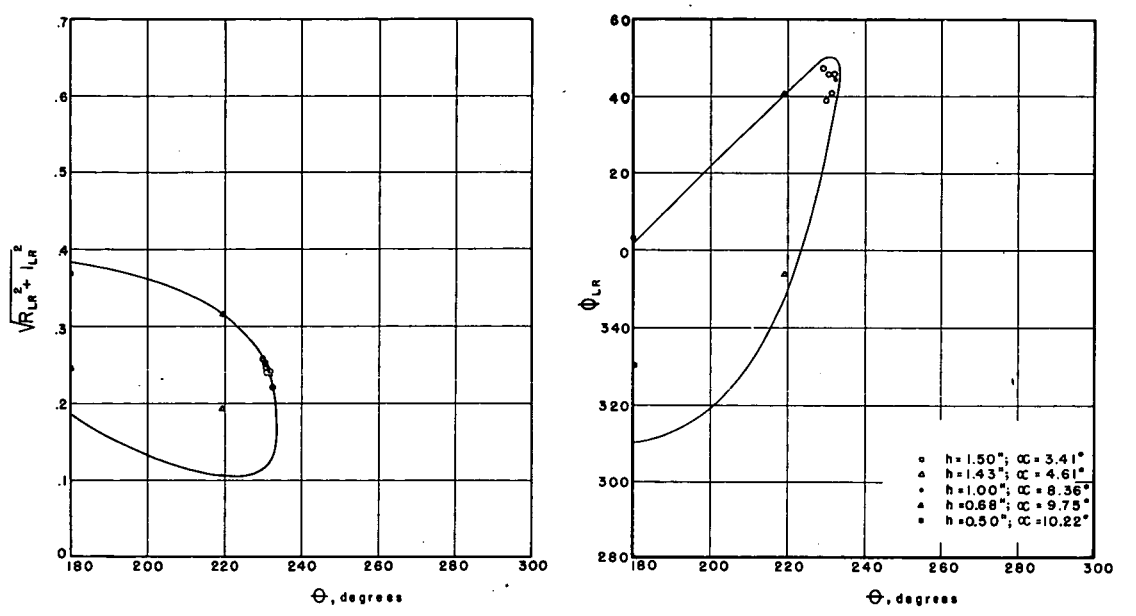

(a) Lift.

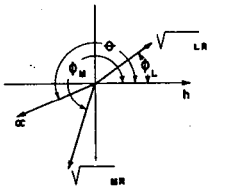

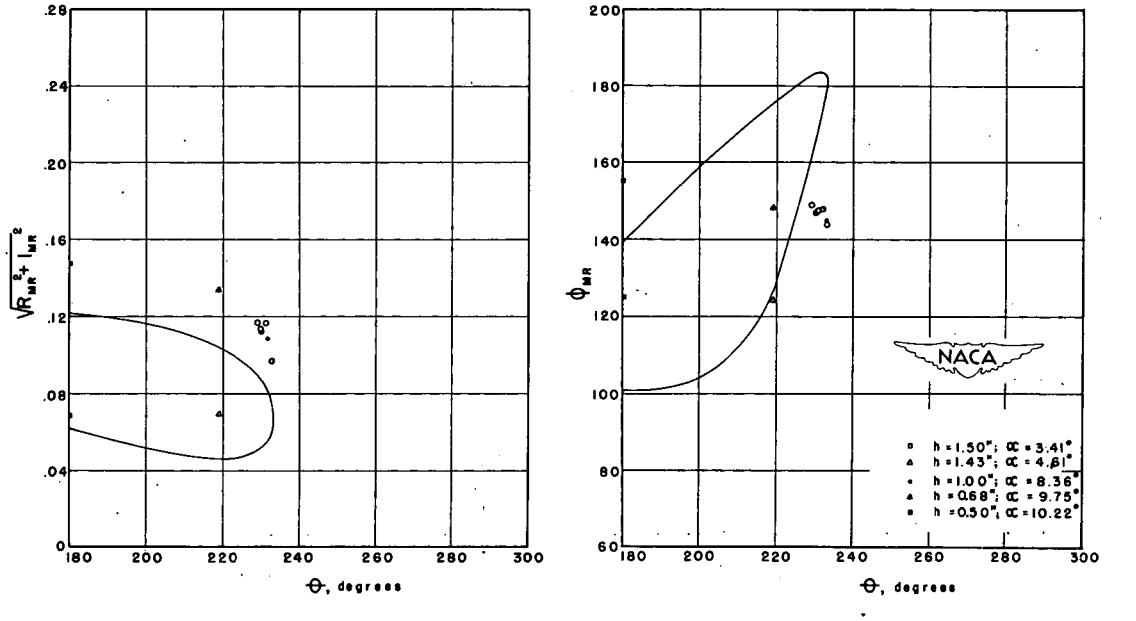

(b) Moment.

Figure 16.- Lift and moment in combined motions. k = 0.30.

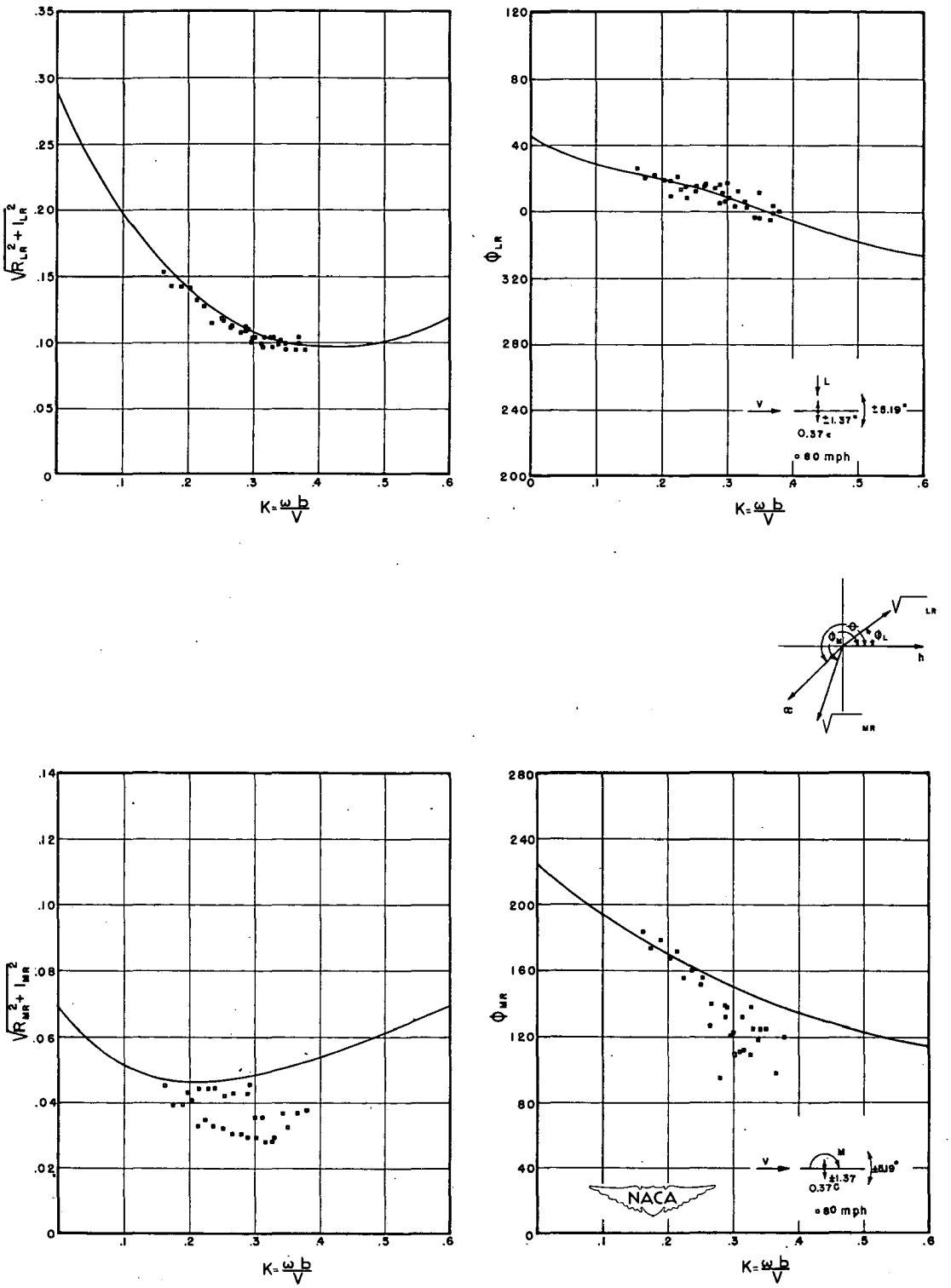

Figure 17.- Lift and moment in combined motions. $\theta = 225.1°$; $h_o = \pm 1.4$ inch; $\alpha_o = \pm 5.2°$.

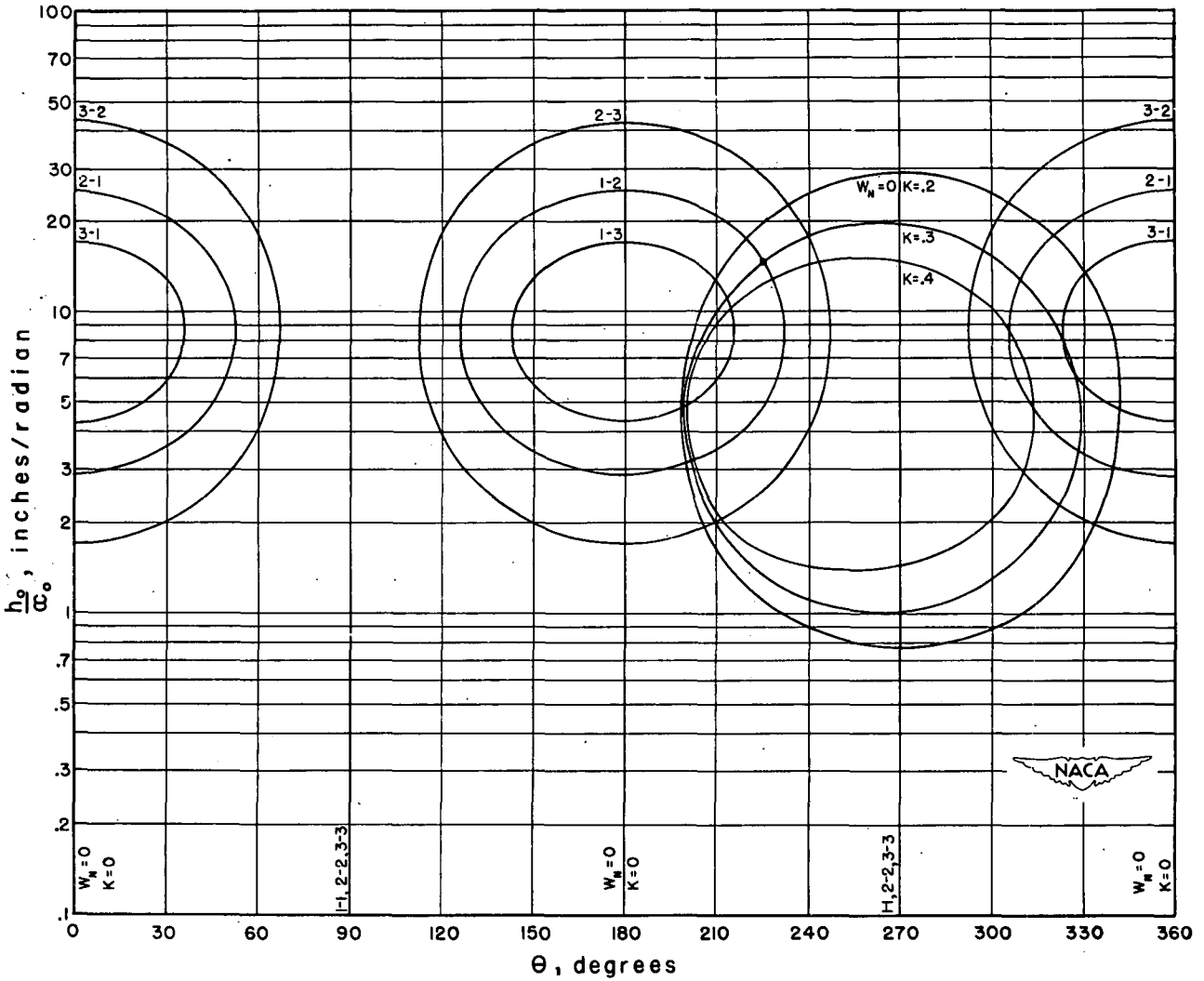

Figure 18.- Graphical solution for the flutter conditions.

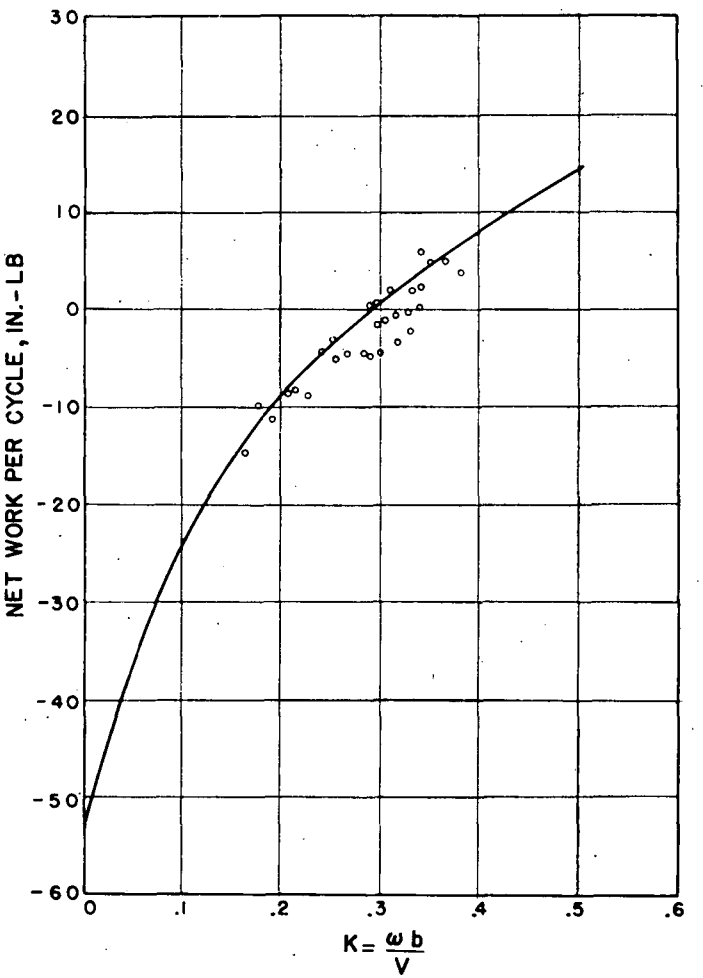

(a) $\theta = 225.5^{\circ}$; $h_o/\alpha_o = 15$.

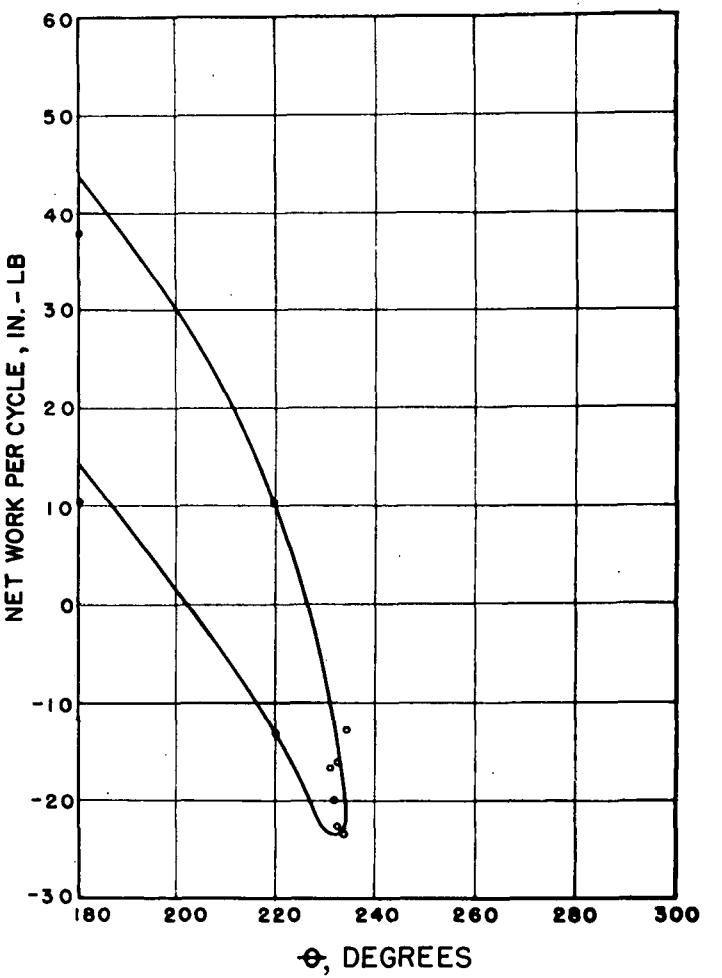

(b) k = 0.3.

Figure 19.- Work per cycle in combined motions.

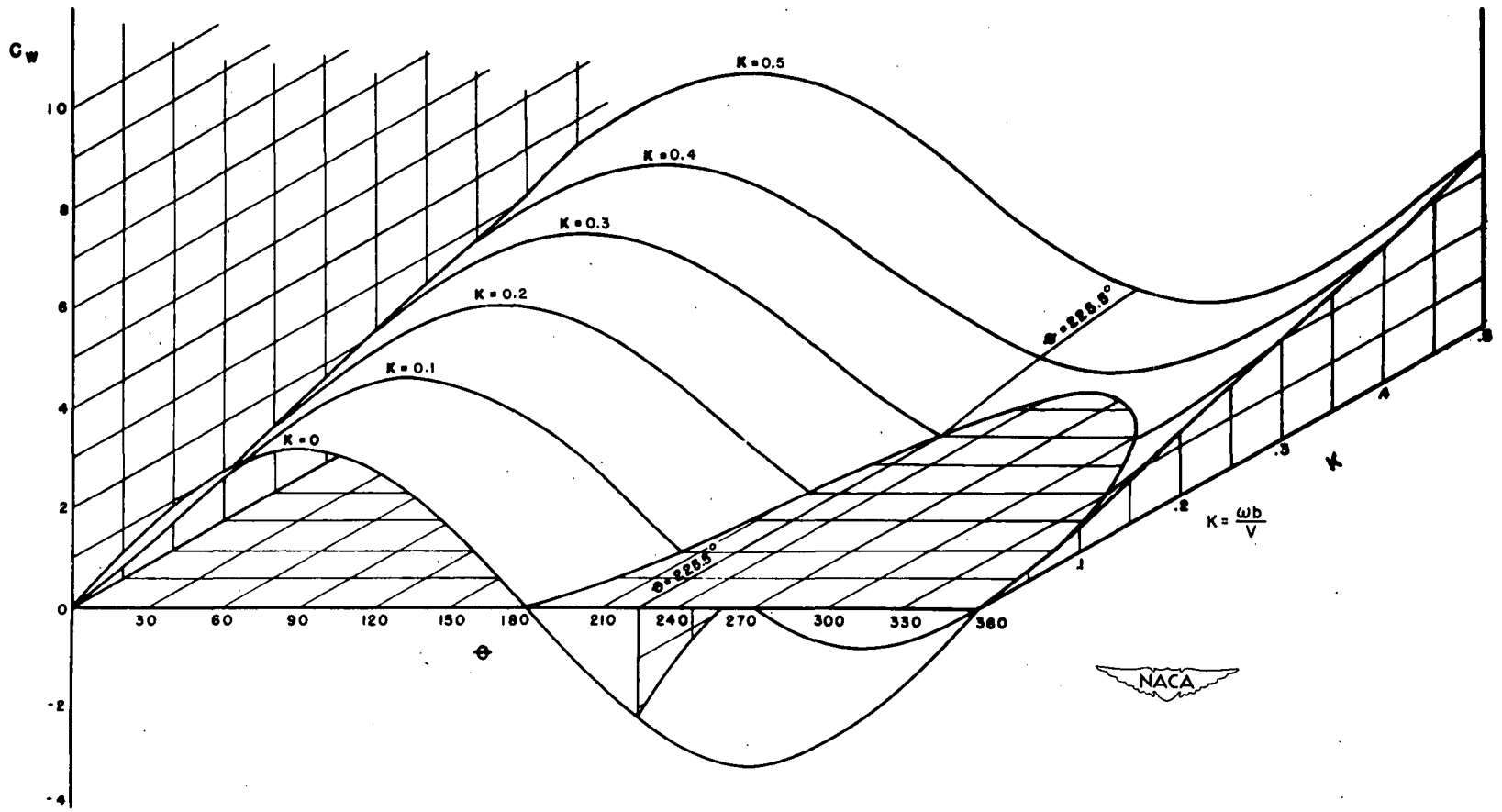

Figure 20.- Work per cycle in combined motions. $h_o/a_o = 15$.

$$C_W = C_{W_M} - C_{W_L} = \frac{W_N}{4qba_\phi h_o}.$$

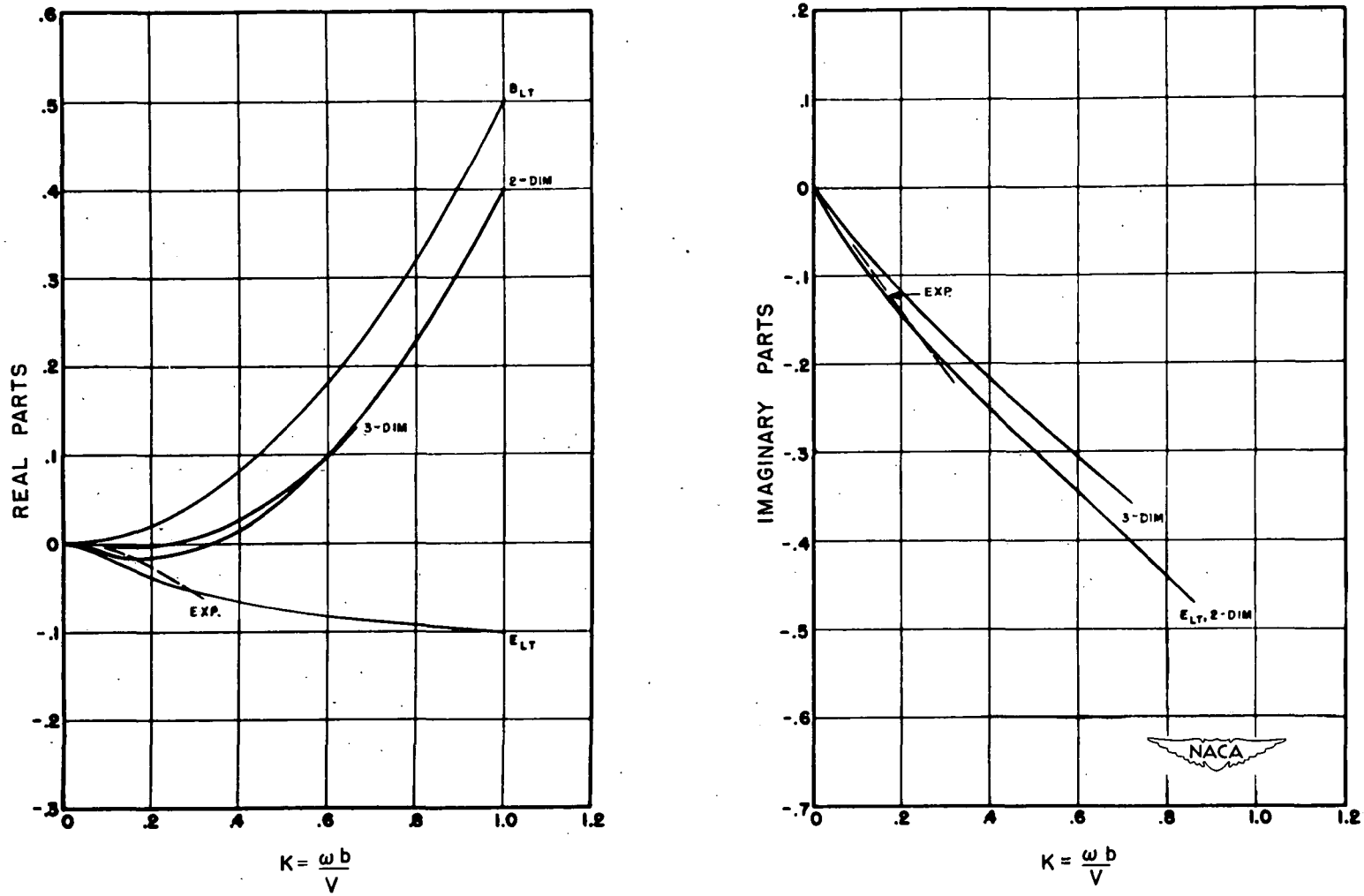

Figure 21.- Component analysis. Lift in pure translation. $B_{LT} = \frac{k^2}{2}$; $E_{LT} = ikC$.

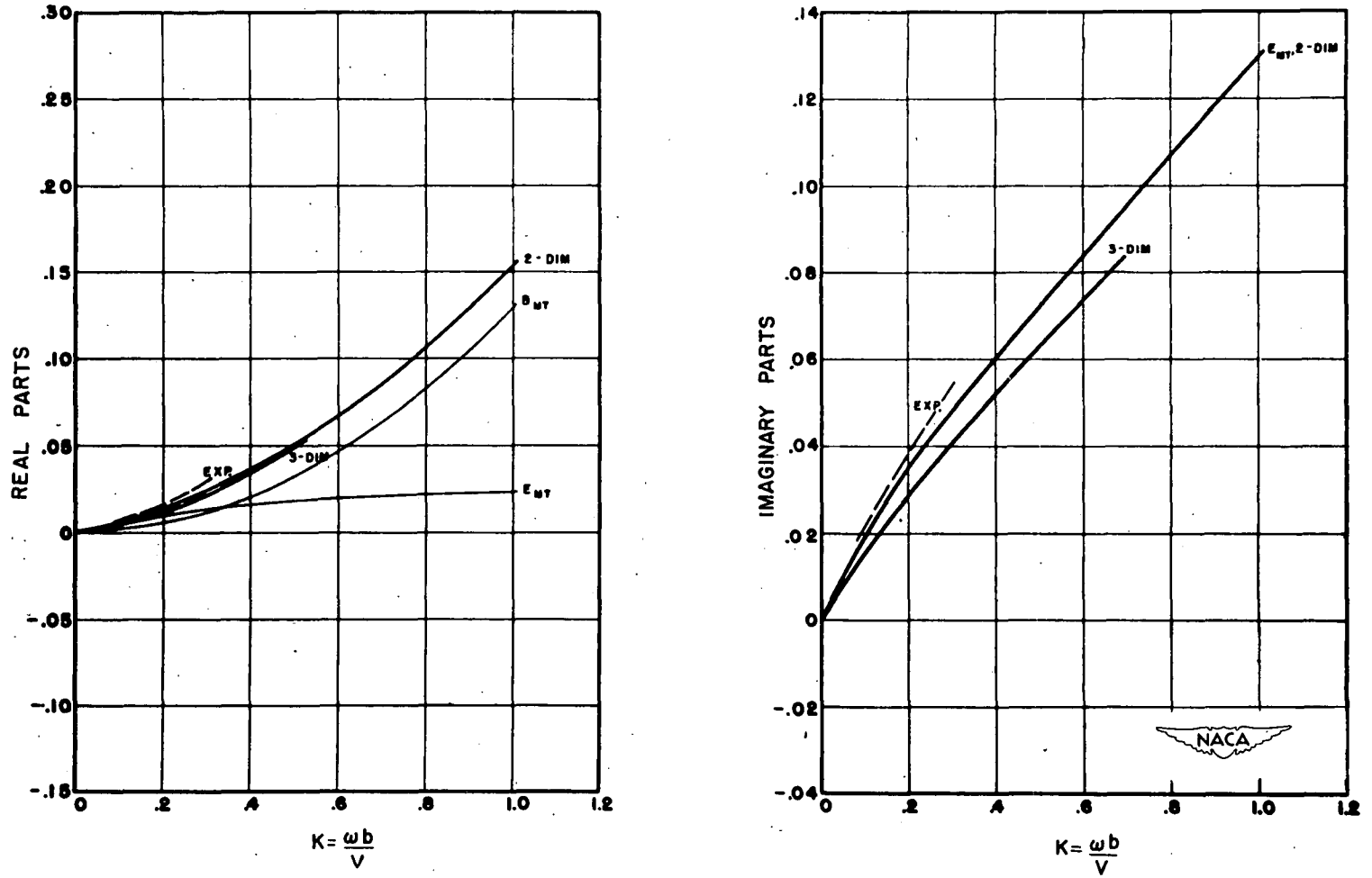

Figure 22.- Component analysis. Moment in pure translation. $B_{MT} = -\frac{ak^2}{2}$;
$E_{MT} = \left(\frac{1}{2} + a\right)ikC = \left(\frac{1}{2} + a\right)E_{LT}$.

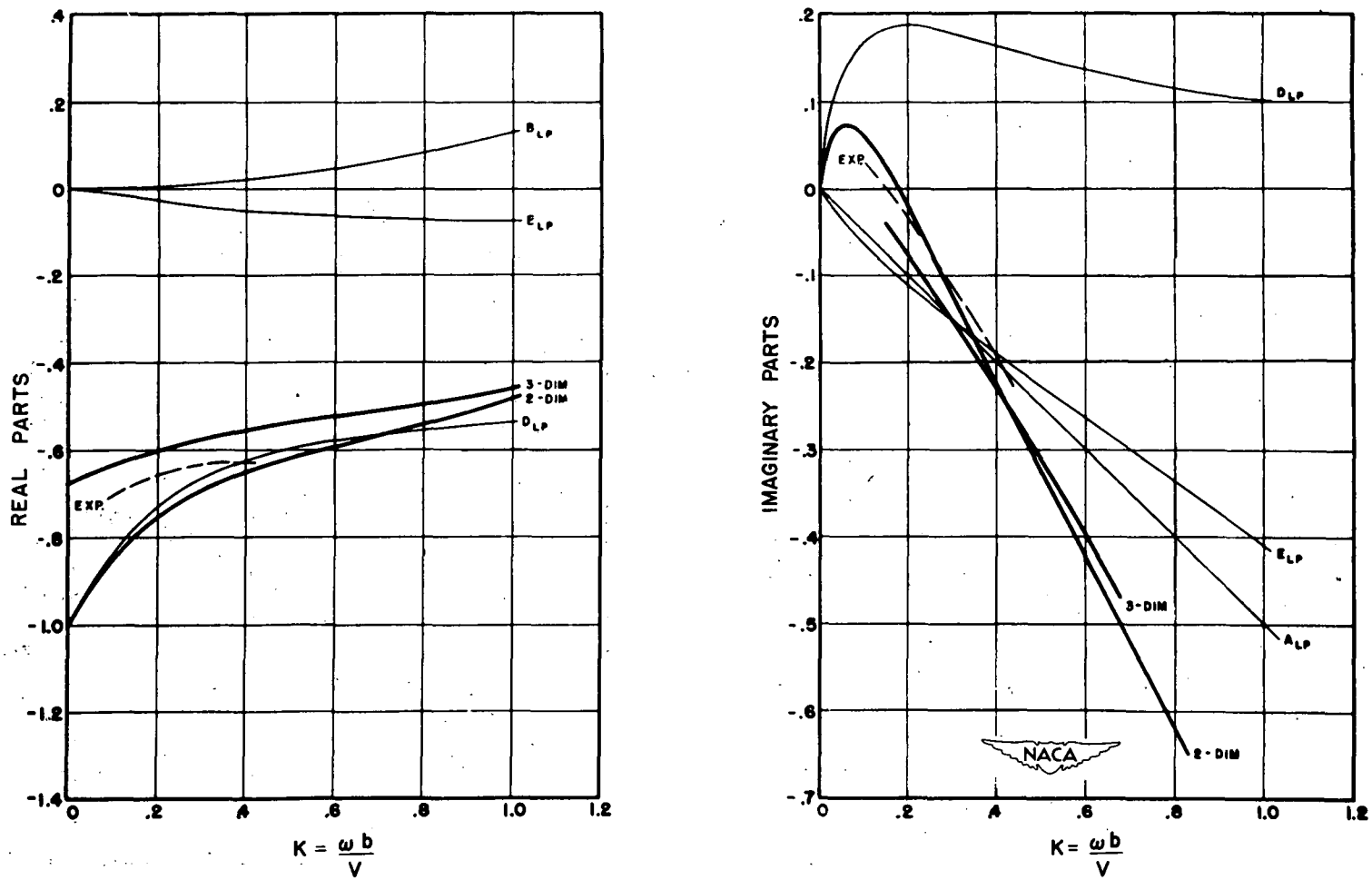

Figure 23.- Component analysis. Lift in pure pitch. $A_{LP} = -\frac{ik}{2}$; $B_{LP} = -\frac{ak^2}{2}$; $D_{LP} = -C$; $E_{LP} = -\left(\frac{1}{2} - a\right)ikC$.

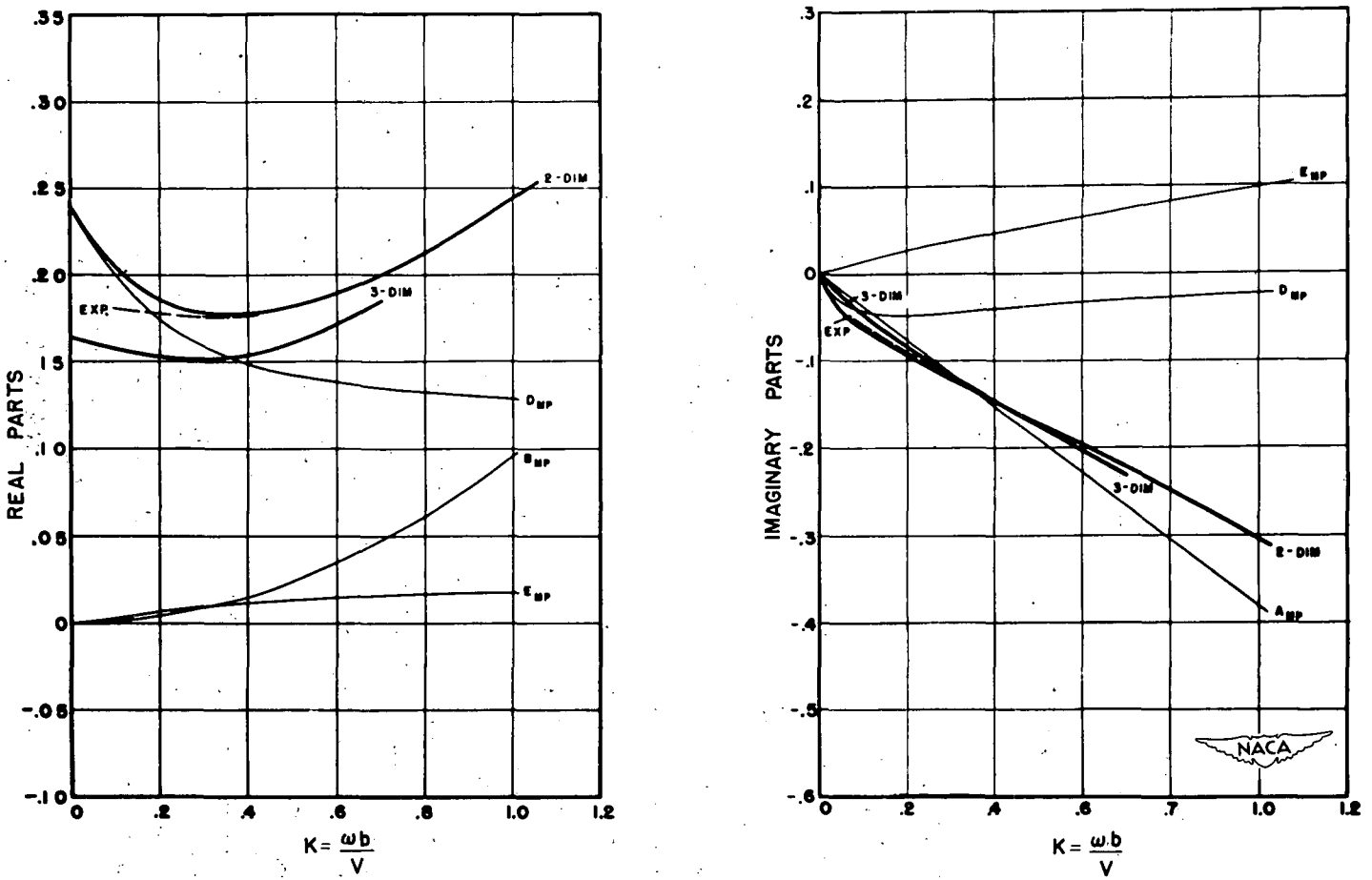

Figure 24.- Component analysis. Moment in pure pitch.

$$A_{MP} = -\frac{ik}{2}\left(\frac{1}{2} - a\right) = \left(\frac{1}{2} - a\right)A_{LP}; \quad B_{MP} = \frac{k^2}{2}\left(\frac{1}{8} + a^2\right);$$

$$D_{MP} = \left(\frac{1}{2} + a\right)C; \quad E_{MP} = \left(\frac{1}{4} - a^2\right)ikC.$$

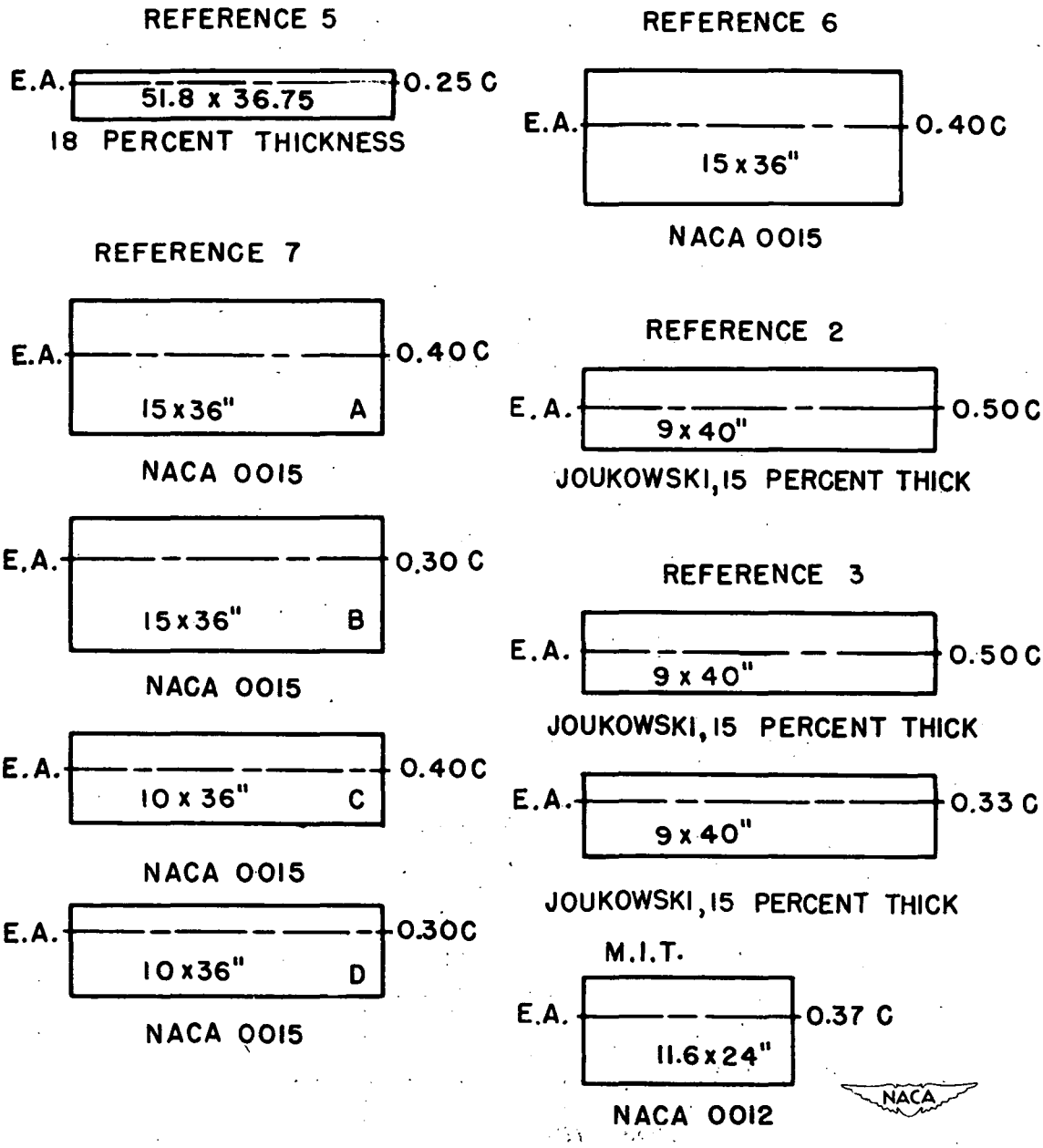

Figure 25.- Airfoil dimensions.

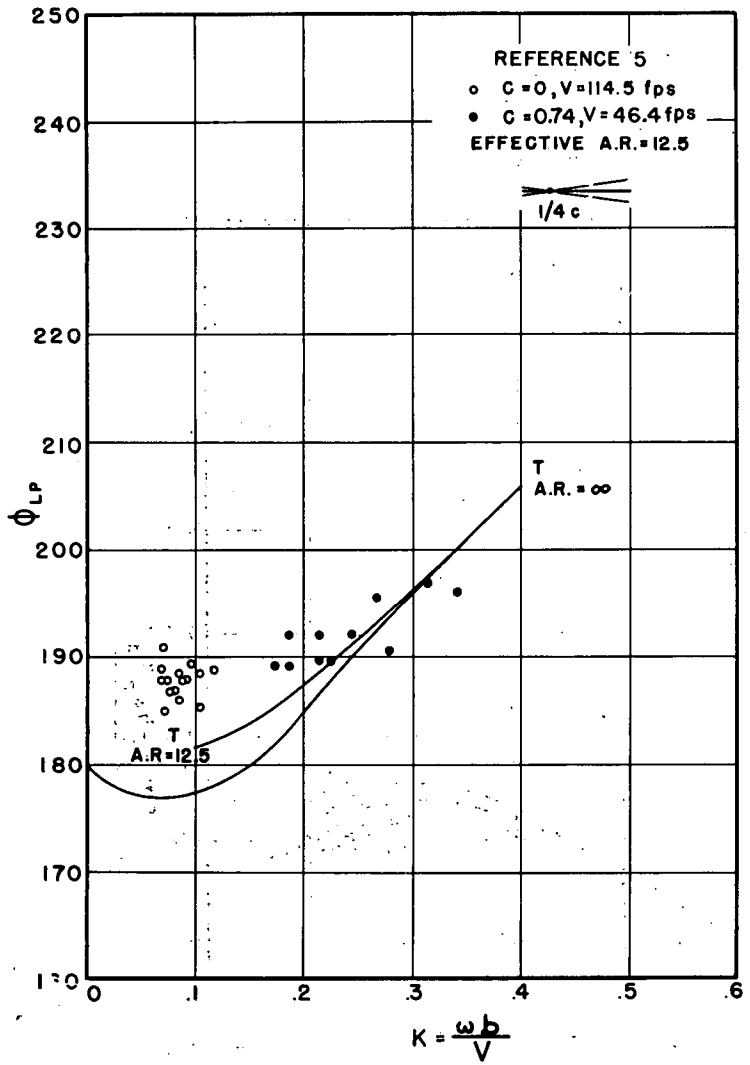

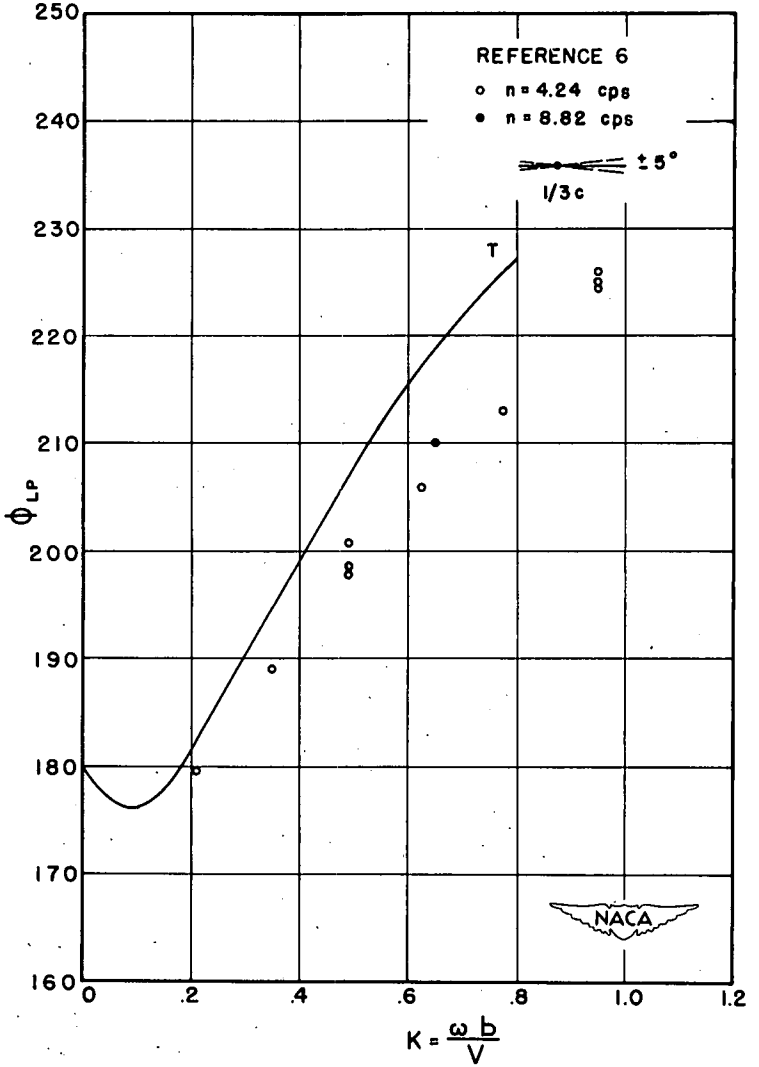

Figure 26.- Lift phase angle in pure pitch. From references 5 and 6.

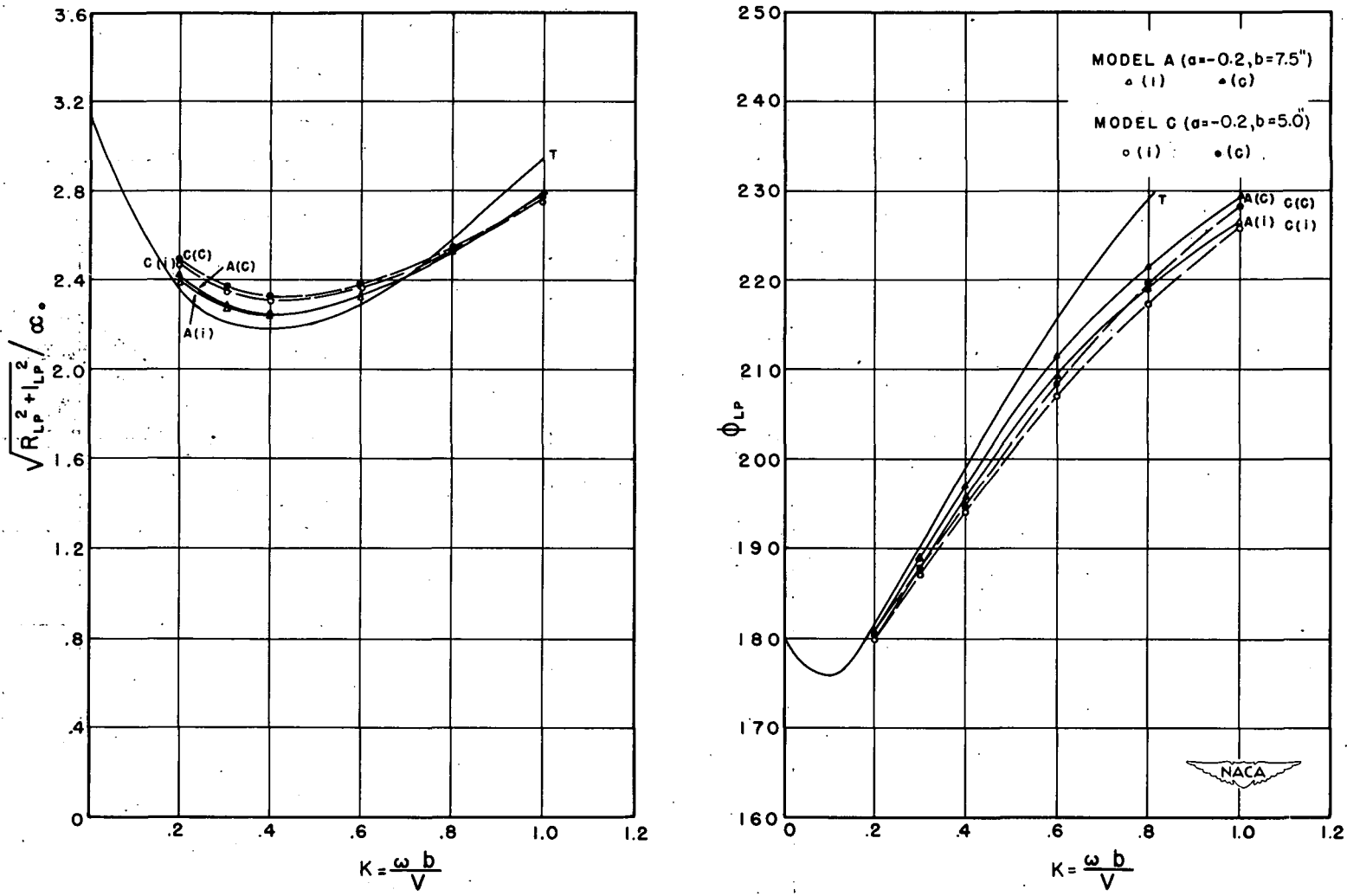

Figure 27.- Lift in pure pitch. Stanford models A and C. Oscillation amplitude, ±2.5°.

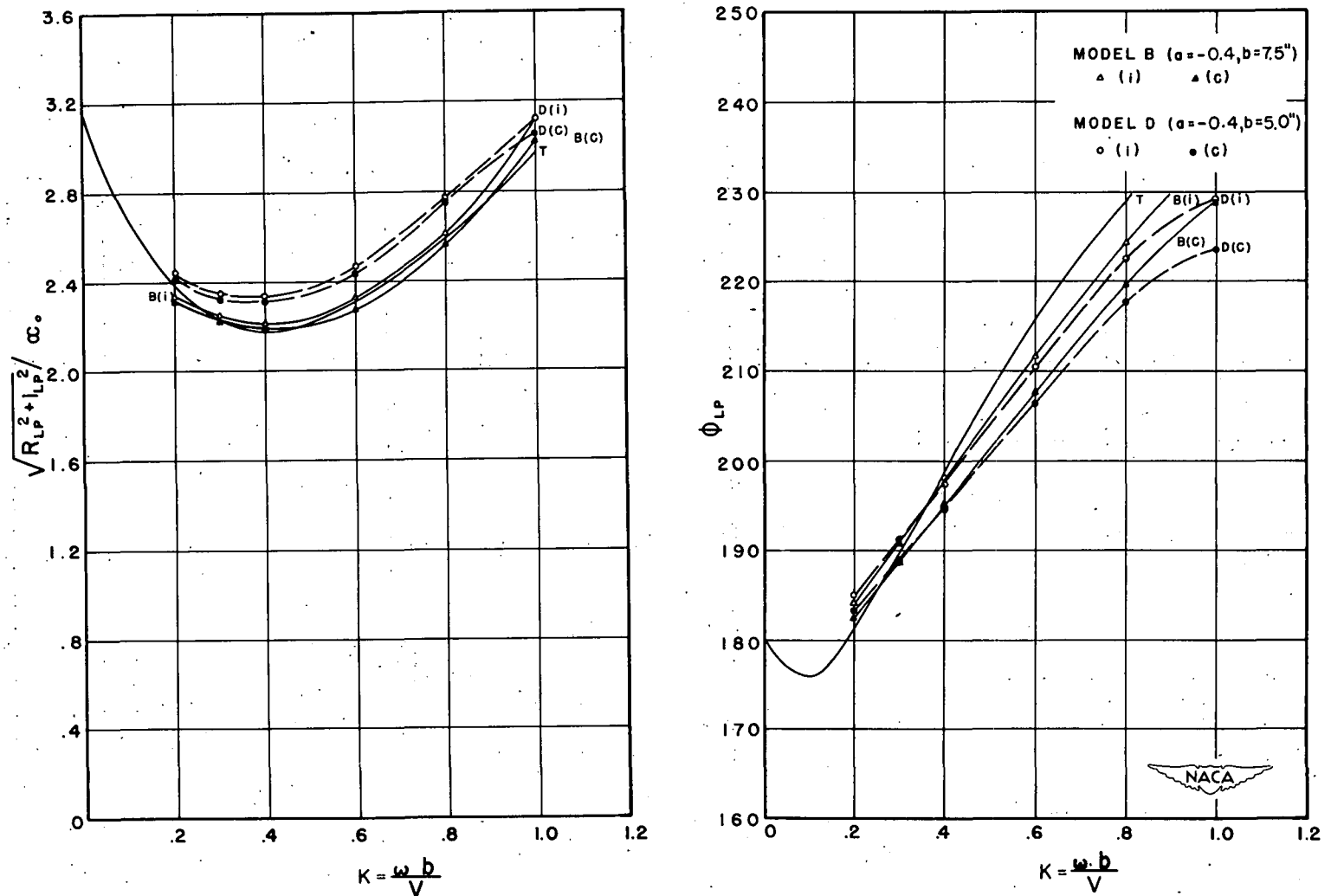

Figure 28.- Lift in pure pitch. Stanford models B and D. Oscillation amplitude, ±2.5°.

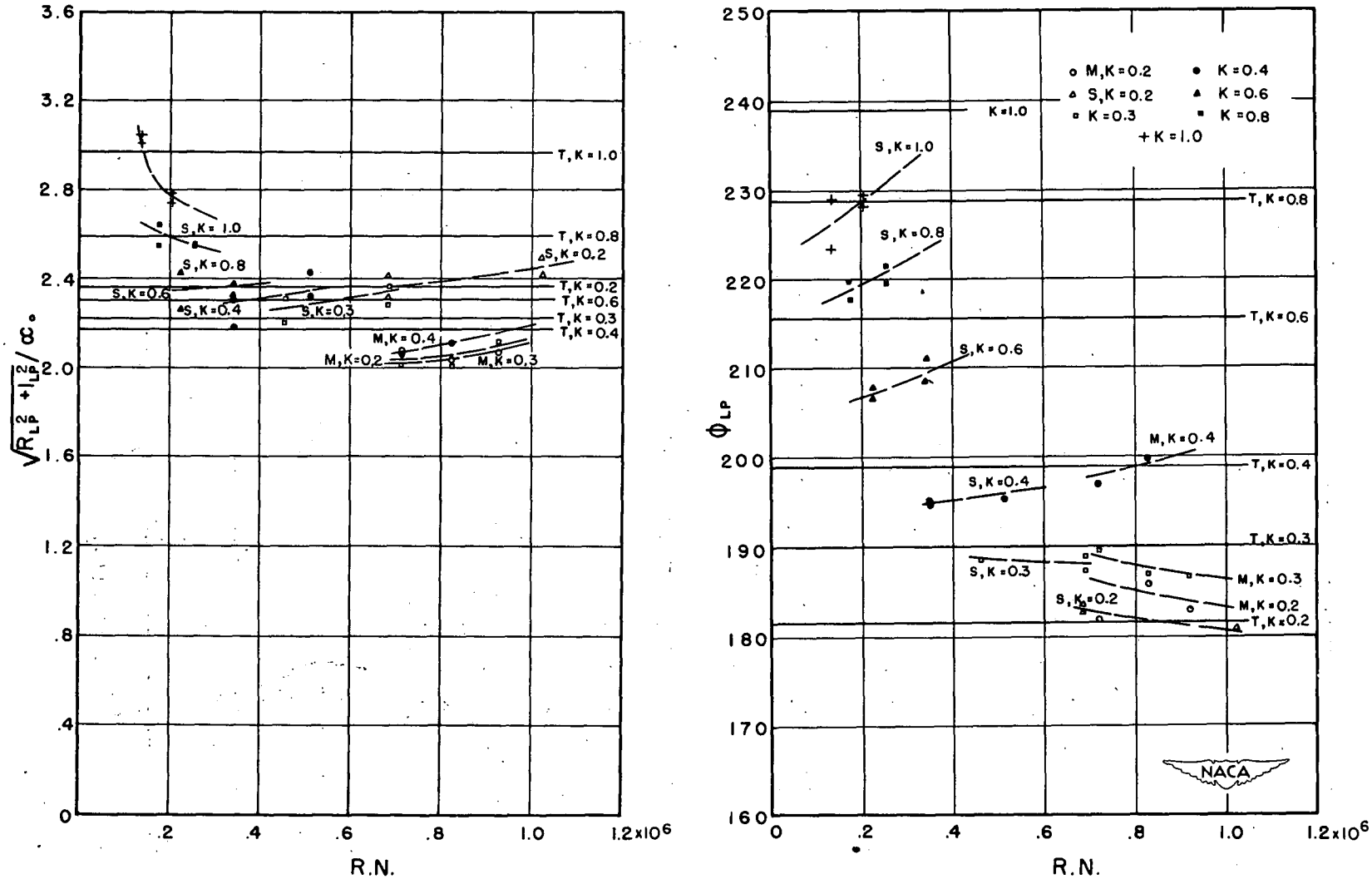

Figure 29.- Reynolds number effect - lift in pure pitch.

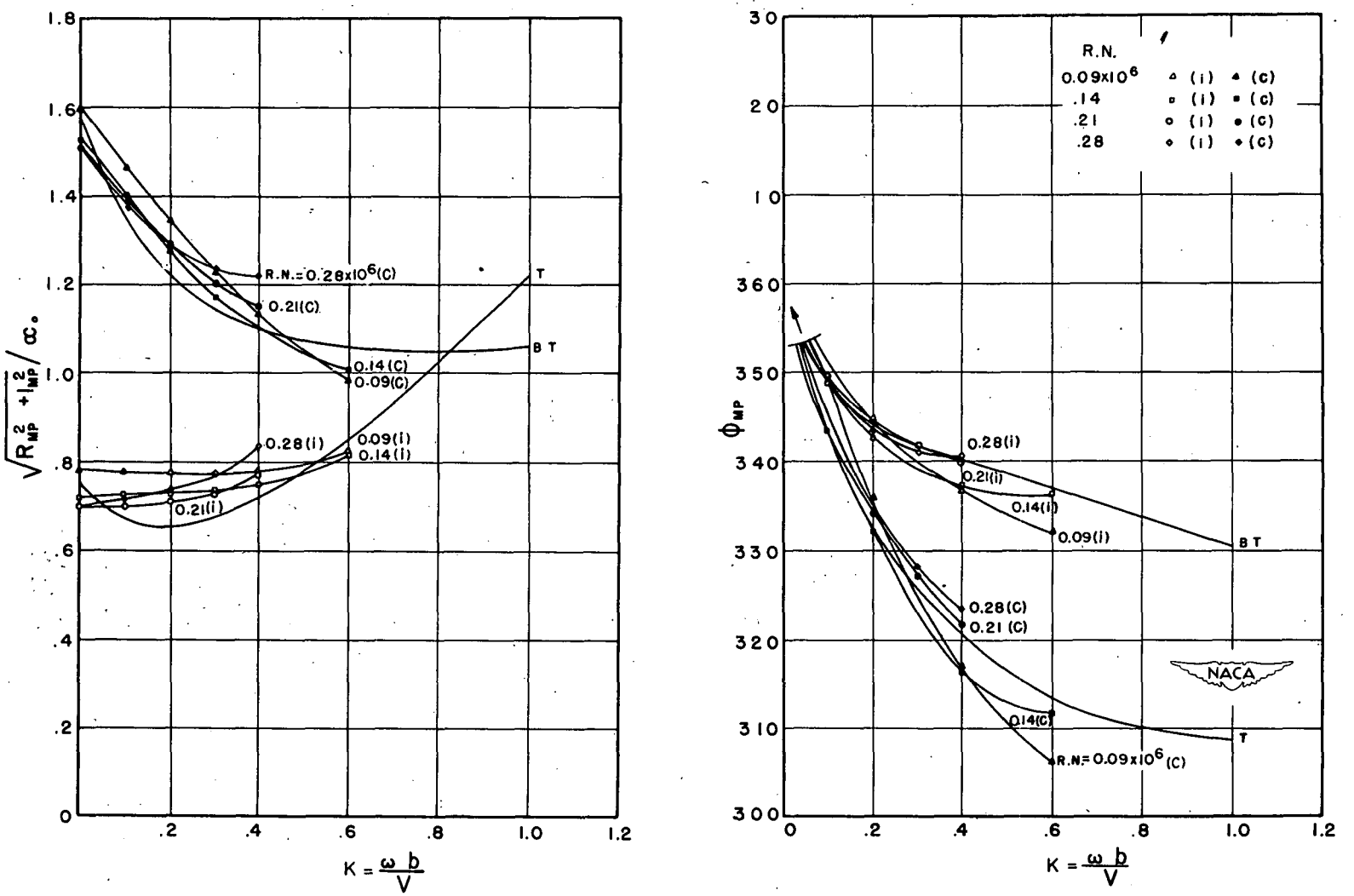

Figure 30.- Moment in pure pitch. $\alpha_o = \pm 5.13^\circ$. Reference 2.

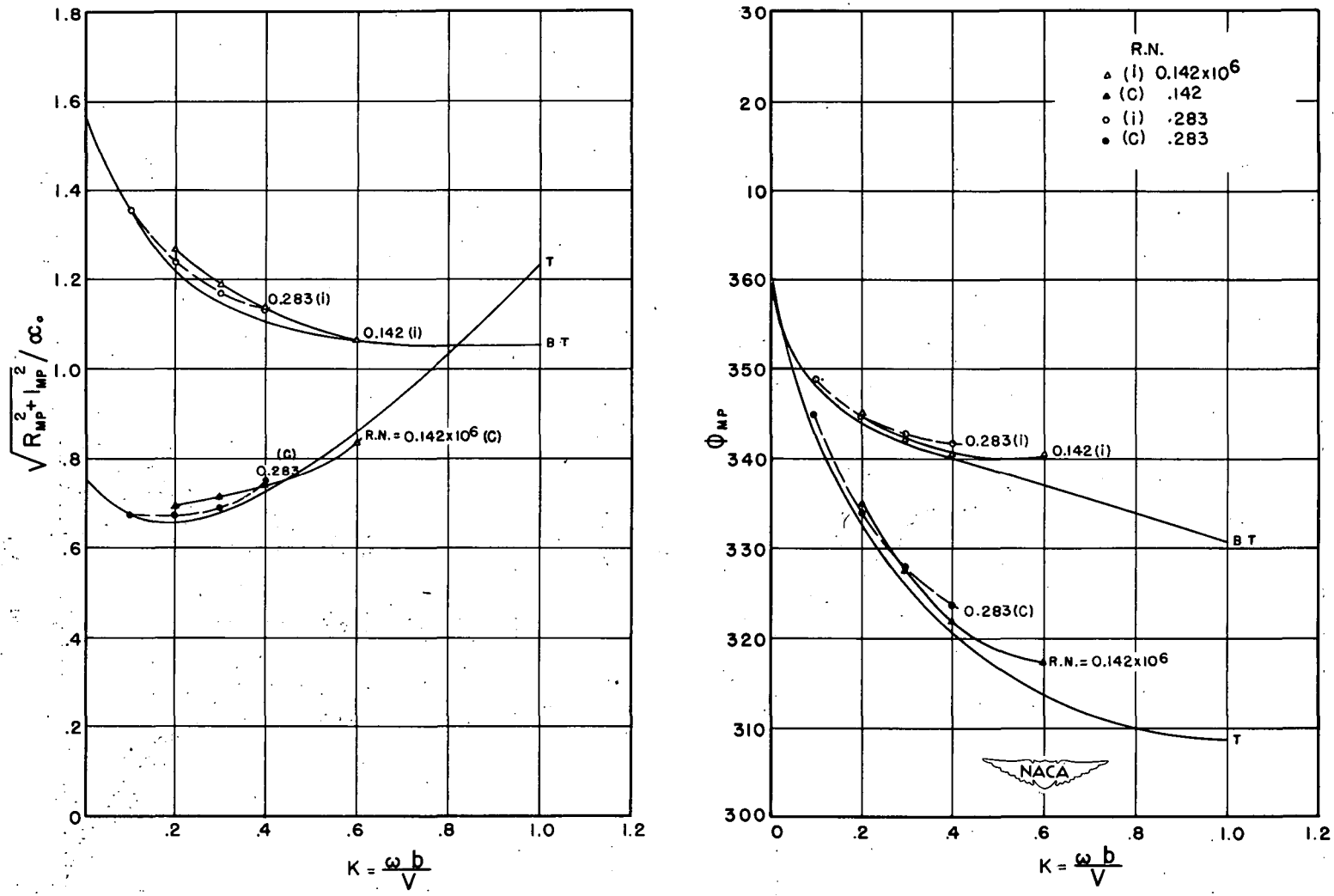

Figure 31.- Moment in pure pitch. $\alpha_o = \pm 6.0^o$. Elastic axis at half-chord, with center bearing. Reference 3.

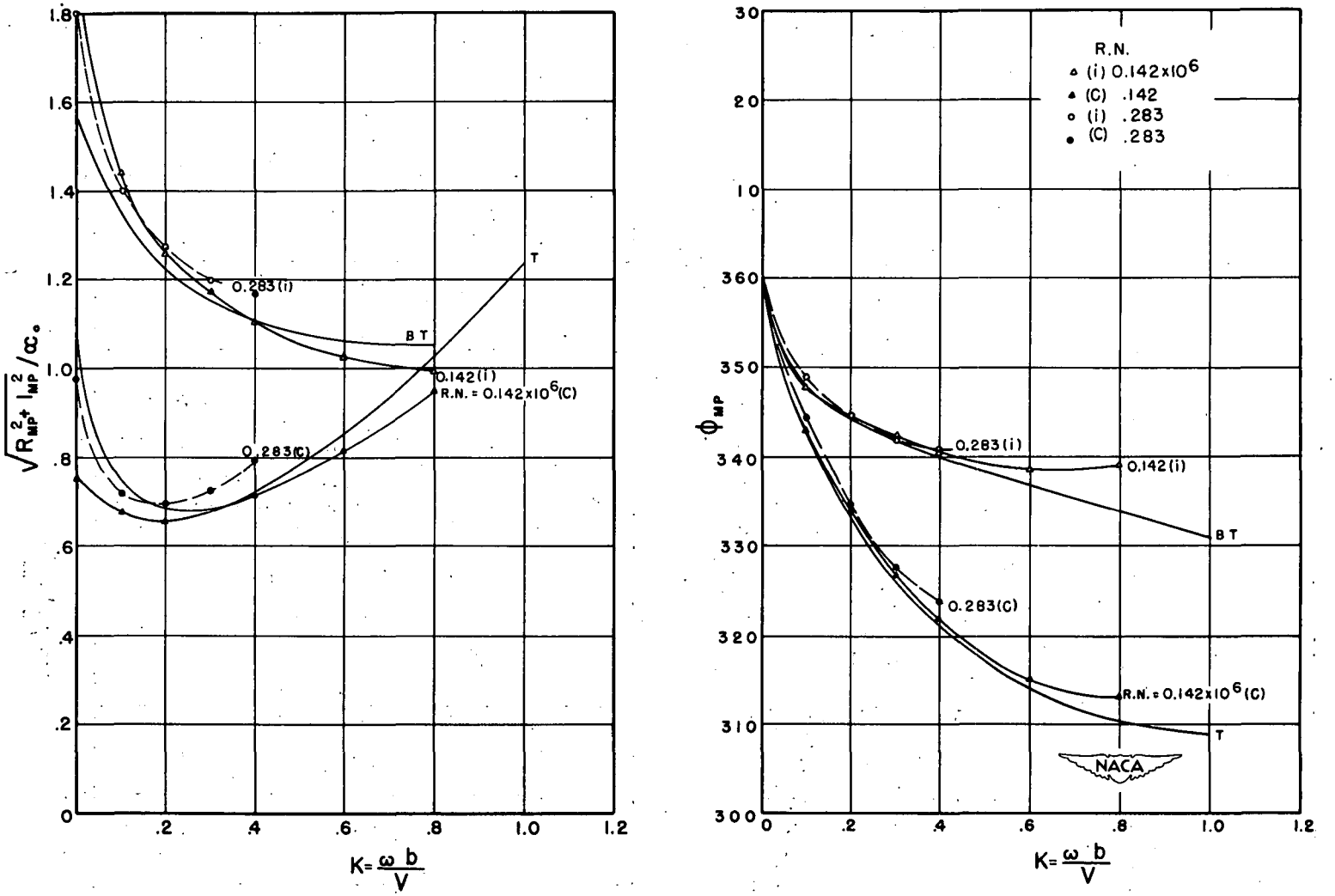

Figure 32.- Moment in pure pitch. $\alpha_o = \pm 6.0^\circ$. Elastic axis at half-chord, without center bearing. Reference 3.

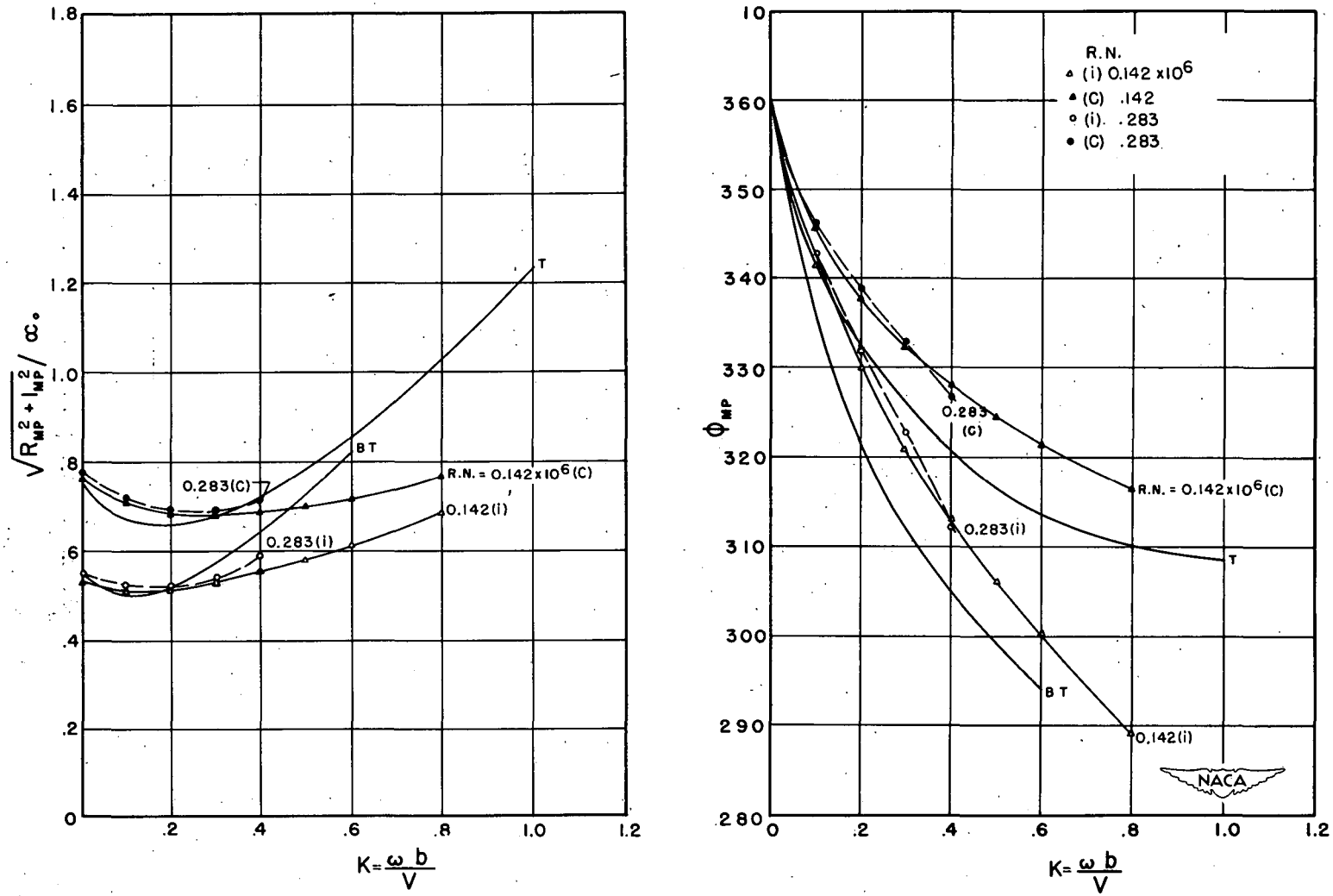

Figure 33.- Moment in pure pitch. $\alpha_o = \pm 6.0°$. Elastic axis at third-chord. Reference 3.

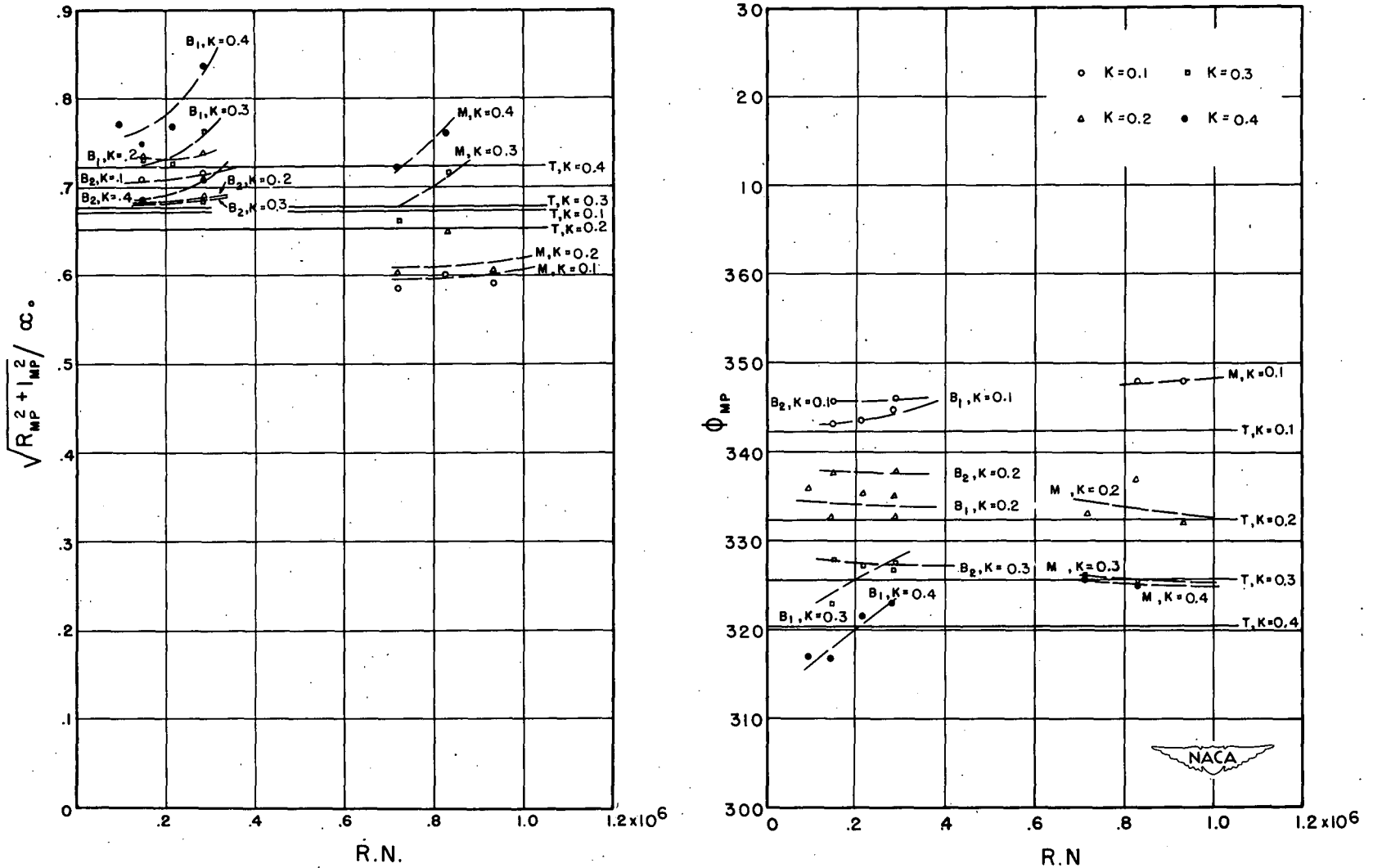

Figure 34.- Reynolds number effect. Moment in pure pitch.